TECHNISCHE UNIVERSITÄT MÜNCHEN

Fakultät für Chemie

Flow-based chemiluminescence bioassays for rapid screening of fungi, antibiotic resistant bacteria and diclofenac

Katharina Sollweck

Vollständiger Abdruck der von der Fakultät für Chemie der Technischen Universität München zur Erlangung des akademischen Grades einer

Doktorin der Naturwissenschaften (Dr. rer. nat.)

genehmigten Dissertation.

Vorsitzender:	Prof. Dr. Martin Elsner
Prüfer der Dissertation:	1. Priv. - Doz. Dr. Michael Seidel
	2. Prof. Dr. Andreas Thiem

Die Dissertation wurde am 12.07.2021 bei der Technischen Universität München eingereicht und durch die Fakultät für Chemie am 11.10.2021 angenommen

Be like a pineapple.

Stand tall.

Wear a crown.

And be sweet on the inside.

Table of Contents

Preface

First of all, I would like to thank my supervisor PD Dr. Michael Seidel for giving me the possibility to do my dissertation on such interesting research topics. I would also like to thank him for his support and the fruitful discussions. My thanks also go to Prof. Dr. Martin Elsner who, with his supportive nature, always found a way to encourage me even when times were hard.

Without my students, this research would not have been possible. I want to thank Gerhard Schwaiger who worked with me on and off through almost my entire PhD time. I also would like to thank Andreas Auernhammer and Philipp Streich, who contributed a lot to my work. The months where it was the four of us together, were some of the best months of my thesis. I also would like to thank my other students, Elmedina Shimaj, Leonhard Lorenz, Michael Zollo and Leong Jin Rui.

A PhD would not be what it is if it were not for colleagues, the very people you share all the difficult and beautiful moments with. I was very blessed to have such supportive souls around me which to this day are my friends. Lisa, you are the kind of person who would never say no if anyone needed help, that is such a beautiful trait of yours. Caddi, your laughter and your tears both are contagious, we have had some very happy, sad, and angry moments together, thank you for that! Verena, even if we only got closer when you had already left the institute, what a wonderful friendship was born! Thanks for being so supportive in every aspect of my life, you keep me grounded. Julia N., keep on spreading positivity with your friendly nature. Julia K., you have my deepest admiration for all the things you do to make this world a better place, rock on girl! And Yanwei, you have had some rough times but nevertheless you never lost your motivation to go on and accomplish great things. Fabio, even though we only shared three months, you are the best example for a very busy person who will never loose sight of others even though they have way too much on their plate already. Emilio, my Italian anchor, always helping me out when I needed input from out of my bubble, you always helped me, listened to me, no matter how stupid the issue. I want to thank all of you for nice conversations, scientific discussions and most of all, emotional support.

Of course, I also want to thank every other person at the institute who contributed to the nice working environment and who like Conny and Christine kept the whole place running!

I want to thank my wonderful parents, who went through some rough times while I did this research and still never stopped supporting me. Same goes for my brother, thank you for always believing in me.

The greatest thanks of all goes to my partner Tim, who became my husband during these crazy times. He is the person who gets me through every day, who encouraged me when times were hard and who celebrated every tiny success with me. Thank you for being my personal cheerleader, I honestly do not know what I would do without you!

Publications

Parts of this work were published in peer-reviewed journals:

Sollweck K., Streich P., Elsner M., Seidel M.

A chip-based colony-fusion-recombinase polymerase amplification assay for monitoring of antimicrobial resistance genes and their carrying species in surface water.

ES&T water 2021. https://doi.org/10.1021/acsestwater.0c00110

Sollweck K., Schwaiger G., Seidel M.

A chemiluminescence-based heterogeneous asymmetric recombinase polymerase amplification assay for the molecular detection of mycotoxin producers.

Analyst. 2021. https://doi.org/10.1039/D0AN02000A

Conference contributions

Parts of this work were presented on the following conferences:

VDI/BAuA Expert Forum Bioaerosols in Berlin, November 2019

Poster presentation and oral presentation:

Sollweck K., Schwaiger G., Elsner M., Seidel M.

A chemiluminescence based microarray detection system for mycotoxin producers in indoor air

AC@TUM Conference in Raithenhaslach, July 2019

Poster presentation:

Sollweck K., Schwaiger G., Shimaj E., Streich P., Elsner M., Seidel M.

Chemiluminescence based microarray detection systems for environmental contaminants

ANAKON Conference in Münster, March 2019

Oral presentation:

Sollweck K., Seidel M.

Development of detection methods for mycotoxin producers in indoor air

Medical Biodefense Conference in Munich, October 2018

Oral presentation:

Sollweck K., Seidel M.

Development of detection methods for mycotoxin producers and mycotoxins in indoor air

Abstract

In this dissertation, three chemiluminescence-based assays for application with a fully automated chip reading platform (MCR 3) were developed. The first assay was designed for the analysis of mycotoxin producers. Mold in indoor air is a prominent topic for residential and occupational safety as the latter can have a number of health impacts for humans. These can range from allergies, skin irritations, headaches, respiratory infections to even cancer. Current methods used for quantification of microorganisms in indoor air are culture-based and relatively inaccurate as only viable cells are detected and many molds are not culturable. An alternative method is counting the total number of microbial cells under the microscope, but this requires a lot of expertise. These methods are not capable of translating the on-site situation to analytical data reliably. In this work, a molecular biological, chemiluminescence-based method for the detection of mycotoxin producers through isothermal amplification of mycotoxin biosynthesis genes on glass and polycarbonate carriers was developed. This proof-of-principle study showed the successful detection and quantification of zearalenone producers via heterogeneous asymmetric recombinase polymerase amplification (haRPA). An appropriate lysis method for fungal spores was developed in order to rapidly access DNA of fungal spores. To be more cost and time effective, the assay was transferred from glass to polycarbonate surfaces. A system calibration with spores of *Fusarium culmorum* as zearalenone-producing organism resulted in a limit of detection (LoD) of 2.7×10^5 spores/ml. The assay was shown to be specific for zearalenone producers and preliminary results showed the possibility of detecting trichothecene producers by a second primer set.

A second project focused on the detection of antibiotic resistance genes and their carrying species. For risk assessment, it is important to be able to link resistance genes to their carrying species in order to evaluate their potential pathogenicity for humans. This cannot be achieved by the molecular biological methods currently used in this field. This second proof-of-principle study presented a solution by the introduction of a colony-based fusion recombinase polymerase amplification (RPA) starting from bacterial culture plates. With the here designed workflow, it is possible to detect species and resistance genes simultaneously within 1.5 h. In a first step, the fusion product of these genes is generated by homogeneous RPA, while

detection occurs in a second step via haRPA. This assay successfully discriminated between *Escherichia coli* colonies carrying blaCTX-M cluster 1 resistance genes and *E. coli* carrying blaCTX-M genes of other clusters as well as other bacterial species carrying blaCTX-M resistance genes. A cutoff value of 17% was defined for the differentiation between positive and negative samples. The assay was confirmed to be usable for environmental samples by analysis of water from the river Lech. Preliminary results indicated a suitable primer set for fusion product formation in *Klebsiella pneumoniae*.

The third assay which was worked on in this thesis, was an indirect competitive immunoassay for the detection of diclofenac in milk. Non-steroidal anti-inflammatory drugs can accumulate in animal-derived foods when inappropriately fed to animals. As they pose danger to human health, there is a need for surveillance. An assay which had previously been developed for analysis of diclofenac did not compete with enzyme-linked immunosorbent assay (ELISA) in terms of detection limits (0.26 µg/L vs. 0.08 µg/L). Therefore, the following approaches were tested to improve its performance: Transfer of the assay from glass to polycarbonate surfaces, modifications in spotting procedure and spotting buffer composition and modification of the amount of immobilized antigen. Optimization of these parameters did not yield much improvement, resulting in an LoD of 0,17 µg/L. Furthermore, the regenerability of polycarbonate chip surfaces was not satisfactory with a recovery of only 74% of the original signal after 14 cycles of regeneration. It was concluded that antibody properties, steric hindrances, or assay differences such as missing equilibrium formation were likely the cause for this, but more investigations have to be done in the future.

Kurzfassung

In dieser Arbeit wurden drei Methoden zur Anwendung mit einer Chemilumineszenz-basierten, automatisierten Chip-Ausleseplattform (MCR 3) entwickelt. Die erste Methode zielt auf die Detektion von Mykotoxinproduzenten ab. Schimmel in Innenräumen ist ein weit verbreitetes Problem vor Allem in den Bereichen Wohn- und Arbeitssicherheit, da dieser gesundheitliche Probleme auslösen kann. Durch Schimmel ausgelöste Beeinträchtigungen reichen von Allergien oder Asthma über Atemwegsinfektionen bis hin zu Krebs. Gängige Methoden zur Quantifizierung der Belastung von Innenraumluft mit Mikroorganismen sind meist kulturbasiert und relativ ungenau, da viele Schimmelarten nicht kultivierbar sind und nur lebende Zellen quantifiziert werden können. Eine Alternativmethode ist die mikroskopische Auszählung von Zellen, die jedoch sehr viel Zeit und Expertise erfordert. Auf diesen Wegen ist es nicht möglich die Situation analytisch korrekt in Daten umzuwandeln. Daher wurde im Zuge dieser Arbeit wurde eine molekularbiologische, Chemilumineszenz-basierte Methode für die Detektion von Mykotoxinproduzenten mittels isothermaler Amplifikation von Mykotoxin-Biosynthesegenen auf Glas- und Polycarbonatoberflächen entwickelt. In der Prinzipstudie gelang es Zearalenon-Produzenten spezifisch mittels heterogener, asymmetrischer Rekombinase Polymerase Amplifikation (haRPA) zu detektieren und zu quantifizieren. Eine Lyse-Methode wurde entwickelt, um schnell und unkompliziert an die DNA der Pilzsporen zu gelangen. Außerdem wurde der Assay von Glasoberflächen auf Polycarbonatoberflächen übertragen, um schneller und kostengünstiger zu sein. Eine Kalibrierung des Arbeitsablaufs mit Sporen der Art *Fusarium culmorum* als Zearalenon-Produzenten ergab eine Detektionsgrenze von 2.7×10^5 Sporen/ml. Vorläufige Ergebnisse mit einem zweiten Primerset zeigten die Möglichkeit auch Trichothecene-Produzenten spezifisch zu detektieren und quantifizieren.

Als zweite Methode wurde ein Assay für die Detektion von Antibiotikaresistenzgenen und deren tragenden Spezies entwickelt. Für eine zuverlässige Risikoanalyse ist es neben der Identifizierung von Resistenzgenen auch wichtig die tragende Spezies zu ermitteln, um die Pathogenität gegenüber dem Menschen bewerten zu können. Dies können die gängigen molekularbiologischen Methoden, die für diesen Zweck verwendet werden, nicht leisten.

Deshalb wurde in dieser Arbeit eine *colony-based fusion recombinase polymerase amplification* (RPA) ausgehend von Bakterienplatten entwickelt. Bei dieser Methode werden Resistenz- und Spezies-spezifische Gene gleichzeitig innerhalb von 1,5 Stunden identifiziert. Im ersten Schritt wird mittels homogener RPA ein Fusionsprodukt aus beiden Genen gebildet, welches im zweiten Schritt mittels haRPA auf einem Chip detektiert werden kann. Dieser Assay konnte erfolgreich zwischen blaCTX-M cluster 1 tragenden *Escherichia coli*-Kolonien und *E. coli*, die blaCTX-M Gene anderer Cluster oder anderen Spezies unterschieden. Der Schwellenwert für die richtige Zuordnung positiver und negativer Kolonien wurde bei 17% festgelegt. Auch die Anwendbarkeit mit Umweltproben wurde bestätigt, indem Wasser des Flusses Lech erfolgreich analysiert wurde. Vorläufige Ergebnisse mit einem weiteren Primersystem zeigten außerdem die Möglichkeit einer Erweiterung des Anwendungsgebiets auf *Klebsiella pneumoniae*.

Im dritten Projekt dieser Arbeit wurde ein Chemilumineszenz-basierter, indirekt-kompetitiver Immunoassay zur Detektion von Diclofenac in Milch genauer betrachtet. Nicht-steroidale Entzündungshemmer können sich bei inkorrekter Anwendung in tierischen Produkten wie Milch anreichern. Aus gesundheitlichen Gründen müssen daher regelmäßige Kontrollen erfolgen. In diesem Teil der Arbeit wurde ein bereits etablierter Assay auf Glasoberflächen genauer untersucht, da dieser im Vergleich zu einem ELISA eine 10-fach höhere Detektionsgrenze aufwies (0.26 µg/L vs. 0.08 µg/L). Durch das Testen folgender Optionen wurde versucht dieses Problem zu lösen: Die Übertragung des Assays auf Polycarbonatoberflächen, sowie die Veränderung der Spotting-Bedingungen, des Spotting Puffers und der Menge an immobilisiertem Antigen. Dies brachte nur eine bedingte Verbesserung (0.17 µg/L). Auch die Regenerabilität des Assays auf Polycarbonatoberflächen ist verbesserungswürdig, da bereits nach 14 Zyklen nur noch 74 % des ursprünglichen Signals festgestellt werden konnte. Gründe für diese Probleme könnten die Antikörper-Beschaffenheiten, sterische Hinderung oder Unterschiede im Assay-Ablauf sein, die die Einstellung eines Gleichgewichts verhindern. Genauere Beobachtungen und weitere Optimierungen sind in Zukunft nötig.

Motivation

Analytically monitoring harmful substances in the environment has become very important since industrialization. Contamination of air, water, soil etc. is part of humanity's daily life[1]. This is the reason why even a new geological epoch is being suggested by some scientists: the Anthropocene, which is thought to have begun in the mid-20th century as shown by geochemical signatures.[2] The increase of global population and the advancing of technology goes hand in hand with changes in soil, water, air, and climate. The pollution of the environment does not remain without consequences, most agents which enter the environment can be harmful to human health or to ecosystems by finding their way into food, water, soil and air.[3,4] This fact has created the need for a whole new research field called environmental analytics. While practices and entities for environmental surveillance exist since the 1960s,[5] the growing issue of pollution and stricter regulations call for more analytical, rapid, multiplex-able and automated methods in the present. At the heart of this field stands environmental monitoring, the science of surveillance of the environment. This is especially important regarding harmful substances such as pharmaceuticals, pathogens, combustion products, toxins and many more. Monitoring is needed to provide information about the state of a particular environment to scientists and decision-makers.[6] Several organizations have environmental monitoring systems in place in order to distribute this type of information globally. To give some examples, the United Nations (UN) administer programs to monitor water[7] and air[8] quality. The Food and Agricultural Organisation (FAO) monitors the environmental impact of everything related to food production and agriculture.[6] Since 1975, UN agencies also manage the Global Environment Monitoring System (GEMS) which is a collaboration between many organizations.[5,6] It is required that new and reliable methods are developed in order for programs such as these to be successful. Methods of course need to be designed to be suitable both for the environment they are intended for and the polluter or pollutant which is aimed to be analyzed. Monitoring techniques usually require to be rapid, easy to use and applicable on-site as well as in low-resource settings. This work aimed to contribute to this scientific field by the development of three easy-to-use and on-site

screening methods (detection of fungi in air, antibiotic-resistant bacteria in surface water and pharmaceutical contaminants in food).

The first project focuses on the detection of mycotoxin producers. Modern society spends most of its time indoors either at home or at the workplace.[9] Mold which produces mycotoxins can be very harmful to human health and is a big issue for residential and occupational safety.[10] In this work, a method was developed which is able to detect and quantify spores of zearalenone and trichothecene-producing *Fusarium* species by heterogeneous asymmetric recombinase polymerase amplification (haRPA) on polycarbonate surfaces.

The second method aimed to create a contribution to the rising problem of antibiotic resistance in the environment. This issue has been ranked as one of the top health issues for humanity in the 21st century by the World Health Organization (WHO).[11] Therefore, rapid, on-site methods are needed for the simultaneous detection of antibiotic resistant bacteria and their carrying species. This was done using a colony-fusion-haRPA workflow for the detection of CTX-M cluster 1 carrying *Escherichia coli*.

The contamination of animal-derived foods such as bovine milk with pharmaceutical residues is a prominent topic, too.[12] A chip-based immunoassay for the detection of the non-steroidal anti-inflammatory drug diclofenac in milk was aimed to be improved in this work.

All three of these methods contribute in their own way to the establishment of more user-friendly monitoring methods which can be used on-site also in low-resource settings where environmental contamination is often the heaviest. In addition to minimizing humanity's footprint on the environment, the future also asks for more transparent, applicable, and global monitoring systems to ensure safety for humans and ecosystems.

1. Theoretical background

This work focuses on the detection of mycotoxin producers in air, antibiotic resistant bacteria (ARBs) in water and the nonsteroidal anti-inflammatory drug (NSAID) diclofenac in bovine milk by application of analytical microarray methods. This is why, at first analytical microarray systems, especially the one used in this work will be introduced. Theoretical background information on the contamination of indoor air with mold, the contamination of surface water with ARBs and the contamination of milk with NSAIDs, especially diclofenac will follow.

1.1. Analytical microarray systems

One of the first applications for microarrays was the analysis of gene expression patterns developed 30 to 40 years ago.[13] The first breakthrough was achieved by Fodor and colleagues in 1992, who based on their research founded Affymetrix Inc.[14] In 1992, the first immunoanalytical microarray was presented by Ekins and Chu.[15] The first mRNA analysis to track protein expression was done 1995 by Patrick Brown and colleagues,.[16,17] Both of these studies showed the immense potential of these systems. Since then, microarray technology has been used for many different techniques and applications. The main point, which makes these systems so powerful, is their multiplex-ability. There are plenty of different systems now to analyze matrices such as food[18], feed[19], water[20,21], body fluids[22] and many more. The analytes of interest can be microbes[19,21,23], viruses[23], toxins[24], proteins[25,26], DNA[18,20,21,23,27,28] , pesticides[29], pharmaceuticals[22] etc. The general setup of microarray systems is the same, specific bio(molecular) recognition elements are immobilized on a surface by physical or chemical interaction (Figure 1.A). This immobilization is usually done by microprinting or microdispensing on chemically modifiable materials. This creates a 2D structure which can be read out by imaging for the data analysis (Figure 1. C+D). The research question that is always aimed to be answered with these methods, is how much of a set of analytes is present in the sample.

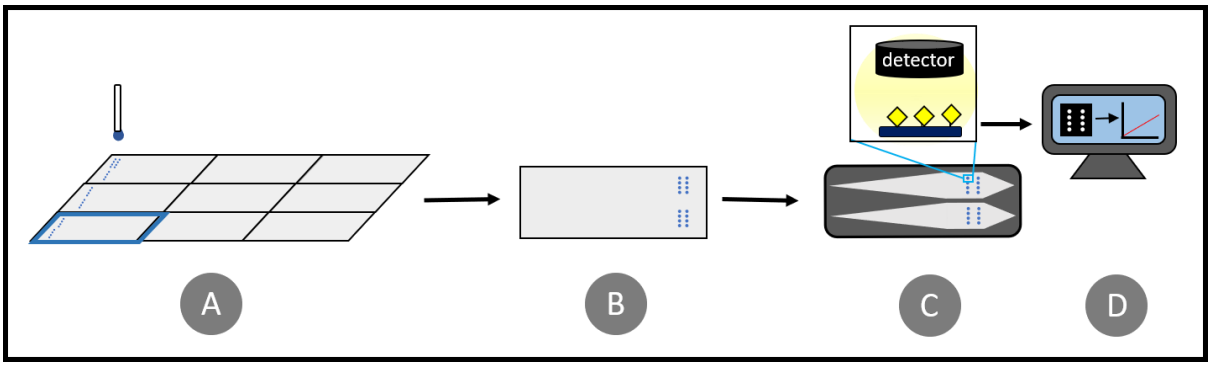

Figure 1: Schematic overview over analytical microarrays. (Bio)molecules are immobilized on a surface via printing or dispensing **A**. The resulting analytical surface **B** is then used for a microarray immunoassay (MIA) or DNA-based assay (hybridization or NAT) and the label of choice is captured by the detector **C**. The data from the detector can then be analyzed and for example converted into a calibration curve **D**.

Thereby the exact quantity of analyte can be determined. In general, the detection of small organic molecules, proteins, cells and viruses can be done using microarray immunoassays (MIAs),[30,31] whereas the analysis of genetic material can be done by hybridization assays[32] or nucleic acid amplification tests (NATs).[31,33] When the two principles are combined, they can be referred to as NAMA (nucleic acid amplification and microarray analysis).[31] For MIAs, either antibodies or other proteins which can bind the analyte or the analyte itself are immobilized. Upon addition of the analyte, it can either directly bind to the compound on the surface or compete for an antibody or other detecting molecule with the analyte on the surface. The detection then happens with a detection antibody or other detecting molecule.[34] Aside from antibodies, affimers have gained popularity in recent years and are often times performing similarly well to antibodies.[35] Detection antibodies or other compounds are often labelled with (bio)molecules which enable some kind of visual readout. In the case of DNA hybridization assays, oligonucleotides complementary to the sequence of interest are immobilized on the surface, the labelled DNA of the sample then hybridises according to sequence homology. The bound oligonucleotides can then be read out spatially.[36] When it comes to NAMAs, genomic sequences of interest are either amplified before microarray analysis or on the surface itself. Readout mostly occurs by a labelled oligonucleotide which was incorporated into the sequence on the surface by amplification.[23,37] The major point in

which microarray systems can be differentiated is their readout system. Since the beginning of microarray visualization, fluorescence has been one of the preferred optical detections. It is a very sensitive, fast, nontoxic, nondestructive, and cheap method. On the other hand, analytes need to be labeled, which is an additional preparation step and can interfere with binding on the surface.[38] In general, analytes or detecting agents are labeled or tagged with a luminophore which can then in turn be excited by a laser and its emission be detected.[34] As there is a high variety of different luminophores with different excitation and emission spectra, multiplexing is possible. Many different luminophores are used for fluorescence microarrays. Organic fluorophores, such as cyanines[39], or fluorescein derivates also known as Alexa dies are most commonly used.[40] Nanoparticles such as quantum dots or organic polymer nanoparticles and fluorescent proteins are other, less often, used alternatives.[38] Label-free surface plasmon resonance imaging or total internal reflection fluorescence assays have also been used for analytical microarray detection.[34] Detecting devices for fluorescence applications are rather complex as they require an excitation source and two monochromators.[41] Label-free methods also exist and their name describes them fully: They require no label for detection of analytes. Some of the methods counting to this category are surface plasmon resonance imaging, atomic force microscopy, electrochemical impedance spectroscopy and MS.[42] Especially electrochemical multianalyte biosensors are gaining popularity in recent years.[43] Via chemiluminescence is another way to evaluate analytical microarrays. Here, a chemical reaction or an enzymatic reaction results in emission of light through energy release. It has a number of advantages like superior sensitivity, speed, safety and a controllable emission rate depending on the amount of excited species which either deactivate to ground state or transfer energy on a luminophore.[44] Chemiluminescence images can be recorded using photomultiplier arrays or highly sensitive CCD cameras.[45] The amount of emitted light is directly proportional to the concentration of a limiting reactant. On microarrays, the emission of light is focused on the spots on the surface thereby spatially confining the signal.[46] Enzymes which can be used as labels for this purpose are alkaline phosphatases, luciferase, microperoxidases, β-galactosidase or horseradish peroxidase (HRP). The excitation is caused by a chemical reaction which requires the oxidation of an organic

compound like luminol, isoluminol, acridinium ester or luciferin by oxidants such as hydrogen peroxide, hypochlorite or oxygen in presence of one of the mentioned enzymes.[47] For the implementation of analytical microarray assays, platforms are needed. These can be automated or non-automated. Automated microarray analysis platforms make the process more user friendly and independent from a laboratory.[31] In the following, the microarray platform which was used in this work will be introduced together with its detection system and applications.

1.1.1. The MCR 3 and its applications

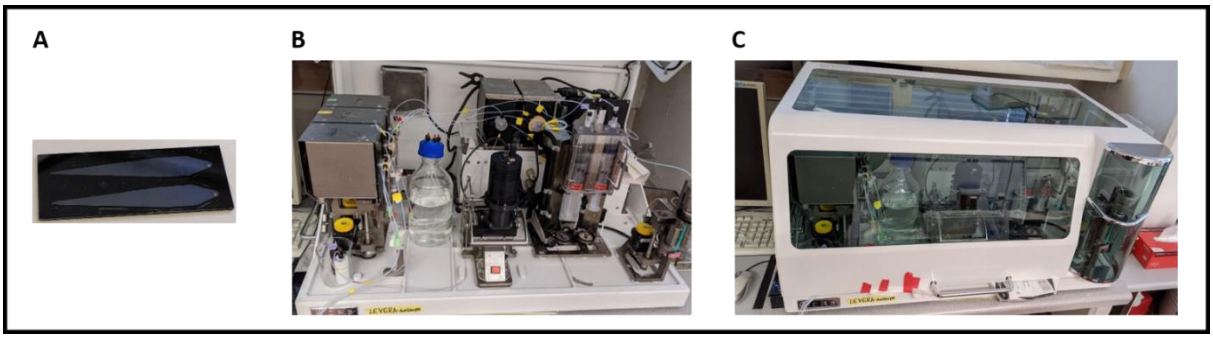

Figure 2: The MCR 3. A shows a chip used for analysis in the MCR 3, **B** shows the open device with pumps, valves, syringes, chip-loading unit and CCD camera and **C** shows the closed device.

The MCR 3 (microarray chip reader, third generation) is a fully automated microarray reader, which was developed by the (IWC-TUM) in collaboration with GWK Präzisionstechnik (Munich). It was designed for flow-injection-based, multianalyte, regenerable, indirect competitive immunoassays with chemiluminescence detection. It contains pumps and valves for automated washing procedures, sample injection, antibody binding and detection The syringes connected to the pumps hold enough volume for the reagents of an entire workday. This way, the MCR 3 presents a portable platform for microarray-based analysis.[31,48] This is placed in the chip-reading unit of the MCR 3 before measurement. On top of the chip-loading unit there is a CCD camera, which records chemiluminescence. The MCR 3 contains a computer and only needs to be connected to a monitor. Chemiluminescence images are

converted to .txt. file by a software from GWK Präzisionstechnik (Munich) and can be evaluated with the latter. Another software, named MCR_Spot_Reader is also available on GitHub. It was developed by Stefan Weißenberger in collaboration with IWC-TUM during this work.[49] For MIA, a new generation of chip readers was developed in the meantime named MCR-R, with a more compact and user-friendly layout. In the following, a short overview over the types of assays which have been performed in the past and were performed during this work on the MCR 3 will be given.

1.1.1.1. Immunoanalytical analysis on the MCR 3 by indirect competitive immunoassay

The MCR 3 is not the first platform which allowed the automation of flow-based chemiluminescence microarray processing.[31] Its predecessors were the parallel affinity sensor array (PASA)[50] and the Immunomat[51]. On the PASA, the principle of regenerable surfaces for chemiluminescence microarray chips was introduced for the first time. This instrument contained a fluidic system with tubing, pumps, and valves and was developed for the detection of small organic molecules by indirect or direct competitive MIAs. On this platform, assays were developed for the detection of triazines, atrazine and trinitrotoluene (TNT) in 29 minutes as well as an assay for the multiplex detection of 24 allergens in less than 1 hour.[31,50] Its successor the Immunomat, was equipped with syringe pumps, a set of tubing, and a chemiluminescence-detection system. On this system, very fast, indirect competitive MIAs became possible. 10 different antibiotics in raw milk were detected in as short as 5 minutes. The disadvantage of this assay was the high cost, as surfaces were not regenerable. Quantification of bacteria in a sandwich MIA was also performed on the Immunomat with an assay time of 3 hours.[31,51] The fluidics of the Immunomat were then adjusted in order to design a platform for hybridization-based oligonucleotide detection assays. The detection of PCR products from the DNA of waterborne pathogens was performed in 7 hours.[31,52] Then, the MCR 3 was developed, as the first chemiluminescence microarray analysis platform which was initially designed for flow-injection-based, regenerable, multianalyte, indirect competitive chemiluminescence immunoassays. The MCR 3 was meant to be a portable stand-alone device which also allowed storage of all reagents which are required for one working day. The first application of the MCR 3 was the detection and quantification of 13 different antibiotics in raw milk by indirect competitive

immunoassay published in 2009 by Kloth et al. Again, a very valuable point of this assay was the regenerability of the chip surfaces.[48] These glass surfaces were coated with diamino-polyethylene glycole (PEG) and subsequently activated with diepoxy-PEG. The antibiotics were then immobilized on the activated surface by microcontact printing. An internal calibration was performed and subsequently samples could be measured on the same chip with a total of at least 50 measurements. Due to this promising study, the MCR 3 was further used for routine screening of antibiotics in raw milk.[53] This type of assay was then performed with many different analytes and matrices. Antibiotic derivatives could also be detected and quantified in honey with some assay adjustments.[54] Other small molecules could be detected and quantified on the MCR 3 as well. Examples are the quantification of Ochratoxin A,[55] Aflatoxins, Deoxynivalenol, Fumonisins,[56] Saxitoxin, Ocadoic acid, Domoic acid,[57] enterotoxin B and ricin.[24] Figure 3 shows an overview over the mechanisms of this assay type (left) and its differences to indirect competitive ELISA (right). The analyte is immobilized on the chip surface through covalent binding, which is the key point for creating a regenerable surface. In ELISA, antigens are mostly immobilized only through adsorption of the antigen directly or the antigen coupled to a protein such as bovine serum albumin (BSA). This makes ELISA plates single-use and expensive. Before contact with the chip surface, the primary antibodies and the sample are mixed and incubated together (Figure 3, left, A). After that, the sample in which the antigens are already bound to a primary antibody, is lead over the chip surface. There, the antigen on the surface competes with the antigen in the sample for primary antibodies (Figure 3, left, B). The more primary antibodies remain bound to the chip surface, the less antigen was in the sample. For detection, a secondary antibody targeting the primary antibody is led over the chip. This detection antibody has a HRP bound to it, which produces the detectable chemiluminescence upon addition of hydrogen peroxide and luminol (Figure 3, left, C). This entire assay from sample injection to chemiluminescence detection on the chip takes nine minutes.[48]

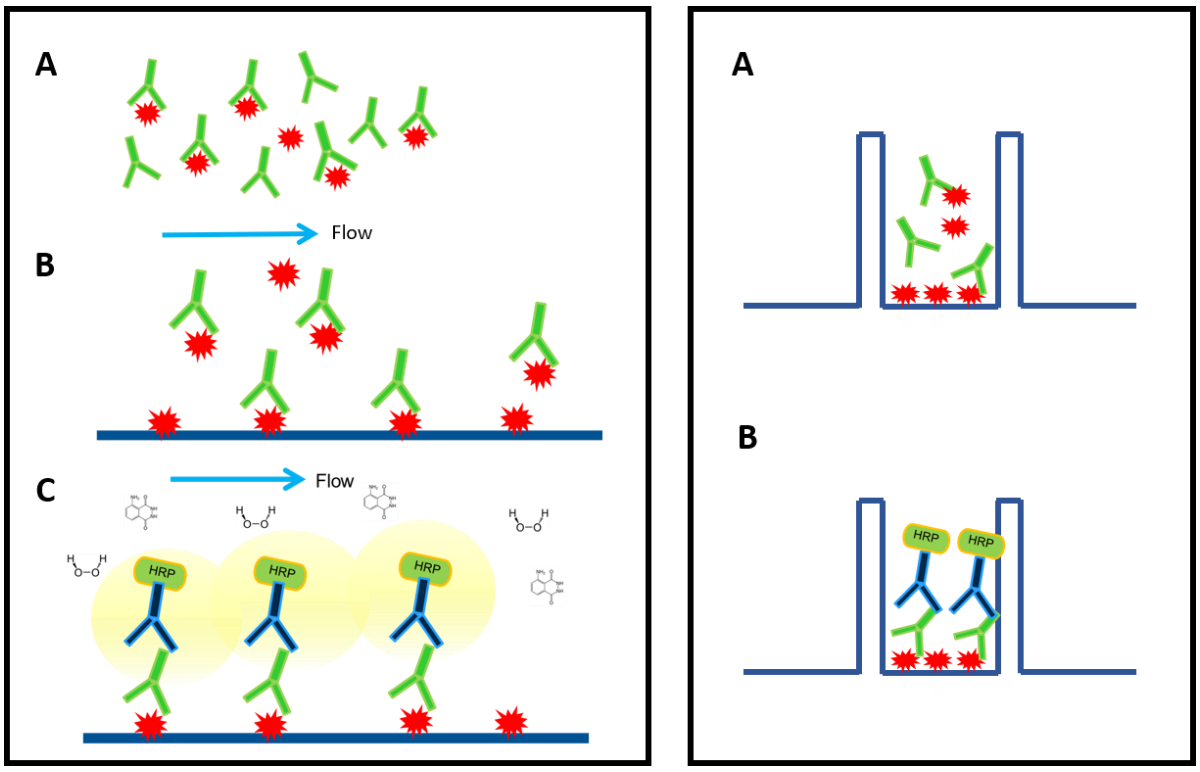

Figure 3: Schematic overview of chemiluminescence-based indirect competitive immunoassays. On the left, the flow-based chip assay performed on the MCR 3. **A** shows the incubation of sample and primary antibodies, **B** shows the competition reaction on the chip surface and **C** the chemiluminescence detection. On the right, the ELISA version of this assay is shown. **A** shows the incubation of sample and primary antibodies in the well, **B** shows secondary antibody binding and chemiluminescence detection.

In ELISA, this type of assay takes a lot longer. As an example, the previously mentioned indirect competitive ELISA detecting diclofenac requires 1 hour and 45 minutes.[58] The main reason for this is that ELISAs are performed in well plates in bigger volumes which is the major difference to flow-based assays as performed on the MCR 3. The incubation of the sample and the primary antibodies for competition with the surface is performed directly in the well for thirty minutes (Figure 3, right, A). After this, the wells are washed and incubated with the detection antibodies, which usually takes one hour. (Figure 3, right, B). After this the detection follows which can be done by chemiluminescence as well (Figure 3, right, B). The incubation steps in ELISA need more time because the distribution of the reagents is solely based on diffusion. While in the flow-based assay, the contact of the liquid phase and the solid phase is ensured by pumping, in ELISA, this only happens through diffusion which can be enhanced

by shaking the plate. Because of this, the concentration of antibodies also has to be a lot higher (10 - 100-fold) in the flow-based assay, as no diffusion or equilibrium formation can occur. This fact can be easily overlooked in light of the advantages of such a short assay time and regenerable surfaces. On top of this, the chip-based assay is multiplex-able whereas in ELISA only one analyte can be analyzed per well. Here, a chip-based indirect competitive immunoassay targeting diclofenac was assessed.

1.1.1.2. Molecular-biological analysis on the MCR 3 by heterogeneous asymmetric recombinase polymerase amplification

The first molecular biological application for the MCR 3 was a hybridization-based assay published in 2009 by Donhauser et. al. Here, biotin-labelled PCR products were detected on a microarray chip by hybridization to oligonucleotides on the surface.[52] This assay did not make the MCR 3 independent of a PCR cycler, therefore another assay was developed which did not require an additional device. Kunze et al. developed the haRPA on the MCR 3 in 2016. The underlying amplification method, RPA is an isothermal method, which does not require a thermal cycling device, instead a steady temperature is sufficient.[23] In their study, DNA from human adenovirus 41, PhiX 174 and the bacterium *Enterococcus faecalis* was detected by amplification on the chip surface. The next haRPA assay was able to detect *Legionella ssp*. and *Legionella pneumophila* with the additional feature of viability determination through propidium monoazide (PMA) treatment of cells before DNA extraction.[21] Another study showed that it is possible to detect CTX-M cluster 1 β-lactamase genes by haRPA and the results were compared with qPCR.[28] All of these haRPA assays were developed on glass surfaces which are rather time and cost intensive in production. This work focused on the transfer of the haRPA reaction to polycarbonate surfaces, which was already shown to work in principle previously but had never been attempted for a full assay.[59]

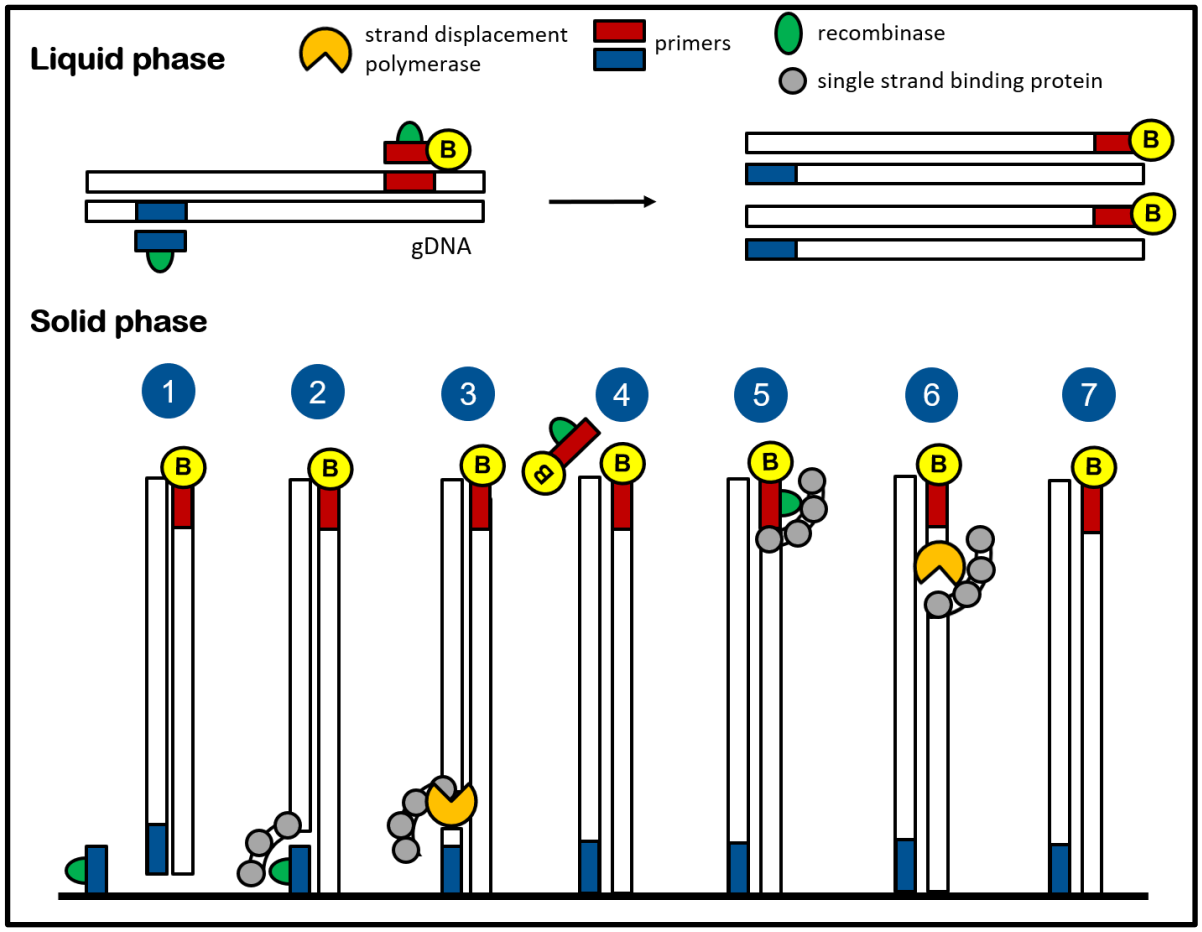

Figure 4: Schematic overview over the haRPA reaction mechanism. The kick-off reaction takes place in the liquid phase, where a small amount of amplicon is generated from genomic DNA (top-left, depicted as a small double strand for simplicity reasons. Here a biotinylated forward primer (red) and a reverse primer (blue) which is only present in very limited amount are used. The resulting amplicons (top-right) then act as template DNA for heterogeneous amplification on the chip surface. There, the amplicon attaches to the immobilized reverse primer (blue) **1** and the recombinase (green) which forms a complex with the primer opens up the double strand which is then stabilized by single strand binding proteins (grey) **2**. A strand displacement polymerase (orange) then prolongs the immobilized reverse primer by amplification **3**. Once this strand is completed **4**, the biotinylated forward primer can bind to its complementary region on this strand and the process starts again for the other strand **5**, **6**. At the end of the reaction time, the immobilized double strands with incorporated biotin which are present on the surface are detected via chemiluminescence **7**.[20]

Figure 4 shows the reaction mechanism of haRPA. Instead of thermal cycling, enzymes have to step in for haRPA. Where a heat denaturation step is performed to separate strands in PCR, the *E. coli* RecA recombinase is used in haRPA (Figure 4, green). Single-strand DNA binding proteins protect resulting single strands (Figure 4, grey) and a DNA polymerase which has

strand-displacement activity (for example Sau polymerase from *Staphylococcus aureus*) performs replication (Figure 4, orange). There are also accessory proteins and cofactors which support the RPA reaction such as T4 UvsY, a recombinase loading factor or polyethylene glycol, as crowding agent. The enzymes are powered by ATP which is generated by a creatine kinase through hydrolyzation of phosphocreatine. In short, the haRPA mechanism is as follows. In the liquid phase, a kickoff reaction takes place to generate more template material for heterogeneous amplification (Figure 4, upper part). The amplification transfers to the chip surface once the unlabeled homogeneous primer, which is only present in very low amount, is depleted (Figure 4, upper part, blue primer). On the chip that same primer is present on the surface enabling an amplification there together with the biotinylated primer (Figure 4, red primer). The recombinase is assisted by a loading factor and forms a complex with the primers (Figure 4, green and blue or red). This complex scans the double-stranded DNA (dsDNA) target for homologous sequences and invades the dsDNA when homology is found (Figure 4,1). The resulting single strand is then protected by single strand binding proteins (Figure 4, 2, grey). The recombinase disassembles from the complex upon ATP hydrolyzation, allowing the strand displacement polymerase to bind and start replication (Figure 4, 3, orange). This process is then repeated from the other side, thereby stably incorporating the biotin on the labeled primer (Figure 4, 4-7). Just as in the immunoassays, a streptavidin-labeled HRP will bind to the biotin, producing local chemiluminescence upon addition of hydrogen peroxide and luminol. The RPA-cycle continues until exhaustion of the primers on the surface or exhaustion of the phosphocreatine pool. haRPA is executed at 39 °C and incubated for either 20 or 40 minutes. In this work, haRPA assays were developed for the detection of mycotoxin producers and ARGs and their carrying species.[23,60–62]

1.2. Mold in indoor air

Molds are fungi which grow multicellulary with hyphal structures and which mostly belong to the divisions of Zygomycota and Ascomycota. They reproduce by the development of asexual spores at the tips of their hyphae. These spores can germinate in order to form new colonies when provided with the right conditions. Fungal spores are ubiquitously present in the human environment but rarely pathogenic.[63] They have the ability to grow on nearly all materials, natural or synthetic. Especially when there is a certain degree of moisture involved, these organisms can reach a level of growth which is dangerous to human health.[10] Moisture can lead to a degradation of building materials which facilitates the invasion of microorganisms.[64] As modern society spends a lot of time indoors (65% of the time in Germany)[65] elevated levels of mold growth in indoor environments can affect occupational and residential health. It has been reported that residents of mouldy or damp buildings have a higher risk of developing respiratory symptoms or infections.[64] The number of health effects fungi can cause on humans is vast. From mild symptoms such as respiratory tract irritations to allergies and asthma[63], intoxications[66], infections or even cancer[67]. An analysis of a number of published research studies estimated the percentages of increase of health damage risk for people living in dampness and mold affected houses resulting in 50% for current asthma, 33% for ever-diagnosed asthma, 30% for asthma development, 50% for cough, 44% for wheeze and 52% for upper respiratory tract symptoms.[68] Most healthy individuals are less likely to suffer from these effects, but preconditions which weaken the immune system can severely increase the chances of suffering from mold-related health problems.[69,70] The concentration of fungi in the air varies a lot depending on the circumstances. While in winter outdoor air harbours around 100 colony forming units (CFU)/m³, in summer there are as many as 10,000 CFU/m³ present.[64,71] The concentration of fungi in indoor air always has to be set into relation to the respective outdoor air contamination. A room is considered contaminated once it contains 1,000 to 10,000 CFU/m³.[72] Here, the concentration changes in the opposite direction, in winter the colony count is a lot higher than in summer. This originates from heating and ventilation behavior of residents as well as from humidity in heated rooms. Aside from these

commonly known residential problems, lesser-known high risk workplaces exist as well. People employed in industries such as composting, tobacco, agriculture, paper, wood or cork often suffer from allergies or toxic symptoms.[73] In paper sorting facilities the spore count was measured to be as high as $1{,}8 \times 10^6$ CFU/m³ to which workers were exposed all day long.[74] Diseases such as exogenous allergic alveolitis almost exclusively occur when mold contaminations are above 10^6 spores/m³. This inflammation can lead to serious lung damage even leading to fibrosis.[75] All of these health effects occur due to allergens, volatile organic compounds or fungal particles, but mold also produces other small organic compounds which can have much more severe impacts on human health. Some of these are also known as mycotoxins. They are volatile molecules that fungi produce in order to keep other organisms from invading their living spaces. Deadly for other microbes and plants, these toxins can be very dangerous to humans, too. Their effects can be anywhere from neurotoxic to immunoactive to carcinogenic.[76] Occasions where this danger made its way into society's awareness are mostly related to food poisoning.[77] Although there is no scientific consensus as to how inhalation of indoor mycotoxins can affect human health[78], mycotoxins have been measured in the sera of residentially exposed people[79] and models suggest that especially at agricultural workplaces the exposure can be above the threshold of toxicologic concern (TTC)[80].

1.2.1. Mycotoxins in indoor air

Respiratory tract problematics caused by mold exposure have been investigated a lot, while health effects related to mycotoxin inhalation are not yet thoroughly studied.[81] It is known that the inhalation of spores leads to exposure of certain mycotoxins, and that this can lead to mycotoxicoses but the precise dosages and exposure rates are unknown. Ochratoxin, sterigmatocystin and trichothecenes have reliably been isolated from homes in the US.[82,83] On top of this, there are a number of reported cases in which mycotoxins in work places and homes led to health impacts. In a home in Chicago, trichothecenes have been associated to health impacts of residents.[83] It was shown that farm workers as well as factory employees

who work with animal feed or nuts have an increased risk of cancer which is caused by exposure to airborne aflatoxins.[84] Also, aflatoxin, ochratoxin A and zearalenone were detected in the air in poultry farms[85] and trichothecenes were detected in a ventilation system of an office building[86]. This shows that airborne mycotoxins might be an underestimated risk. If and in what quantity fungi produce mycotoxins depends on the living circumstances such as moisture, temperature, substrate or oxygen availability.[76] As mycotoxin producers do not always produce toxins, the analysis of mycotoxins themselves can be very shortsighted. It is only a snapshot in time. As an example, if mycotoxin analysis is negative in summer, it is not excluded that toxin producers are present and that toxins will be produced in winter when humidity is higher. Therefore, methods are needed which can state whether a detected mold is harmful and a potential toxin producer. In the following, current detection methods will be evaluated with regard to this question.

1.2.2. Detection systems for mold, mycotoxin producers and mycotoxins

Culture-based methods are most commonly used in mold analytics. In fact, these are the methods proposed by the regulatory guidelines in Germany (VDI DIN ISO 16000-16-21).[75] Air samples have to be taken by impaction, filtration or impingement, and then be plated on different types of culture media and incubated for up to ten days for the count of CFU.[75] They are used because they are easy to handle and do not require trained personnel but they do have a number of disadvantages. One of the most pressing issues is the non-cultivability of many molds and the formation of aggregates by multiple spores, falsifying the results.[75,87] On top of this, also dead spores or other fungal particles are not recorded, even though they can be dangerous as allergens or due to bound mycotoxins or other organic compounds.[64] Often, the fungal species determination is more important for human health than the estimation of the total fungal load itself. This point requires a high degree of expertise when using a culture-based method. In conclusion, culture methods for fungi are time intensive and still often result in a large under or misestimation of fungal load.[88] Another rather established and old

method is the counting of spores by microscopy.[89] This method is often combined with analysis by culture.[75,90] As environmental samples are often rather dirty, staining of fungi by fluorescence or other stains like lactophenol cotton blue or trypan blue is often needed to distinguish fungi from dust and other contaminants.[75,88,89] Unfortunately, for this kind of analysis a high degree of expertise is needed as samples are mixed and are dirty. Especially for species identification a lot of experience is required. This method is up to 6-times more accurate than culture methods but very tedious and time intensive.[88] Due to these points, the requirement for new, faster and more accurate methods was and is pressing. Therefore, DNA-based molecular biological methods have gained popularity in the past decades.[22] The advantages of the latter are mainly that it is not of importance whether the cells are viable or cultivable or not, as only their genetic material is analyzed. On top of this, sampling can be longer as no viable organisms are needed and storage by freezing is very convenient. Though being reliable, reproducible and sensitive, there are no standardized protocols for them yet.[75] Amongst molecular biological methods, the quantitative polymerase chain reaction (qPCR) is the most established and most used.[91–94] Often, qPCR is used on genetic material of air and dust samples to identify and quantify the fungal species present. This is mostly done by amplification of species-specific genes.[88,91,92,94] For detection of mycotoxin-producing molds, this method is usable, too, as genes coding for proteins in mycotoxin biosynthesis pathways can be amplified.[85,95,96] Although the result of qPCR methods are copy numbers of genes, they can be correlated to cell numbers by calibrating systems with a known amount of conidia or spores. This way, a communication between culture-based and molecular biological methods can be established. [95,97,98] Whilst nowadays almost all biological laboratories are equipped with qPCR devices and also the use of the latter is straight forward, it remains a laboratory only method. While for culture-based methods only agar plates and temperature incubators are needed, qPCR requires a clean bench and laboratory environment as it is prone to contaminations. While culture-based analysis is feasible also in the field or in low-resource settings, this is not so much possible with qPCR. Therefore, a method which can combine in-field application with molecular analysis is required. Isothermal amplification methods carry this potential. Loop mediated isothermal amplification (LAMP) assays have already been used

for the analysis of mold.[99–101] In principle, LAMP is very well applicable in the field[102] with the disadvantage that it requires a set of 4-6 primers per amplicon and the design of these is rather complicated.[103] RPA is an alternative isothermal method, which requires only two primers per gene which can be similar to or the same as PCR primers.[104] This method has been used for the detection of other fungi so far but not for mold.[105–107] Mycotoxins on the other hand are mostly detected by methods such as ELISA, high performance liquid chromatography (HPLC) or mass spectrometry (MS).[85,108,109] While these methods are well established mostly for food-borne mycotoxin analysis as well as being accurate and reliable, they require expertise and a well-equipped laboratory. Also, mycotoxin production strongly depends on the conditions the producing organism is facing. Circumstances such as water activity, temperature and pH strongly influence toxin production.[110,111] Change of seasons or even just time of the day influences these factors. In conclusion this means that by only detecting mycotoxins, important information might be missed. Even if no measurable toxins are present, toxin producers might still be there and start production of the latter at any moment.

1.3. Antibiotic resistant bacteria in water

One of the major issues resulting from humanity's irresponsible handling of pharmaceuticals is antibiotic resistance. Classified as one of the most important public health problems of the 21st century by the WHO, this issue requires outmost attention.[112] Interestingly enough, this problem was already predicted in 1945 by the father of Penicillin, Alexander Fleming, who said: "The time may come when penicillin can be bought by anyone in the shops. Then there is the danger that the ignorant man may easily underdose himself and by exposing his microbes to non-lethal quantities of the drug make them resistant."[113] The early warning of this problem has not been able to prevent the spread of this often lethal issue. ARBs are now emerging at a high rate and spreading amongst humans, animals, plants and the environment.[114] In the European Union (EU) alone, ARBs are responsible for more than 33,000

deaths per year.[115] With a total number of over 650,000 infections, healthcare costs and productivity losses amount to 1.5 billion EUR a year.[116] Mainly, the overuse and misuse of broad-spectrum antibiotics is responsible for the development of antimicrobial resistances which consequently reduces the effectiveness of existing antibiotics.[117] The two main entry points of ARBs into the environment are wastewater facilities and runoff from feedlots and fields fertilized with manure.[118–120] From there, antibiotic resistances are distributed to groundwater, lakes, rivers and sea water.[118,120] The reason for this is that ARBs develop where antibiotics accumulate. Hospital or municipal sewage but also sewage from antibiotics producing pharmaceutical companies contains antibiotics from human or livestock excretion as well as through incorrect disposal. Consequently, there is a high density and diversity of microorganisms in wastewater treatment facilities coming from human, animal, and environmental origin. A high availability of carbon sources, optimal growth conditions and particles on which to form biofilms favours this special microbiome.[121,122] On top of this, wastewater contains antibiotics, disinfectants and metals all of which can favour a selection pressure for antibiotic resistance.[123] Bringing together this exceptional microbiome, with these peculiar living conditions, wastewater is a potential hot spot for a process called horizontal gene transfer.[123] Horizontal gene transfer is the mechanism by which genes or mobile genetic elements disseminate between compatible bacterial cells and species. Antibiotic resistance genes (ARGs) are typically located on or associated with mobile genetic elements such as plasmids or transposons which are especially suitable for the transfer by conjugation, transformation or transduction.[124] Conjugation is believed to be the predominant way, as it is very efficient and provides protection to the genetic information which is being shared.[125] Horizontal gene transfer in wastewater is especially dangerous as genes can spread from commensal to pathogenic species due to the diverse microbiome.[124] The importance of environmental reservoirs as the origin for this has been acknowledged in recent years by several examples, one being the spread of *bla*$_{\text{CTX-M}}$ genes.

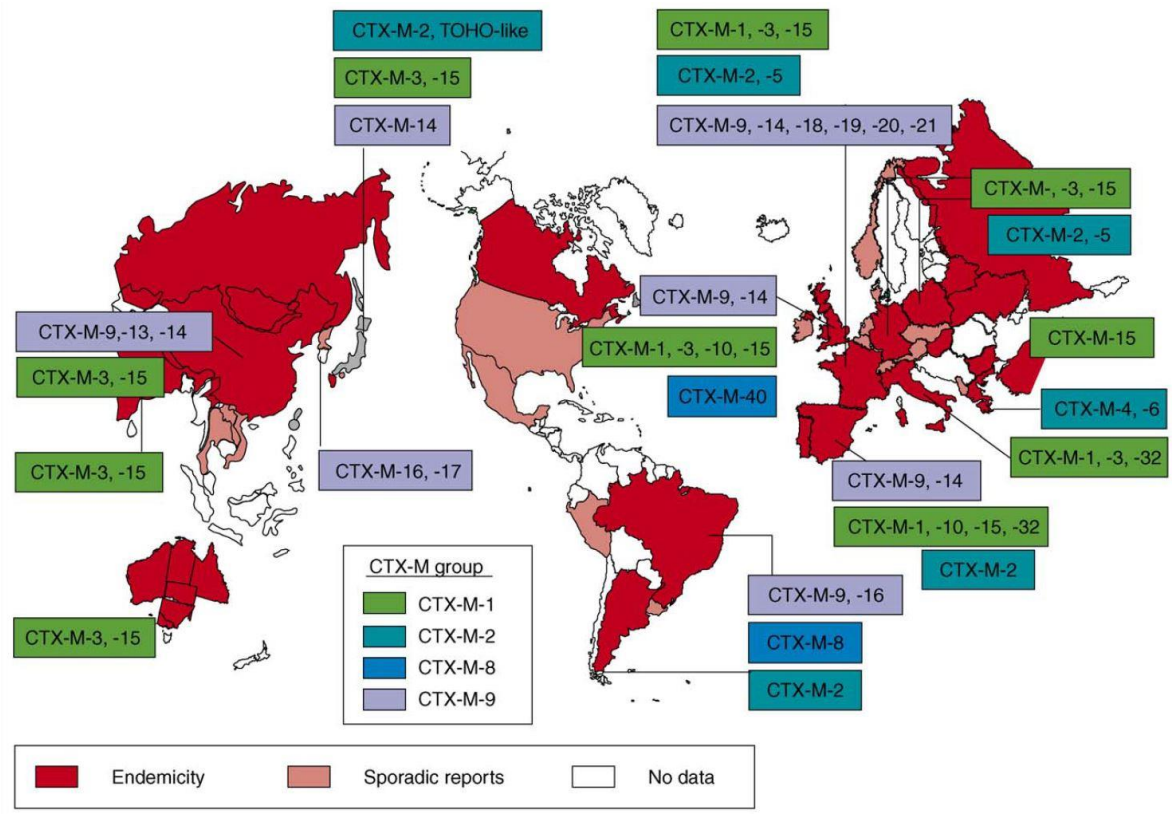

Figure 5.: World-map showing the distribution of CTX-M β-lactamases.[126] The prevalent genes in Germany are CTX-M-3 and CTX-M-15 which belong to cluster 1. Therefore, this work focuses on the detection of *E. coli* carrying the latter. (Reprinted from Current Opinion in Microbiology, Vol. 9/edition 5, Cantón R., Coque T. M., The CTX-M β-lactamase pandemic, Pages 466-475., Copyright 2006, with permission from Elsevier).

These genes now are the main cause for the expression of extended spectrum β-lactamases (ESBLs) in mainly *Enterobacteriaceae* but also other opportunistic pathogens worldwide and they cause large problems at the level of clinical treatment.[124,127] They can ubiquitously be found in samples of humans, animals and the environment. The origin of these genes is suspected to lie on the chromosomal DNA of some environmental species such as *Kluyvera spec.* From there, they were spread to a large number of bacterial species. This was accelerated due to *bla*$_{\text{CTX-M}}$ genes being located on plasmids at some point, which are easy to spread across strains, species and even genera of bacteria. [124,126] When it comes to the variety of ARGs that exist, it is vast. Of course, the more used a class of antibiotics is, the more resistances to it emerge in the environment. β-lactam antibiotics are prevalently used

worldwide.[127] Therefore, this is especially happening with the latter and the β-lactamase genes which infer resistance to the them. Since the 1970s, roughly 900 different unique β-lactamase enzymes have evolved.[128] ESBLs in particular render their hosts resistant to penicillins and third-generation cephalosporins by hydrolyzing their β-lactam ring. The increase in distribution in their most prevalent members, the of *bla*$_{CTX-M}$ genes, is especially relevant in Europe.[129] It has even been shown that CTX-M enzymes have nearly displaced other ESBL enzymes of *Enterobacteriaceae* over the last 10 years. Some examples are TEM and SHV type β-lactamases.[127] CTX-M enzymes have a high degree of clinical importance, since they confer resistance against the antibiotics cefotaxime, ceftriaxone and ceftazidime depending on the specific gene.[130] So far, at least 109 CTX-M genes have been identified starting from CTX-M-1 which was found in Munich in 1990.[130,131] Unlike other ESBLs, the CTX-M enzymes are a family of very diverse β-lactamases which most likely originated from punctual mutations and dispersion on mobile genetic elements. They were classified in seven different clusters.[127] The most common variants of these genes worldwide are CTX-M-15 and CTX-M-14 followed by CTX-M-2, CTX-M-3 and CTX-M-1.[130] With the exceptions of China, South-East Asia, South-Korea, Japan and Spain, CTX-M-15, belonging to cluster 1, is now prevalent everywhere.[127] In Germany, the most relevant genes are CTX-M-15 and CTX-M-3, both belonging to cluster 1, as can be seen in Figure 5.[126]. Researchers refer to a "CTX-M β-lactamase pandemic" which is clinically very relevant, as the spread of ESBLs leads to more prescription of carbapenem antibiotics. This in turn promotes the development of carbapenemase-producing *Enterobacteriaceae,* which cause potentially untreatable infections. Monitoring the spread of ARGs such as these is therefore crucial.[126,129] In 2017 the WHO classfied *Enterobacteriaceae* carrying ESBLs amongst the most urgent antibiotic resistance (AR) threats for which antibiotics are urgently needed.[11] *Escherichia coli* is the most widespread CTX-M carrying organism, often responsible for problems in clinical settings.[126,129] Because of these points, this work focuses on the monitoring of *E. coli* carrying CTX-M cluster 1 genes.

1.3.1. Detection of ARBs in water

Surface water is the matrix which was targeted in this work. It is one of the main distribution points of ARBs out of their origins into the environment and therefore a critical spot for monitoring. As for most microbiological analyses of environmental settings, culture-based methods are prevalent here, too.[132–134] Depending on the medium which is used for cultivation, these methods can give information about the antibiotic the organism is resistant to the susceptibility and when chromogenic media are used, also the class of bacteria which is being analyzed.[135] For monitoring of environmental samples, this is not ideal. Firstly, no differentiation between intrinsic and acquired resistances is possible. Secondly, the genes which are responsible for the resistance cannot be identified.[134] This is why, environmental monitoring is now making use of more modern, molecular biological methods. Examples for these are the PCR, qPCR as well as hybridization or sequencing based techniques.[120,134,136,137] These methods have the advantage that they can indeed identify the gene which infers resistance as well as the species. Although, they cannot do this at the same time. DNA extracts for these methods are produced from mixed environmental samples, resulting in a mixture of genetic information of different species present in the sample.[136,138] Therefore, these methods can show which resistance genes and which species were present in the mix, but not on which species carried which gene exactly. Unfortunately, this is a very important piece of information. When non-pathogenic bacteria carry resistances, it is far less dangerous than when human pathogenic bacteria do so. On the other hand, the presence of a resistance gene does not imply gene activity or viability of the organism, which therefore cannot be determined by molecular biological methods. With this in mind, the combination of a culture-based method which singles out bacteria and a molecular biological method which can determine the gene and the species would be ideal for monitoring. There already are sophisticated methods using single-cell-fusion-PCR by spatially confining amplification of species-specific genes and genes of interest and then creating a fusion product of the latter. The resultant amplicons are sequenced and analyzed, revealing the population of ARGs and

their carrying species.[139–141] While these methods are very valuable for research, they are too complicated for in-field monitoring. Laboratory or even clean room equipment is needed, DNA extracts have to be very pure and PCR requires instruments which enable temperature cycling. Also, the possibility of sequencing and sequencing data evaluation is required. As alternative also in the field of AR, isothermal methods, especially LAMP, have gained popularity.[102,103,142–144] In this project, RPA, which again provides an easy-to design alternative to LAMP was worked on. With the aim of combining the singling-out effect of culture-based methods and the molecular analysis of bacteria, this work aimed to create an appropriate workflow for this. To be used in accordance with standard environmental sampling methods, RPA was aimed to be starting from single colonies isolated by culture. Colony-based analysis of bacteria is often done by PCR (colony-PCR) as it is very convenient and does not require DNA extraction[145,146] but had never been shown for RPA.

1.4. Veterinary anti-inflammatory drug residues in bovine milk with focus on diclofenac

Anti-inflammatory drugs (corticosteroids and NSAIDs) are often used in dairy farming. They limit losses in milk production by treating diseases associated with pain, muscosceletal disorders, fever, endotoxins, and inflammation.[147] The excessive use of the latter on dairy cows is associated with the appearance of residues in milk.[148] Together with antimicrobial drugs, growth promoters, sedative drugs, anticoccidials and antihelminthics, NSAIDs belong to the main veterinary drugs that potentially contaminate food of animal origin.[149] They act via inhibition of cyclooxygenase (COX) isozymes, which are responsible for the formation of prostaglandins in humans and larger mammals. While COX-1 is involved in processes such as aggregation in blood clotting or the production of gastric acid, COX-2 is increasingly formed in the event of inflammation, pain reactions or tissue damage. Therefore, the pain-relieving and anti-inflammatory effects of NSAIDs derive from the inhibition of COX-2 whereas the inhibition of COX-1 leads to side effects such as stomach problems or blood coagulation.[150,151]

Contamination of food with NSAIDs can have hazardous health effects for humans and other animals. This strongly depends on the pharmacokinetic characteristics of the compounds and physicochemical or biological processes of the ingesting animals. Contamination of food can also act as in indicator for environmental dissemination, where diclofenac can have other types of influences on ecosystems and humans as well. Figure 6 gives an overview over possible distribution processes of diclofenac starting from its manufacturing.

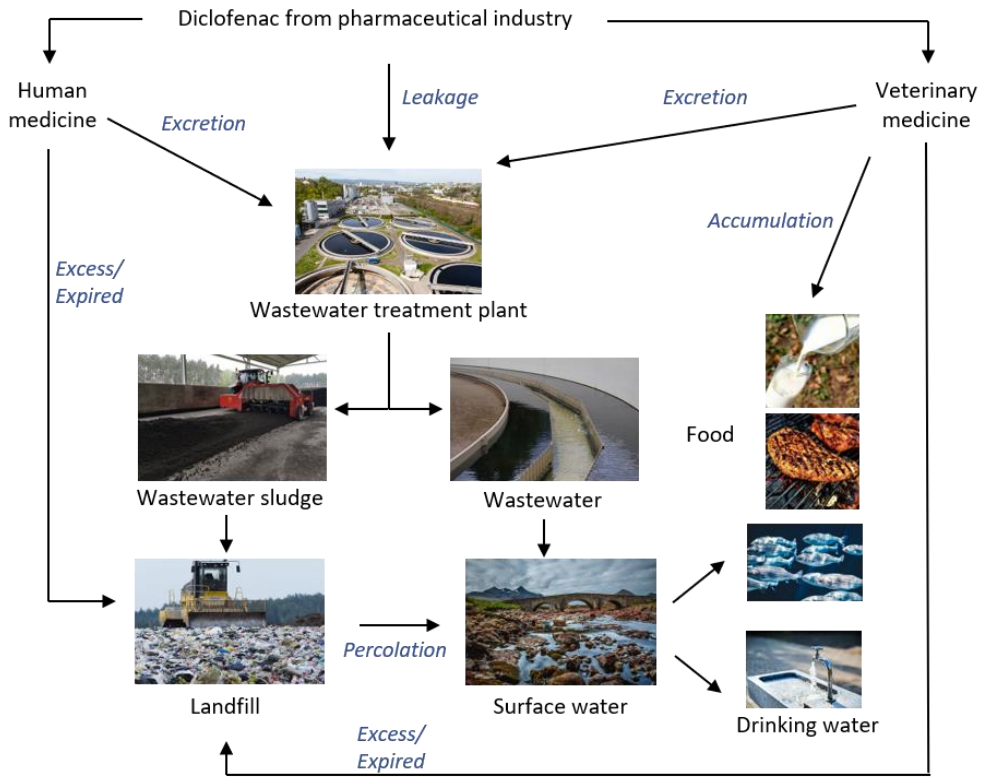

Figure 6: Entry routes of diclofenac into the environment. Veterinary medicine plays an important role, making monitoring of diclofenac in livestock and animal-derived food an important task.[152]

Most residues in food come from inappropriate drug usage or failure in maintaining withdrawal periods.[149] NSAIDs are often used in combination with antibiotics[153] and for the treatment of mastitis which makes them prone for their appearance in milk.[154] Also, they bind to plasma proteins and thereby are distributed through tissues and fluids, which favors an accumulation in milk, too.[155] Therefore, very few NSAIDs are allowed for treatment of dairy

cows. In order to regulate milk contamination with NSAID residues, the EU has established maximum residue values (MRLs). There are MRLs in milk for flunixin (40 µg/kg), meloxicam (15 µg/kg), tolfenamic acid (50 µg/kg), metamizole (50 µg/kg), and diclofenac (0.1 µg/kg).[154] The compound diclofenac became famous in 2006 as it endangered the survival of three species of vultures in South Asia. This was the result of vultures feeding on cattle carcasses with high doses of diclofenac residues in their flesh.[156] Since then, this problem arose also in Africa in 2009 as diclofenac was further promoted on this continent.[157] As an answer to this, many affected regions have banned or heavily regulated the use of diclofenac on livestock.[158,159] Even though a ban has been in discussion also for Europe, the EU only banned the use of diclofenac for milk-producing animals.[160] Some European countries such as Italy or Spain still use diclofenac for livestock treatment, endangering local bird populations.[161] Not only is diclofenac toxic for birds, it has a high ecotoxicity in general with special emphasis on aquatic habitats.[162–164] Therefore, the MRL which was set for milk by the EU rather has the purpose of monitoring diclofenac, as it is also excreted with feces and eventually finds its way into water bodies.[152] As it is also used for treatment in humans, diclofenac residues in food rarely reach toxic levels. Caution with the use of diclofenac is recommended when breastfeeding and during pregnancy.[165,166] Although there is a MRL for diclofenac in bovine milk in the EU and it is banned for the use of dairy-producing animals, several cases of exceeding limits are reported.[167,168] In this work, a chip-based indirect competitive immunoassay was aimed to be optimized in order to achieve a limit of detection (LoD) below the MRL. As shown above, the MRL for diclofenac is particularly low which is challenging for analytical methods.

1.4.1. Analytical methods for the detection of diclofenac in bovine milk with focus on immunoassays

There are many different analytical methods which can be used to detect NSAIDs in bovine milk. The most used ones from literature involve chromatography methods often coupled to MS.[153,154,169] In these methods, the individual compounds contained in a sample are separated

by thin layer, gas or liquid chromatography. Because of their high sensitivity they are quite popular, although they often require special sample pretreatment. On top of this, analyzing multiple compounds at a time, which is required when looking for pharmaceuticals, is rather difficult. Operating these analytical systems requires a high degree of expertise for device maintenance, experimental procedure and especially for data evaluation. These points make chromatography methods less attractive for screening and on-site measurements. Immunoassays present a more user-friendly way of analyzing samples such as drug-contaminated milk. The most prominent one probably is the ELISA [170–172] There are different setups of ELISAs, named sandwich-ELISA and competitive ELISA, direct ELISA and indirect ELISA. Typically, in a sandwich ELISA, antibodies are immobilized on a well surface, capturing the analyte which is then detected by a second antibody. In an indirect competitive ELISA, the antigen is immobilized on the surface and competes with the analyte in the sample for antibodies.[173] If possible, the latter is preferred, as it is more cost efficient by requiring less antibodies. Competitive ELISAs are practicable when the antigen is stable, which is often the case for small molecules such as diclofenac. ELISAs are well established in most biological laboratories and therefore techniques are optimized. They are performed in a 96 or 384 well plate format and can thus handle a high number of samples per run. In routine laboratories, ELISA kit plates are often purchased for reasons of reproducibility and convenience. Usually, ELISA experiments take several hours to produce results, depending on the antibodies and antigens, the setup and the matrix. This method is used so frequently because it is very sensitive, easy to handle and offers high throughput. On the downside, ELISA plates are not reusable, and they are expensive. Also, laboratory equipment is needed to perform the assays. Especially the detection step requires a reading device which can transform colorimetric, chemiluminescence or fluorescence reactions into numbers. This again is no method for on-site analysis of samples. Therefore, many researchers have taken advantage of the ELISA method while transferring it onto more handy platforms. Some examples are dip-stick or lateral flow-based assays[174], chip-based[169,175,176] and lab-on-a-chip ELISAs[177] as well as electrochemical systems[178]. The low MRL for diclofenac is challenging also for sensitive assays such as ELISA. The group of Prof. Dr. Knopp at the Institute of Water Chemistry of the

Technical University of Munich (IWC-TUM) developed an antibody which performed well enough in classical ELISA to detect diclofenac below the MRL in surface water and freshwater.[58] Having found this powerful antibody, a transfer to a chip-based detection system was aimed resulting in a LoD of 34 ng/L in water, which is below the MRL.[179] In this work, a similar assay was reproduced and optimized for the detection of diclofenac in milk.

2. Experimental procedures

2.1. Chip production and spotting

2.1.1. Glass chip production

Glass chip preparation was done in house as described elsewhere[23,180] In short, the procedure consists of hydroxylation and silanization of glass slides after which the resulting epoxide groups react with Jeffamine® ED-2003 which is a polyetheramine. The product is a surface with exposed amino groups which can be further used. The preparation is described in the following. Glass slides were numbered by engraving with a sinograph and subsequently sonicated in a 2% Hellmanex® solution for 30 min for cleaning. After this, the the Hellmanex® solution was renewed and the glass slides were incubated in it overnight. After another sonication of 30 min the glass slides were washed 5 times with a total volume of 1 l of water by shaking. In a next step the glass slides were incubated in a freshly prepared 1:1 mixture of concentrated hydrochloric acid and methanol for 1 h. After washing 5 times with a total volume of 1 l of water, the glass slides were incubated in 97% sulfuric acid for one hour. The sulfuric acid was washed off by rinsing 5 times with a total of 1 l of water. After that, the glass slides were dried with a nitrogen stream and left in an oven at 70 °C for 15 min to dry. For silanization, 600 µl of (3-Glycidyloxypropyl)trimethoxysilane (GOPTS) was pipetted onto the surface of one glass slide and by placing a second glass slide on top of it, a sandwich was formed which was left to incubate for 3 h at room temperature. After separation of the sandwiches, the glass slides were washed in ethanol by hand and by sonication cycles for 15 min in ethanol, methanol and ethanol each. In

the end, the glass slides were dried with a nitrogen stream and placed in an oven for 15 min at 70 °C. They were then stored in an exicator until further use.

2.1.2. Polycarbonate chip production

Polycarbonate chips were produced in-house, as described elsewhere.[59] In short, a transparent, 1 mm thick Makrolon® polycarbonate sheet was precut into two 78 x 228 mm rectangles, each containing nine 26 x 76 mm chips. Around 4 ml of melted, succinylated (for haRPA) or 70% (in water) non-succinylated (for diclofenac) Jeffamine® ED-2003 were coated onto these precut 1 mm thick Makrolon® polycarbonate sheets via screen printing. The sheets were then incubated for 2 h at 100 °C in an oven. After that, they were washed twice for 15 min with ultrapure water in an ultrasonic bath. Finally, they were dried under nitrogen flow and stored at low humidity, in a drying cabinet (below 20%) until further use. A detailed overview of the polycarbonate chip production for haRPA can be seen in Figure 7.

2.1.3. Spotting for haRPA on glass chips

Glass slides were activated and spotted as described elsewhere.[21,23] In short, the used forward primer concentration was 150 µM. As negative control, ultrapure water and as spotting (positive) control, EZ-Link™ amine-PEG2-biotin (1 µg/mL) was used. Each chip contained one row of primer spots, three rows of negative controls and one row of spotting control. Every row contained five spots. For the spotting process, a piezo-spotter (SciFlexArrayer) was used. The drop sizes ranged from 350 – 400 pl. After spotting, the chips were incubated at 60 °C and 55% humidity in an incubator.

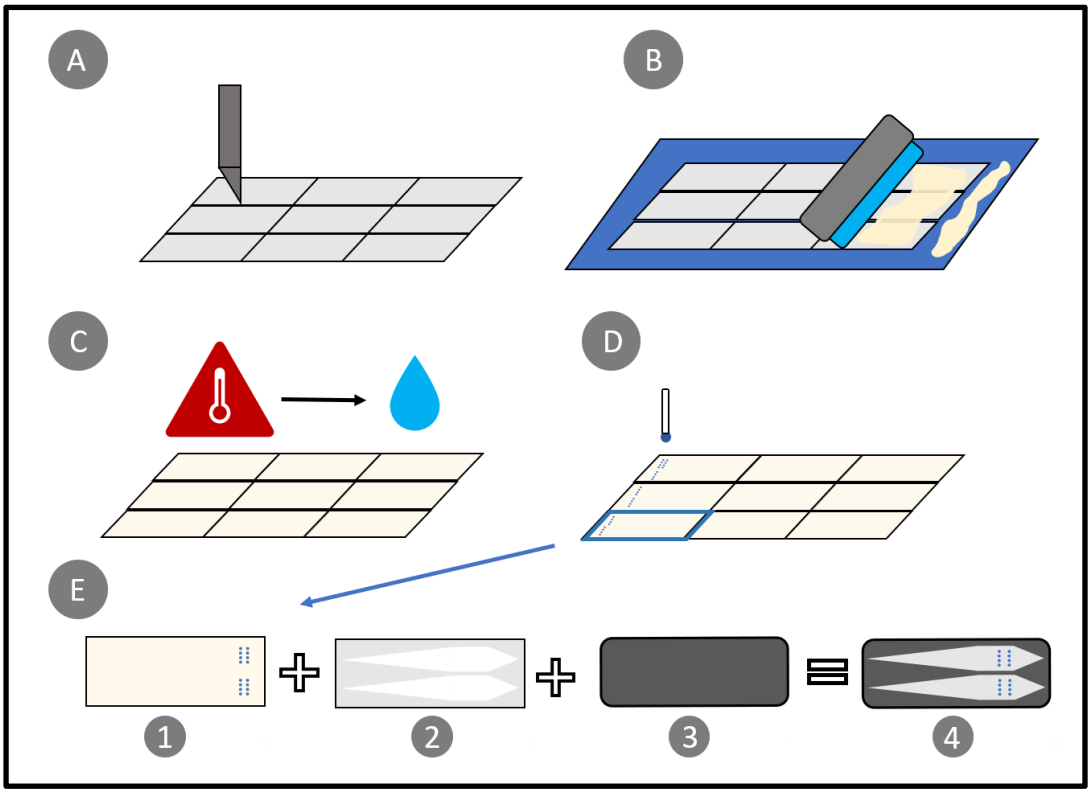

Figure 7: Polycarbonate-chip production workflow for haRPA. The polycarbonate sheet is precut by a cutting plotter to contain 9 chips which therefore can be handled all at the same time **A**. This sheet is coated with a paste of succinylated Jeffamine® ED-2003 by screen printing **B**. The sheet is then washed after 2 h of incubation at 100°C by being placed in water in an ultrasonic bath for 2 times 15 min C. After drying under a nitrogen flow, the spotting is done by contact printing. After that, the sheet is placed in an incubator at 25 °C and 55% humidity overnight **D**. At the end, the chip is assembled to form the flow cells **E**. The polycarbonate sheet is divided into the single chips (**D**, blue box). These will then become the top of the chips **E**.1. A double-sided adhesive tape with pre-cut flow cells acts as the middle layer and therefore connects top and bottom of the chip **E**.2. A black, 1 mm thick PMMA-carrier acts as the bottom part **E**.3. The final assembled chip can be stored at 4 °C until use **E**.4.[27]

2.1.4. Spotting for haRPA on polycarbonate chips

For spotting of the coated polycarbonate sheets, a micro-contact spotter (BioOdyssey Calligrapher® MiniArrayer) was used. For activation, the crosslinking reagents 1-ethyl-3-(-3-dimethylaminopropyl) carbodiimide hydrochloride (EDC) and N-hydroxysulfosuccinimide sodium salt (S-NHS) were used. The reverse or forward primer for immobilization contained a 5'-NH_2-C_{12}-modification. It was mixed with crosslinking reagents just before spotting. The final concentrations were, 75 µM primer, 0.4 mg/ml EDC and 1.1 mg/ml S-NHS in PBS-buffer

(pH 7.4). As a control for successful spotting, 1 µg/ml of EZ-Link™ amine-PEG2-biotin mixed with activation reagents in PBS buffer was spotted. As a negative control, only the activation reagents in PBS buffer were spotted. The reagent mixtures were spotted with a solid pin SNS 9 at 25 °C and humidity of 55%. Chips contained one row of spotting control, one row of primer and three rows of negative controls respectively. Each spotting row held four spots. After spotting, the chips were incubated at the spotting conditions for 16 h. After that, they were assembled to form flow-through chips by gluing the polycarbonate surface to a PMMA carrier containing inlet and outlet holes via a double-sided adhesive tape with two cut out flow cells as can be seen in Figure 7 and were stored at 4 °C until further use[21,23,59] Before measurements, the flow cells were blocked by being filled with a blocking buffer consisting of 10 mg/ml bovine serum albumin and 5 mg/ml casein in PBS buffer and were left to incubate at 4 °C for 6 to 16 h. A detailed overview of the polycarbonate chip production and spotting procedure can be seen in Figure 7.

2.1.5. Spotting of diclofenac on glass chips

The micro-contact spotter BioOdyssey Calligrapher® MiniArrayer was used for spotting here as well. 300 µL of a diclofenac solution containing 0.13 mg/mL diclofenac dissolved in 90% dioxane and 10% PBS buffer were mixed with 100 µl of a solution containing 4 mg/ml EDC and 4 mg/ml S-NHS in PBS buffer. The final diclofenac concentration in this mixture was 0.1 mg/ml. This mixture was incubated for 1 h at room temperature before spotting. The humidity and the temperature in the spotting chamber were adjusted to 25 °C and 55%, respectively. Every spotted row contained five spots. After spotting, the glass chips were left to incubate 25 °C of 55% humidity overnight.

2.1.6. Spotting of diclofenac on polycarbonate chips

For spotting of diclofenac on polycarbonate chips the same protocol as for glass chips was used. The adjustments in spotting buffer composition which were tested can be seen in the results and discussion section.

2.2. MCR 3 measurements

2.2.1. MCR 3 measurement of haRPA

For haRPA the TwistAmp® Basic kit from TwistDx was used according to the manufacturer's instructions with following adjustments. The concentration of biotinylated forward or reverse primer was 454 nM and of the unmodified forward or reverse primer 45 nM. For amplifications starting from DNA extracts, variable target volumes were used. In case of spore lysates, 10 µl were used. In case of colony-fusion-haRPA 15,96 µl were applied. The final volume was always adjusted to 50 µl with sterile water. As reaction starter, 4 µl magnesium acetate (280 mM) were added. In the end, the reaction mixture was injected into one flow cell of the chip and incubated there at 39 °C for 20 (colony-fusion-haRPA) or 40 min (mycotoxin producers). The haRPA reaction mechanism is shown in Figure 4. Every chip contains two flow cells; therefore, two samples were always handled at a time. For detection, the chip was placed into the MCR 3 (GWK Präzisionstechik GmbH) and after flushing of both flow cells, thereby stopping the haRPA reactions, a blank image was taken which was then automatically subtracted from the following measurement. Running buffer consisted of 0.5% casein in 1 x PBS. The readout continued as described elsewhere and in Table 1.[21,23,28] The chemiluminescence images were evaluated with the software MCRImageAnalyzer (GWK Präzisionstechnik GmbH). Background signal was defined as the mean of four dark spots on the left and four dark spots on the right margin of the spotted area. It was subtracted from the chemiluminescence signals of the samples. The final values were calculated as the mean of four spots in one row.

Table 1.: haRPA measurement program of the MCR 3

Step	Volume	Flow rate
Heating of chip loading unit to 37 °C		
Flushing of flow cell with running buffer (3x)	1000 µl	200 µl/s
Loading with Strep-HRP	150 µl	50 µ/s
Strep-HRP injection	600 µl	2.0 µl/s
Flushing of flow cell (3x)	1000 µl	500 µl/s
Injection of H_2O_2 and luminol into the flow cell	200 µl each	20 µl/s
Image acquisition with CCD camera (exposure)		60 s
Flushing of the fluidic system	1500 µl	500 µl/s
Flushing of the flow cell (3x)	1000 µl	68 µl/s

2.2.2. MCR3 measurement of diclofenac

For measurements of diclofenac, spotted and assembled chips were inserted into the chip loading unit and a blank program flushed the flow cell with running buffer and a blank image was taken. This blank image was then automatically subtracted from all subsequent measurements. As this chip chemistry is regenerable, one flow cell was used for multiple measurements. Before sample measurements, two empty measurements were carried out which were not used for data evaluation, but which served to remove all unbound material from the surface. If not mentioned otherwise, every measurement was performed by the MCR 3 as stated in **Table 2**and as described elsewhere.[48] Running buffer consisted of 0.5 % casein in 1 x PBS and primary anti-diclofenac antibody as well as secondary anti-mouse antibody were diluted in the latter. Chemiluminescence images were evaluated with the software MCR_Spot_Reader.

Table 2 : MCR 3 program for measurement of diclofenac with regenerable chip surfaces

Step	Volume	Flow rate
Injection of sample and primary antibody solution (1:1)	1000 µl	10 µl/ s
Flushing of flow cell with running buffer	2000 µl	500 µl/s
Injection of secondary antibody solution	1000 µl	10µl/s
Flushing of flow cell with running buffer	2000 µl	500 µl/s
Injection of luminol and H_2O_2	200 µl each	68 µl/s
Image acquisition with CCD camera (exposure)		60 s
Flushing of flow cell with running buffer	2000 µl	500 µl/s
Flushing of flow cell with regeneration buffer	3000 µl	1000 µl/s
Flushing of flow cell with regeneration buffer	1000 µl	10 µl/s
Flushing of flow cell with running buffer	2000 µl	500 µl/s

2.3. Molecular biology

2.3.1. Primer design for RPA and haRPA

RPA primer design was always performed based on published PCR primers to ensure specificity. To prolong or to shift primer sequences, their respective or homologous genomic regions were retrieved from the National Center of Biotechnology Information (NCBI) database. Alignments and designs were performed with the software CLC Genomics Workbench 20.0.3 by QIAGEN. To maintain specificity even after change of the sequence, the new sets were checked for cross-reactivity using blastn, a tool provided by BLAST® (NCBI).

While doing this, relevant genomes were chosen for cross-reference. Only when both primers did not result in high homology to other genomes, the primer set was used for further testing.

2.3.2. Primer testing in homogeneous RPA

Once candidate primer sets were designed, they were tested in homogeneous RPA. All possible combinations were tested and resulting amplicons were analyzed by agarose gel electrophoresis. The aim was amplification of right-size amplicons with little to no amplification of side products. If a strong smear or many side products were visible on the gel, the primer set was not used further. If clean product bands of the right size were present, the reaction was repeated, and the bands cut out from the gel. The containing DNA was cleaned up using the Monarch® DNA Gel Extraction Kit by New England Biolabs. Sequencing revealed if the correct region had been amplified with the primer set. After this, the sets were checked for specificity using a number of different non-target genomic DNA samples. If no unspecific amplifications occurred, primers were used and further tested with haRPA.

2.3.3. Fusion-haRPA workflow

At first, the single amplicons from the species-specific gene and the resistance gene were formed by homogeneous RPA. To do this, the TwistAmp Basic kit from TwistDx as used according to the manufacturer's instructions except for splitting the reagents of one kit tube into two. Therefore, 29.5 µL rehydration buffer, 8.2 µl sterile water, and 5 µl lysis supernatant were added to the kit tube to dissolve the lyophilized RPA reagents. The mixture was then split equally into two tubes and 1.2 µl of both forward and reverse primers (10 µM) were added. The reactions were started by adding 1.25 µl of magnesium acetate (280 mM) and incubated at 39 °C for 20 minutes. For the following fusion product formation, again only half of the reagents of one RPA reaction tube were needed. 29.5 µl rehydration buffer were added to the lyophilized reagents and the resulting mixture was divided equally into two tubes. Then, the reagents for fusion product formation were added, being 3.3 µl of the species gene RPA reaction mixture and 3.3 µl of the resistance gene RPA reaction mixture as template and 1.2 µl

of forward and reverse primer, respectively. To start the reaction, 1.25 µl of magnesium acetate (280 mM) were added to the mix. After another incubation at 39 °C for 20 minutes, 15.96 µl of this reaction were used as template for the detection haRPA. Here, an entire RPA kit tube was required in order to fill the entire flow cell of the chip, which amounts to 54 µl. The haRPA reaction mixture contained 29.5 µl rehydration buffer, 15.96 µl template, 2.27 µl forward primer (1 µM), 2.27 µl of detection primer (10 µM), 4 µl of magnesium acetate (280 mM) and the lyophilized RPA reagents. The entire reaction volume of 54 µl was injected into one flow cell of the microarray chip and incubated at 39 °C for 20 minutes. The haRPA detection with the MCR 3 is described in 2.2.1.

2.3.4. PCR

PCR and colony-PCR were done with the Phusion® High-Fidelity PCR and the *Taq* PCR kit by New England Biolabs according to the manufacturer's instructions. As it is less expensive, the *Taq* kit was used for screening and the Phusion® polymerase (high fidelity) was used when the amplicon was meant to be sequenced. For colony-PCR, 5 µl of the lysis supernatant was used as template.

2.3.5. Agarose gel analysis

RPA and PCR amplicons were visualized on a 2% agarose gel supplemented with 0.1 µl/ml SERVA DNA Stain Clear G by SERVA Electrophoresis GmbH by excitation on a BlueLight Table by SERVA Electrophoresis GmbH. PCR amplicons were visualized without purification, RPA amplicons were previously purified using the Monarch® DNA Gel Extraction Kit by New England Biolabs according to the manufacturers' instructions.

2.3.6. Sequencing

Sanger sequencing was performed at the sequencing facility of the LMU Biocenter in Martinsried. Sequencing reactions were pipetted according to the facilities' instructions. The

total volume of the reactions was 7 µl, consisting of a variable amount of template, a variable amount of water and 0.5 µl of 10 µM forward or reverse primer. As template, only purified PCR or RPA products were used. Amplicons were purified using the Monarch® DNA Gel Extraction Kit by New England Biolabs according to the manufacturers' instructions.

2.4. Fungal and bacterial culture

2.4.1. Fungal culture

All fungal species used in this work as well as *Bacillus subtilis* were cultivated on malt extract agar (MEA) plates (20 g/L malt extract, 1 g/L peptone, 20 g/L glucose, 15 g/L agar). Plates were inoculated with hyphal fragments from mother plates or glycerol stocks in the middle of the plate and left to grow for up to four weeks at 25 °C. To obtain fungal DNA, liquid cultures were used. Therefore, 10 ml liquid malt extract medium (20 g/l malt extract, 1 g/l peptone, 20 g/l glucose) was inoculated with hyphal fragments from grown MEA plates and left to grow for 1-2 days (25 °C, 150 rpm).

2.4.2. *Fusarium culmorum* spore extract generation and enumeration

Fungal cultures from six sporulated MEA plates (incubation at 25 °C for 2 weeks) were needed. First, a 20 ml syringe was filled with a 3 cm thick layer of compressed sterile rock wool which was then cleaned with 10 ml sterile water for removal of dust and smaller rock wool fragments. Approximately 5 ml sterile water with 0.05% Tween-20 were pipetted onto each MEA plate and the fungal biomass scratched off with a sterile glass slide while mixing with the water. The suspensions of all six MEA plates were pipetted onto the rock wool in the syringe and pressed through it while the flow through was collected. After that, the rock wool was rinsed with 20 ml sterile water with 0.05% Tween-20 to extract remaining spores and the flow through was collected as well. The resulting spore suspension of approximately 50 ml was then pelleted (5,000 rpm, 20 min) and resuspended in 1 ml sterile water. For

quantification of the spore extract, counting under the microscope (20 × magnification) was done. After that, the spore suspension was pelleted (5 min, 10,000 rpm) and resuspended in 200 µl sterile water.

2.4.3. Bacterial culture

Bacterial culture was always handled under sterile conditions. Liquid bacterial culture was inoculated using one cryo bead from a cryo stock or using cells from a mother plate. 15 ml of LB medium alone or supplemented with 1 mg/ml cefotaxime was used for bacterial growth. For cultivation on plates, solid LB media with or without cefotaxime was used. In case of inoculation from liquid cultures, 20 µl of 1:10,000 and 1:100,000 dilutions were spread on LB plates. In case of reculturing from a mother plate, cells from the original plate were streaked out on the new plate with a sterile pipet tip. In case of culturing river samples, 50 ml of the collected water was spun at 13,000 rpm for 10 min. The resulting pellets were each resuspended in 100 µl sterile water and streaked out on LB plates. Plates were always left to grow at 37 °C for 16 h.

2.5. DNA extraction and lysis

2.5.1. DNA extraction from Fungi

For extraction of fungal DNA, liquid cultures were used. Therefore, 10 ml liquid malt extract medium was inoculated with hyphal fragments from mother plates and left to grow for 1-2 days (25 °C, 150 rpm). The grown fungal cultures were then pelleted (15 min, 3500 rpm) and resuspended in 200 µl sterile water. The concentrated suspensions were transferred into lysis tubes E (MP Biomedicals GmbH) and lysed by bead beating (3 × 40 s, 6 m/s) in a FastPrep-24™ 5G instrument from MP Biomedicals GmBH. In between cycles, tubes were cooled on ice for 1 minute. For further extraction, the InnuSpeed Bacteria/Fungi DNA kit from Analytik Jena AG was used according to instructions with some modifications. 4 µl RNAse A (100 mg/ml)

was added to the lysis solution. After incubation the lysate was spun down (4500 rpm, 2 minutes) to pellet cell debris before loading the supernatant onto the column matrix. For elution, 30 µl sterile water were used. DNA was then quantified by UV/VIS spectrometry with the NanoPhotometer® from IMPLEN GmBH.

2.5.2. DNA extraction from bacteria

For the cultivation of bacteria, one bead from a cryo stock was added to 15 ml LB liquid medium under sterile conditions. The culture was incubated overnight at 37 °C. 3 mL of the overnight culture were used for DNA extraction with the QIAamp DNA Mini Kit from QIAGEN following the instruction manual. The resulting DNA samples were stored at -20 °C.

2.5.3. Lysis of fungal spores

Spore extracts (200 µl) were lysed by bead beating (3 × 40 s, 6 m/s) in a FastPrep-24™ 5G instrument (MP Biomedicals). In between cycles, tubes were cooled on ice for 1 minute. After this, 25 µl of proteinase K (20 mg/ml) and 4 µl RNAse A (100 mg/ml) were added. Then, incubation steps followed (5 min, RT; 10 min, 40 °C; 10 min, 95 °C) before the samples were spun again to pellet cell debris (4500 rpm, 2 minutes). The supernatants were carefully taken off and transferred into clean tubes. These lysates were then used as template for haRPA.

2.5.4. Single-colony lysis of bacteria

Colonies (radius ~1 mm) where picked off their plates with pipet tips and were then transferred into microcentrifuge tubes containing 15 µl lysis buffer (TE-buffer (Invitrogen AG) with 0,1% Triton X-100). The pipet tips with the colonies were left soaking in the TE-buffer for 3 min before shaking and pipetting up and down to resuspend the colonies in the buffer. The tubes were boiled (100 °C, 10 min, 300 rpm) in a ThermoMixer® (Eppendorf AG). Afterwards, cells were spun down (13,000 rpm,10 min, 20 °C). 5 µl of the supernatant were used as template in haRPA, RPA or PCR experiments.

3. Results and discussion

3.1. Development of a chip-based detection system for mycotoxin producers using haRPA

3.1.1. Aim of this project

Reliable quantification of mold for monitoring purposes is a difficult task. This project aimed to develop a method for the quantification of mycotoxin producers based on haRPA. To be as close to environmental samples as possible, spores were meant to be used for calibration. Molecular biological methods are more reliable than culture-based ones, but they require more steps which are cost and time intensive. One of them is DNA extraction, which is especially difficult for fungal spores. Here, an alternative protocol, namely mechanical and enzymatical lysis was meant to be used instead of classical kit-based purification. This would reduce the time and cost of the method. On top of this, as haRPA was previously only performed on glass chips[21,23] and the production of the latter is long and expensive, this assay was intended to be transferred onto polycarbonate surfaces. By doing this, both the production time and cost would be reduced substantially. As a proof-of-principle, the development of this assay was to be performed targeting zearalenone producers. Zearalenone is a mycotoxin often found in indoor air environments and produced mainly by members of the genus *Fusaria*.[85,138,181] Here, *F. culmorum* was used as model organism for method development. The multiplex-ability of chip systems is what makes them very valuable for monitoring purposes. In the future, this project aims to develop a chip for the detection of multiple mycotoxin producers at the same time. Therefore, a second primer set targeting trichothecene producers was to be preliminarily tested as well.

3.1.2. Development and testing of RPA primers targeting zearalenone producers

Most published molecular biological assays targeting mycotoxin producers are PCR or qPCR assays. Therefore, respective genomic regions of interest are well chosen for uniqueness and primer sets are well tested for specificity.[92,182,183] As RPA has different requirements for primer sets[104] in comparison to PCR, the sets can seldomly be used as they are. The design of the primer set for this study was based on Meng et al.[184] who used it to detect zearalenone producing *Fusaria* by qPCR. The gene of interest was the polyketide synthase 4 (*PKS4*), a conserved zearalenone biosynthesis gene. Based on the primers of Meng et al.[184] 3 forward and 3 reverse primers were designed and tested in all possible combinations. The design was performed using the full genomic sequence of the *PKS* gene cluster of *Fusarium graminearum* (GenBank number: DQ019316) which was retrieved from the NCBI gene database. This was done, as there is no full sequence of the *PKS4* gene available for *F. culmorum*. From the tested primer combinations, one resulted to be functional in homogeneous RPA. Sequencing of the amplicon revealed that this set was indeed also functional on *F. culmorum* as the result showed a high homology to the *PKS4* region of other *Fusaria* which can be seen in Figure 8. Also, it could be located 7786 base pairs away from an annotated partial mRNA sequence of *F. culmorum PKS4* (GenBank number:EU362992.1). This primer set was then further tested for suitability in haRPA. The sequences can be seen in Table 3, the forward primer (ZEA F) was prolonged to 34 base pairs and the reverse primer (ZEA R) to 30 base pairs. The 5’ ends of both primers contain a cytosine which has been reported to be beneficial for RPA.[104]

Table 3.: RPA primers targeting zearalenone producers and the sequencing primers used to verify correct amplification.

Name	Target gene	Purpose	Primer sequence	Modification for haRPA	Amplicon length
ZEA F	*PKS4*	RPA + haRPA	CTTCGTGATGTCGTCTTCGAGAAGATGACATATG	5‘ - Biotin	268 bp
ZEA R	*PKS4*	RPA + haRPA	CTGCAAGCACTCCGACATCACGCATGATGC	5‘ – NH_2-C_{12}	
ZEA Seq F	*PKS4*	Sequencing	CTTCGTGATGTCGTCTTC G		268 bp
ZEA Seq R	*PKS4*	Sequencing	CTGCAAGCACTCCGACA		

Figure 8: Alignments of the sequencing results of the RPA amplicons generated with the primers ZEA F and ZEA R on different *Fusarium* species. R is the reference sequence, being the *F. graminearum* sequence retrieved from NCBI. **1** is *Fusarium oxysprorum*, **2** is *Fusarium verticilloides*, **3** is *F. culmorum*. Senger sequencing was performed on the gel extracted DNA. Sequencing was performed with the primers ZEA Seq F and ZEA Seq R shown in Table 3. The resulting forward and reverse sequencing data was combined and aligned to the reference sequence **R**. Red color represents gaps or mismatches. The aligments were performed with the CLC Genomics Workbench 20.0.3 by QIAGEN .

As haRPA had previously only been performed on glass chip surfaces, the first experiments for testing were performed on the latter as well. For specificity testing of the ZEA primer set, DNA extracts of different species, belonging to different kingdoms were used. For bacteria *Bacillus subtilis*, for plants *Lotus japonicus* and for fungi *F. culmorum*, *Phoma glomerata* and *Epicoccum nigrum* DNA was applied. *F. culmorum* is the only zearalenone producer amongst these species. Figure 9 shows that indeed *F. culmorum* DNA yielded the highest

chemiluminescence signal. The next highest signal was obtained with *E. nigrum* DNA with 26% of the *F. culmorum* signal. As this species does not carry the *PKS4* gene, this signal is rather high. *B. subtilis, L. japonicus* and *P. glomerata* DNA followed with 13%, 8% and 3% of the *F. culmorum* signal, respectively. This experiment confirmed the selectivity of the ZEA primer set in haRPA.

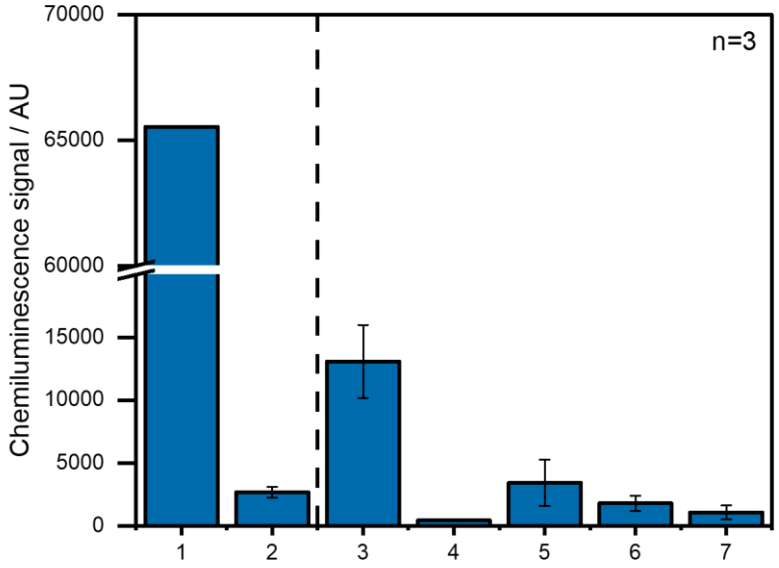

Figure 9: Specificity testing of the *PKS4* primer set on glass surfaces. Chemiluminescence signals from haRPA measurements are depicted in AU. Bars represent the mean values. Lines separate controls from samples. **1** is the spotting control, being immobilized EZ-Link™ amine-PEG_2-biotin, **2** is the negative control, being spotting buffer only, **3** is 50 ng of *F. culmorum* DNA, **4** is 50 ng of *P. glomerata* DNA, **5** is 50 ng of *E. nigrum* DNA, **6** is 50 ng of *B. subtilis* DNA, **7** is 50 ng of *L. japonicus* DNA. n is the number of replicates.[27]

3.1.3. Transfer of the *PKS4* haRPA primer system from glass to polycarbonate surfaces

Production of glass chips is very expensive and takes 5 workdays, of which 2 days for activation and spotting. Bemetz et al.[59] developed a polycarbonate chip surface modification protocol for sandwich immunoassays which could be used for DNA assays too. For this type of chip, only 2 workdays are needed for the preparation, which is a lot cheaper as well. This

protocol had so far only been used for the immobilization of antibodies but was shown to work for DNA in principle, too. In this project, it was adapted further for immobilization of amino-modified primers. In summary, succinylated Jeffamine® ED-2003 was directly melted onto polycarbonate carriers and activation was later performed by addition of the crosslinkers EDC and S-NHS directly to the spotting buffer containing also the amino-modified primer. The NHS-ester can then bind the amino-group of the primer thereby immobilizing it on the surface. A comparison between DNA chip and polycarbonate chip chemistry can be seen in Figure 10. In order to test if polycarbonate surfaces are suitable for haRPA, the concentration dependency of the ZEA primer set was investigated on the latter and specificity was confirmed. This was done by using decreasing quantities of *F. culmorum* DNA and by analyzing the DNA of the previously used fungal species again. Figure 11 shows that in comparison to glass chips, the intensity of the spotting control on polycarbonate chips is 61% lower. This is because it was diluted 100-fold in order to achieve signals below saturation. When the same amount of *F. culmorum* DNA (50 ng) was used, this resulted in a 40% higher signal than on glass chips. The stepwise reduction of the quantity of *F. culmorum* DNA showed an even concentration dependency. The analysis of *E. nigrum* and P. *glomerata* DNA resulted in values even lower than the ones on glass chips, namely in 4.8% and 4.4% of the value for 15 ng *F. culmorum* DNA. This high difference in signal intensities between the zearalenone producer and the non-producing species indicates that the polycarbonate surfaces are more suitable for this assay. A lower level of haRPA background chemiluminescence was observed on polycarbonate surfaces. Also, the negative controls showed a strong decline of 98.2%. A reason for this could be the fact that activation and spotting on polycarbonate surfaces is done simultaneously which might allow for a denser primer immobilization on the spots. This hypothesis is supported by the higher signal of positive samples and lower signal of negative samples and controls in comparison to glass surfaces. Polycarbonate chip surfaces were now shown to be adequate for application of this assay, therefore, further experiments were carried out on the latter.

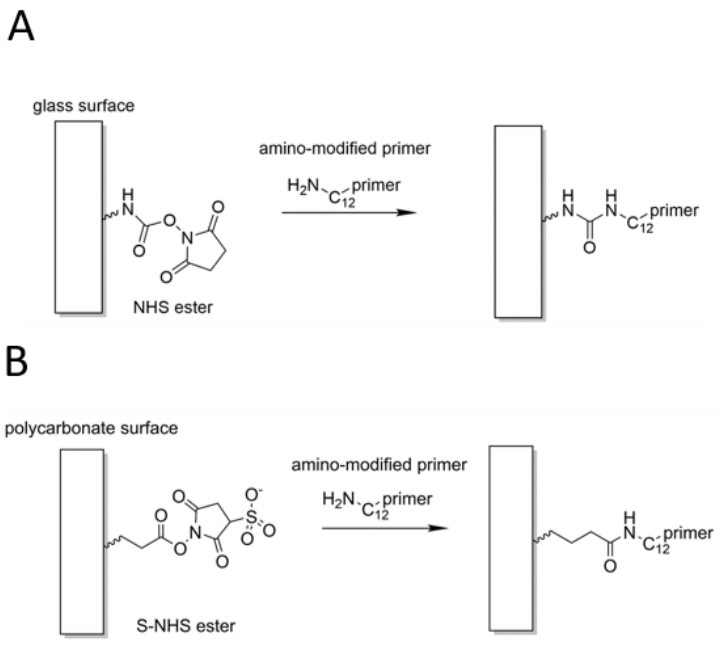

Figure 10: Schematic overview over the glass and polycarbonate chip chemistries used in this project. The glass chip production **A** begins with hydroxylation and silanization of the carrier. The resulting epoxide groups can then react with Jeffamine® ED-2003, a polyetheramine. Activation of the surface with *N,N*-dissucinimidylcarbonate (DSC) which reacts with the amide groups, leads to exposed active ester groups. These ester groups then are able to bind the amino-modified reverse primer in the spotting process**.** This workflow takes 5 days, 2 of which for activation and spotting. Polycarbonate chip production **B** consists of melting succinylated jeffamine onto the carriers. Activation and spotting take place in a single step by adding EDC and S-NHS to the spotting buffer containing also the amino-modified primer. The NHS-ester binds the amino-group of the primer, thereby cross-linking it to the surface. This process only requires 2 working days.

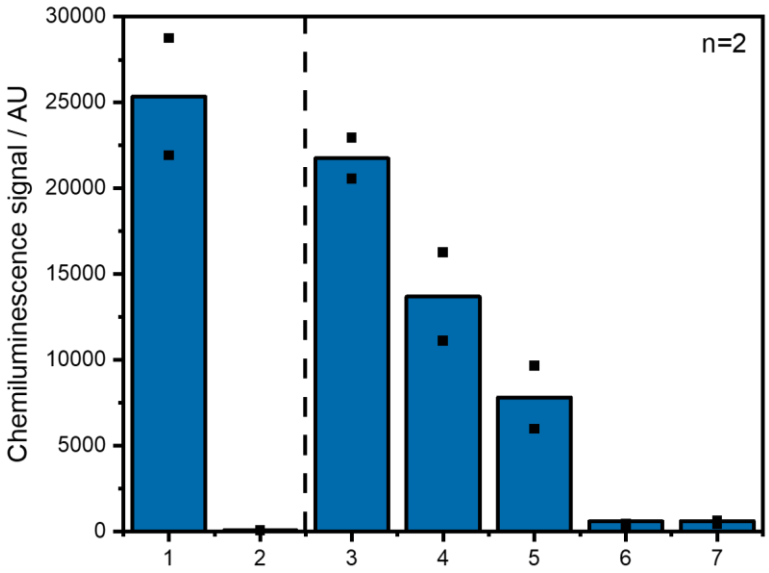

Figure 11: Testing of the ZEA primer set on polycarbonate surfaces. Chemiluminescence signals from haRPA measurements are depicted in AU. Bars represent the mean values, dots the single measurements. Dashed lines separate controls from samples. **1** is the spotting control, being immobilized EZ-Link™ amine-PEG_2-biotin, **2** is the negative control, being spotting buffer only, **3** is 50 ng of *F. culmorum* DNA, **4** is 30 ng of *F. culmorum* DNA, **5** is 15 ng *of F. culmorum* DNA, **6** is 20 ng of *E. nigrum* DNA, **7** is 20 ng of *P. glomerata* DNA. n is the number of replicates. [27]

3.1.4. Development of a protocol for spore extraction and lysis for calibration

In order to develop an effective calibration workflow, samples needed to be as close to real samples as possible. In indoor air, molds pose a danger to human health when their spores are present in high numbers. The inhalation of these spores can lead to health effects such as infections. On top of this, mycotoxins are mostly spore-bound which makes inhalation the most likely route of uptake.[66,185] Therefore, spore extracts were generated as reference for a reliable dose-response curve. The overview over the whole process can be seen in Figure 12. For this, *F. culmorum* hyphae were inoculated on culture plates and incubated for up to 4 weeks until spore formation. The grown fungal biomass was then scraped off the plates and dissolved in water. This suspension was filtered through rock wool for removal of all hyphal fragments and isolation of spores only (Figure 12, 1+2). The resulting spore suspension was

quantified by microscopy using a haemocytometer and stepwise diluted afterwards (Figure 12, 3+4). As DNA extraction from fungal spores is a long and costly process, an alternative was aimed to be found. From other work,[27] it was known that haRPA does not require DNA extracts of high quality. Therefore, the spore dilutions for the dose-response curve were aimed to only be lysed, which saved kit reagents and 2 hours of work in comparison to kit-based DNA purification. For mechanical lysis, a bead beating process was applied to break open the stable cell walls of the spores (Figure 12, 5). For this purpose, ceramic beads, silicon dioxide beads and a mixture of ceramic, silicon dioxide and a glass bead were tested.

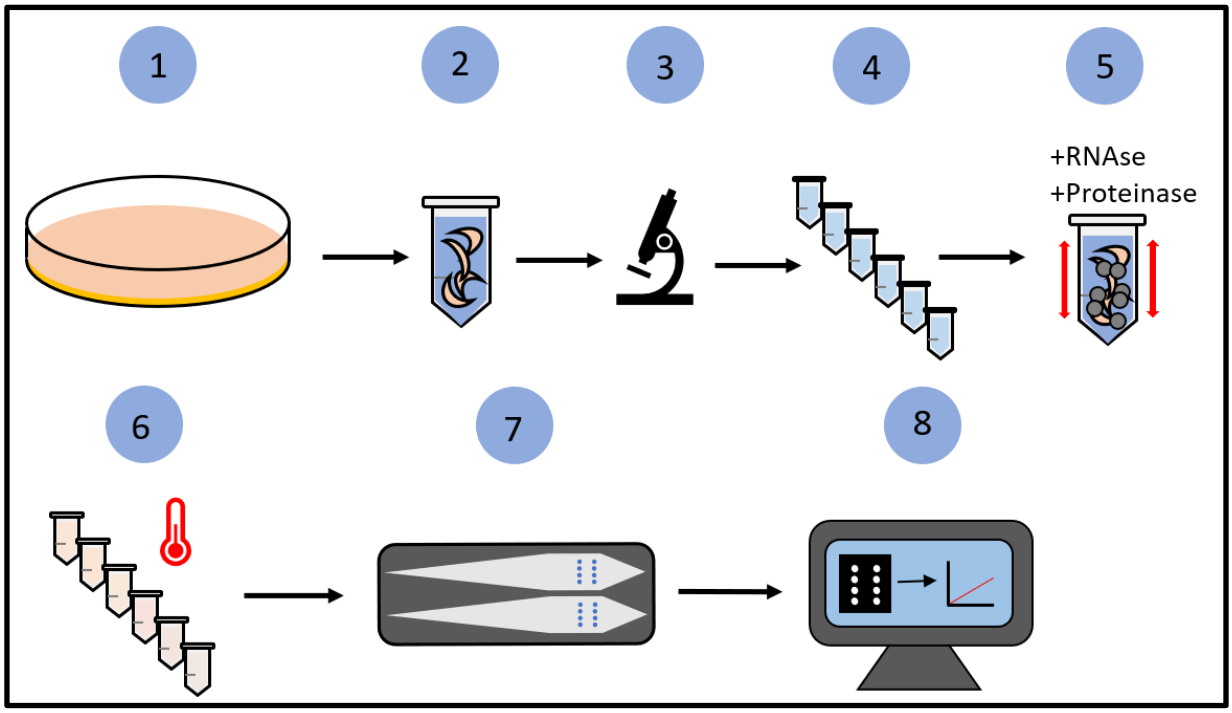

Figure 12: Schematic overview over the calibration workflow. Spore extracts were generated by filtering the whole fungal biomass grown on 5-10 plates through rock wool **1,2**. The resulting spore suspension was quantified by microscopy using a haemocytometer **3**. The quantified spore suspension was adjusted to 10^{10} and diluted downwards **4**. The dilutions were lysed by bead beating with addition of RNAse and Proteinase **5**. The lysates were boiled for 10 minutes for enzyme inactivation **6**. The supernatants were used as templates in haRPA measurements and injected into the chip flow cells for measurements **7**. From the chemiluminescence-signals, the calibration curve was obtained **8**.

The latter performed best and yielded the highest quantities of DNA. More details about this can be read in the Master Thesis of Gerhard Schwaiger, which was part of this work.[186] In order to remove RNA and proteins, RNAse and Proteinase enzymes were added to the lysis buffer (Figure 12, 5). To inactivate these enzymes after incubation, the lysates were boiled (Figure 12, 6). The supernatants of the lysates were then used as templates for haRPA (Figure 12, 6) and the results were used to generate a calibration curve (Figure 12, 7).

3.1.5. Calibration of the *PKS4* primer set targeting zearalenone producers

In order to assess the sensitivity of the assay, a dose-response curve was generated with spore extracts of *F. culmorum* produced as described in Figure 12. The resulting calibration curve is depicted in Figure 13. A sigmoidal correlation between the log of the spore concentrations and the haRPA chemiluminescence signals can be observed. With the help of this curve, the limit of detection of the assay was determined to be at 2.7×10^5 spores/ml. This means that 5.4×10^4 spores have to be present in the 200 µl of spore extract used for the triplicate measurements of each data point. When setting this into relation to the spore load in indoor air of homes it becomes clear that this haRPA assay could be applicable for quantification of spore numbers in the environment but only when above-normal mold contaminations are present. Spore quantities in homes vary a lot between seasons and conditions, they can range anywhere from 40 to 650,000 spores/m^3.[91,187–189] In Germany, guidelines propose that a quantity below 200 colony forming units (CFU) per m^3 air is harmless. Contaminations above 500 CFU/m^3 show a weak infestation and 500-1,000 CFU/m^3 represent a strong infestation. Quantities of 1,000 CFU/m^3 and above are very dangerous and require immediate action.[190] If the haRPA assay was to be used in an average bedroom of 75 m^3, 54 m^3 of air with a concentration of 1,000 spores/m^3 would be needed for a triplicate measurement. The successful generation of a dose-response curve shows the ability of this haRPA assay to generate quantitative results which is valuable for mold analysis.

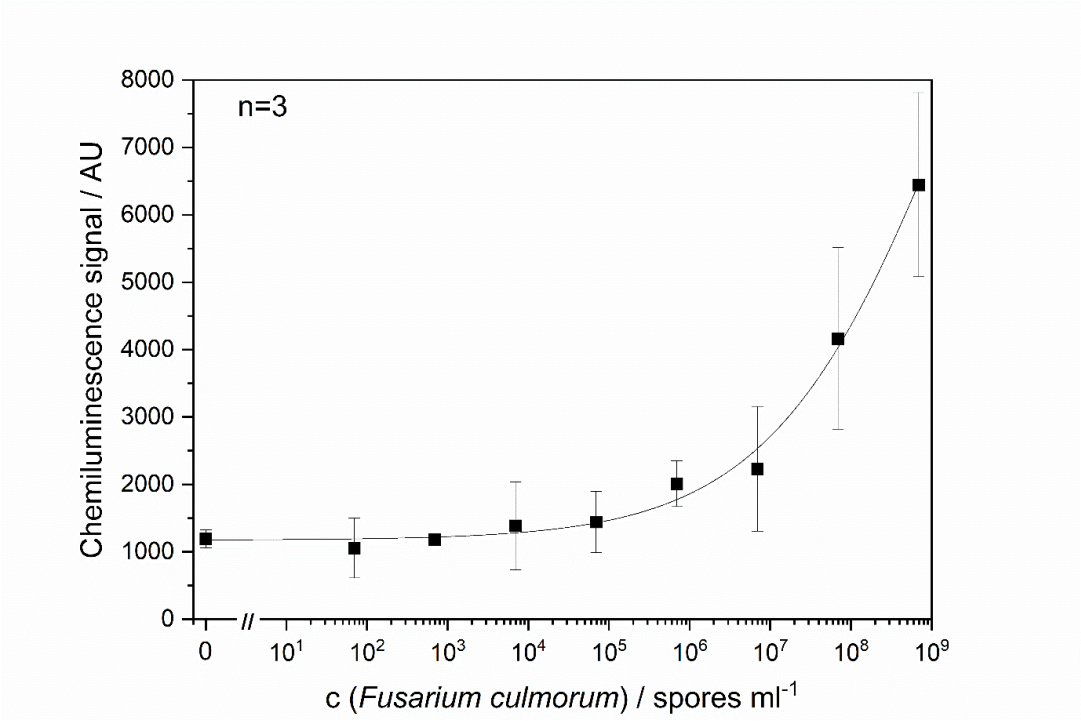

Figure 13: Dose-response curve of the ZEA haRPA assay generated with spore extracts of *F. culmorum*. The chemiluminescence signals from the haRPA measurements are shown in AU. Each black datapoint is the mean value of 3 measurements showing their standard deviation. n is the number of replicates per spore concentration.[27]

3.1.6. Testing of the *PKS4* haRPA primer set on the zearalenone producer *F. oxysporum*

While the calibration curve was generated using spores of *F. culmorum*, it is important that the ZEA primer set is also able to detect other zearalenone producers. Therefore, it was also tested using DNA extract of *F. oxysporum*, another zearalenone producer which is often present in indoor air.[191,192] As can be seen in Figure 14, the ZEA primer set worked for the detection of *F. oxysporum* as well. When the quantity of DNA was reduced from 100 ng to 50 ng the chemiluminescence signal decreased by 48%. These results, together with the sequencing results shown in Figure 8, indicate that the ZEA primer set could indeed be able to detect zearalenone producers in general. What is noteworthy is the difference in signal intensity between 50 ng *F. oxysporum* DNA (Figure 14) and 50 ng *F. culmorum* DNA (Figure

11). The latter is 38% higher, which could indicate that different species behave differently in this system. However, this test was performed using isolated genomic DNA, therefore, calibration experiments using spore extracts would be needed in order to draw reliable conclusions. Spores of different species are also morphologically very different which can impact the lysis efficiency as well as the DNA quantity. If a strong difference in dose-response curves would be the case, the system could be calibrated with the most relevant species for the concerned environmental surroundings.

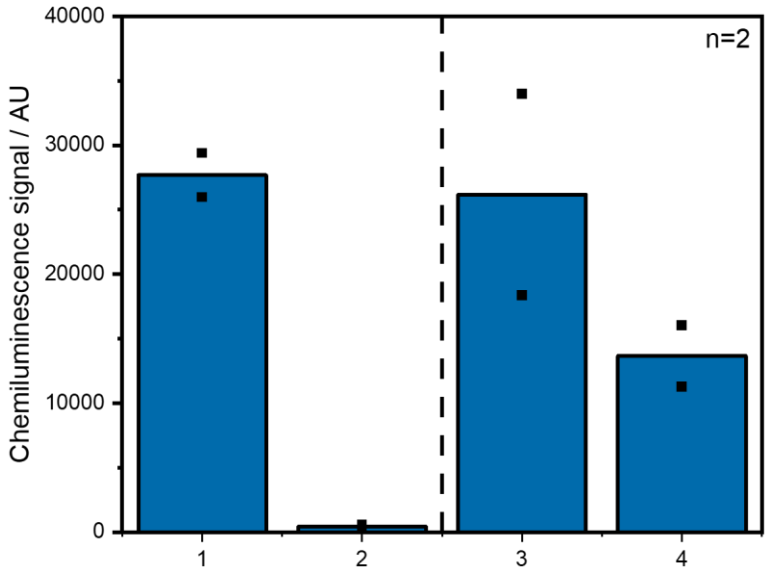

Figure 14: Testing of the ZEA primer set on *F. oxysporum,* a second zearalenone producer. Chemiluminescence signals from haRPA measurements are depicted in AU. Bars show the mean values, dots show the single measurements. The dashed line separates controls from samples. **1** is the spotting control, being immobilized EZ-Link™ amine-PEG_2-biotin, **2** is the negative control, being spotting buffer only, **3** is 100 ng of *F. oxysporum* DNA, **4** is 50 ng of *F. oxysporum* DNA. n is the number of replicates.[27]

3.1.7. Preliminary testing of a haRPA primer set targeting trichothecene producers

The great value of chip systems lies within their multiplex-ability. As the future perspective of this project was the development of a monitoring chip, which could detect multiple mycotoxin producers at the same time, a further primer set targeting trichothecene producers was also worked on. For this purpose, the gene of choice was the trichodiene synthase 5 (*TRI5*) which is conserved in trichothecene producing *Fusaria*. Niessen and Vogel[193] chose this region for PCR-based detection and the tested RPA primers were adapted from their PCR primer sequences. As basis for this, a partial *TRI5* sequence from *F. culmorum* (GenBank: AF480837) and an annotated *TRI5* coding sequence from *Fusarium poae* (GenBank: U15658), which were retrieved from NCBI, were used. As *F. culmorum* is also a trichothecene producer,[194] homogeneous RPA tests were performed using DNA extracts of the latter, just as described for the development of the ZEA primers. This time seven forward and seven reverse primers were tested in all possible combinations. In the final successful set the forward primer was prolonged to 30 base pairs and shifted 16 base pairs in 3' direction in regard to the forward primer used by Niessen and Vogel (TRI F, Table 4) and the reverse primer was a new 30 base pair-long sequence located 16 base pairs in 5' direction compared to the original one (TRI R, Table 4).[193] Figure 15 shows preliminary haRPA measurements using this TRI primer set. For a small specificity analysis, it was tested on *F. culmorum*, a trichothecene producer, *E. nigrum*, a non-producing fungus, *B. subtilis*, a bacterium and *L. japonicus*, a plant. The *F. culmorum* signal resulted to be 92% higher than the highest signal of the other samples. This indicates that the *TRI5* primer set could potentially be a good candidate for future multiplexing experiments.

Table 4.: Primers used for testing the amplification of the *TRI5* gene in trichothecene producers by haRPA.

Name	Target gene	Purpose	Primer sequence	Modification for haRPA	Amplicon length
TRI F	*TRI5*	RPA + haRPA	CTATGCTTACAACAAGGCTGCTCATCACTT	5' - Biotin	700 bp
TRI R	*TRI5*	RPA + haRPA	CATCGTCGAATTCCTTGTAGAACGACATGA	5' – NH_2-C_{12}	

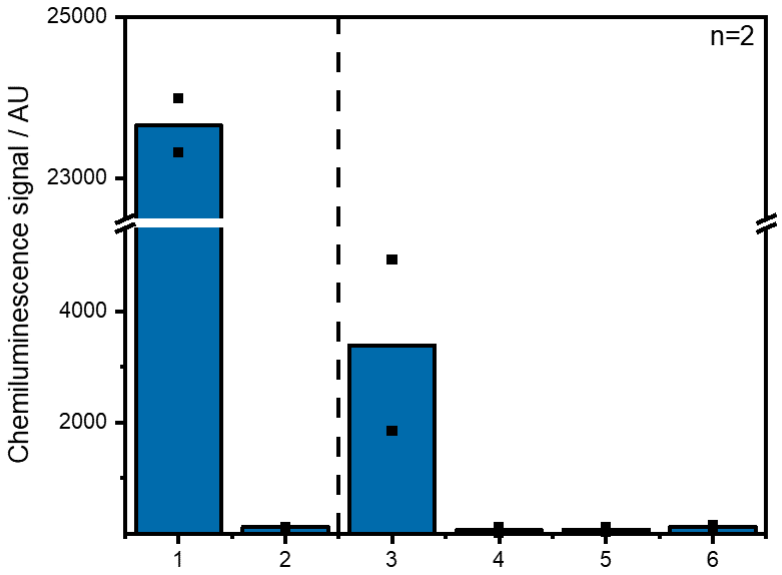

Figure 15: Preliminary haRPA measurements for testing the TRI primer set. Chemiluminescence signals from haRPA measurements are depicted in AU. Bars represent the mean values, dots the single measurements. The dashed line separates controls from samples. **1** is the spotting control, being immobilized EZ-Link amine-PEG_2-biotin, **2** is the negative control, being spotting buffer only, **3** is 100 ng of *F. culmorum* DNA, **4** is 100 ng of *E. nigrum* DNA, **5** is 100 ng of *B. subtilis* DNA, **6** is 100 ng of *L. japonicus* DNA. n is the number of replicates.[27]

4. Development of a chip-based colony-fusion-haRPA method for the simultaneous detection of ARGs and their carrying species

4.1.1. Aim of this project

Monitoring methods which are able to detect ARGs and their carrying species while at the same time being usable in-field are required. This is why, a method was aimed to be developed which combines the benefit of singling-out bacteria of culture-based methods and the genetic analysis of molecular methods. The workflow, which was worked on, was named "colony-fusion-haRPA" as it combines single-colony extraction and heterogeneous asymmetric RPA. This was a proof-of-principle project as neither colony-RPA nor fusion-RPA has ever been shown before. Therefore, prominent ARB species with common ARGs present in surface water needed to be chosen for analysis. As mentioned in the introduction, CTX-M β-lactamases of the cluster 1 are widely spread in Germany. Two relevant species carrying these genes, namely *E. coli* and *K. pneumoniae* were chosen for testing. The use of polycarbonate chip surfaces instead of glass surfaces made the assay more cost- and time efficient. Using haRPA on the MCR 3 as the detection method was meant to enable visual readout to a complex research question. As the method was meant for detection of ARBs in surface water, environmental water samples were aimed to be analyzed with the final method as well.

4.1.2. Establishment of a fusion-haRPA workflow

For ease of understanding, the final workflow will be introduced at the beginning of this section (Figure 16). A sample of interest was cultured on a bacterial plate, supplemented with cefotaxime for colony formation (Figure 16, A). After lysis of a colony (Figure 16, B) the supernatant was used for two reactions (Figure 16, C+D). One, for the amplification of the species-specific gene and the other one for amplification of the resistance gene. In the next

step, a certain volume from each of the two tubes was transferred into a new RPA reaction tube for fusion product formation (Figure 16, E). A part of this reaction was then transferred to a haRPA reaction tube as template for detection of the fusion amplicon on the microarray chip by chemiluminescence. The step-by-step development of this workflow will be explained in the following.

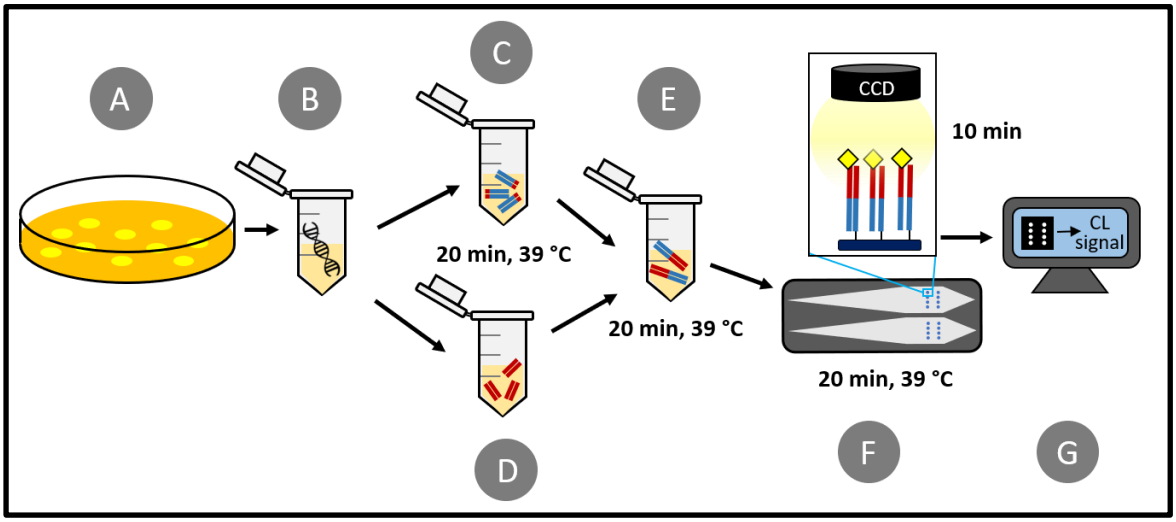

Figure 16: Overview over the colony-fusion-haRPA workflow. A bacterial sample of interest was cultivated on a plate with medium supplemented with cefotaxime **A**. After 16 hours of incubation at 37 °C, a lysis was performed by picking a colony off the plate with a pipet tip, resuspending it in lysis buffer, subsequently boiling it and spinning down the cell debris. The supernatant contained the DNA as template for further reactions **B**. The supernatant was then divided and added into two RPA reaction tubes **C+D**, in which the ITS gene with a CTX-M cluster 1 gene-overhang **C** and the CTX-M cluster 1 gene **D** were amplified separately. As the next step, a certain volume from each of the two tubes was combined together and added into a new RPA reaction tube for fusion product formation **E**. For detection, a specific volume of this reaction was mixed with new RPA reagents and was injected into the microarray chip for haRPA. Chemiluminescence was detected via a CCD camera in the MCR 3 **F**. The chemiluminescence signals were converted in .txt files by an in-house software and subsequently analyzed **G**.[20]

Performing a reaction similar to fusion-PCR with RPA was the first aim of this project. In fusion-PCR, two separate amplicons are generated which are then fused together in a single reaction.[195,196] This was aimed to be done with *K. pneumoniae* and *E. coli* by fusion-haRPA too. For *E. coli*, the species-specific gene was a part of the internal transcribed spacer region (ITS), for *K. pneumoniae* of the phosphatase porin gene phoE. For both of the species, the ARGs of focus were CTX-M genes of the cluster 1. In a first step, primers needed to be

designed which could amplify these regions of interest in a normal homogeneous RPA reaction. As RPA primers are different from PCR primers, a number of different ones needed to be tested and were adapted from existing PCR-primers for best chances of specificity. The CTX-M cluster 1 specific primer set was based on the genomic region Xu et. al[137] used in their studies with PCR. For the ITS region of *E. coli* a qPCR primer set based on Khan et al.[197] and a past Metawater[198] project was used as basis. The phoE genomic region from *K. pneumoniae* was aimed to be amplified with primers based on PCR primers from Shannon et al.[199]

For primer testing, homogeneous RPA reactions were conducted. The amplicons were visualized on agarose gels and if successful, bands were cut out and the cleaned-up DNA was sent for sequencing. Additionally, RPA using a colony lysate as template was tested at the same time. The lysis protocol which allowed a successful RPA reaction consisted of picking the colony off the plate, dissolving it in TE buffer with 0.1% Triton X-100, boiling it for 10 minutes and then spinning down the cell debris. A maximum of 5 µl of the supernatant could be used for the RPA reaction to remain successful. Once working primer sets for the single genes were found, these primers were modified to be able to perform a fusion reaction. Unfortunately, the fusion RPA was not successful in one reaction step as it is usually done in PCR. The reason for this was the high amount of side product formation, which is a common problem in RPA.[61] As all reaction steps take place at the same time, RPA is more prone to unspecific amplifications when more than two primers are used. This is why after much trial and error, it was decided that the amplicons from the two genes (species and resistance) would be amplified separately and then combined in a second step for fusion product formation (Figure 16, C+D+E).

The molecular mechanism of this reaction is explained in detail in Figure 17 by the example of *E. coli.* For *K. pneumoniae,* the species-specific gene which was amplified is phoE instead of ITS. The final primer sequences are stated in Table 5 and their names are used in the following to describe the process. A 148 base pair region from the ITS gene and a 260 base pair region from the CTX-M were amplified using ITS`F and ITS`R-CTXMC1`F and CTXMC1`F and CTXMC1`R respectively (Figure 17, A). ITS`R-CTXMC1`F acts as a bridge-primer, its sequence contains the reverse primer for the ITS gene as well as an overhang complementary

to 5’ end of the 260 base pair region of the CTX-M gene (Figure 17, B). Once incorporated into the amplicon, this overhang acts as forward primer for the CTX-M gene for fusion product formation. In this step, only the primers ITS`F and CTXMC1`R are added, in order to force fusion product formation (Figure 17, C+D). The gel image in Figure 18 shows the successful formation of fusion products for *E. coli* and *K. pneumoniae*.

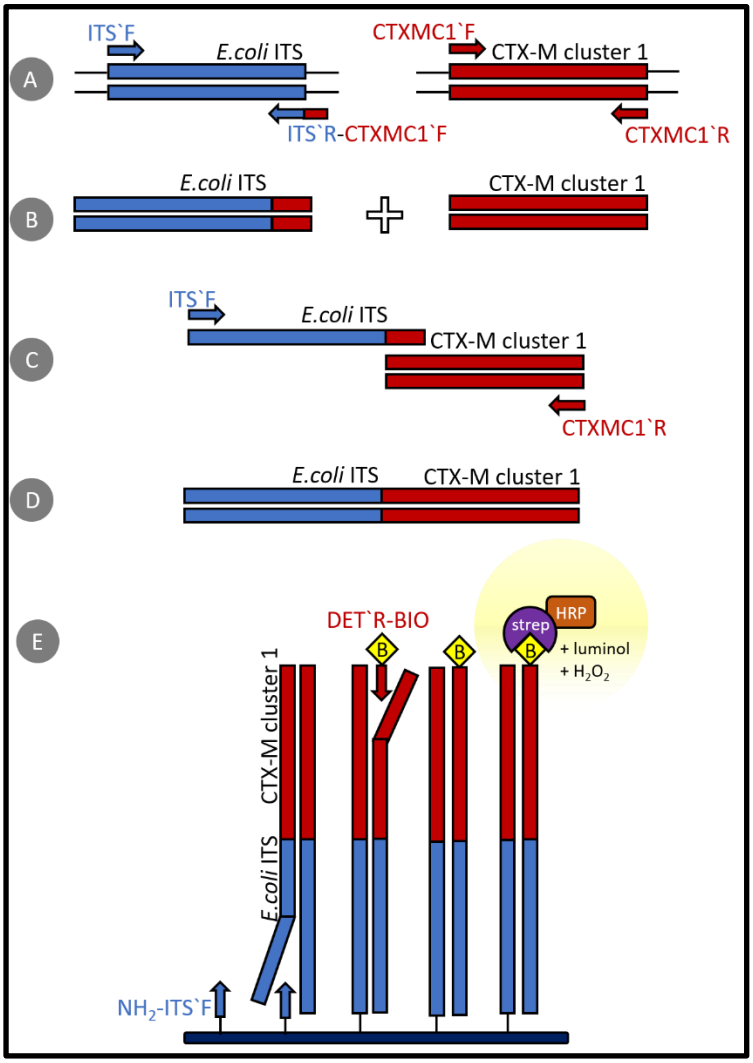

Figure 17: Schematic overview over the molecular process of fusion product formation by the example of *E. coli*. In a first step, the amplicons from the ITS gene and the CTX-M gene are generated separately by homogeneous RPA. During the amplification of the ITS region, the primer ITS‘-CTXC1M‘F incorporates an overhang into the amplicon, which is complementary to the 5’ end of the CTX-M amplicon **A**. In a following step both amplicons are mixed together into a second homogeneous RPA reaction **B** for fusion product formation. As only the two primers ITS‘F and CTXMC1‘R are added to this reaction, there is a selection for fusion product formation as only those can be further amplified **C**. After the ITS-CTX-M fusion product has been formed **D**, it can be detected on the microarray chip **E**. In the detection step, the fusion product is reamplified via haRPA with the amino-immobilized ITS‘F

and the biotinylated detection primer DET'R. This way, the incorporated biotin can be bound by a streptavidin-labeled HRP. This enzyme produces chemiluminescence upon addition of luminol and hydrogen peroxide **E** which can be detected by a CCD camera in the MCR 3. The detected signals can then be further analyzed.[20]

For *E. coli* a fusion product of 408 base pairs was formed (Figure 18, lane 2) and for *K. pneumoniae* one of 363 base pairs was obtained, both corresponding to the correct sizes. This was further confirmed by sequencing of the amplicons which revealed correct fusion products as shown in Figure 19. More details about the establishment of the *K. pneumoniae* primer set can be seen in the Master's Thesis of Philipp Streich, which was part of this work.[200]

Table 5: Primers used for development and application of colony-fusion-haRPA[20]

Primer name	Target	Primer sequence (5'-3')	modification	Amplicon length /bp	Source
ITS`F	ITS region	CAATTTTCGTGTCCCCTTCGTC	none	162	Modified from: Khan et al., 2007
ITS`R-CTXMC1`F	Bridge primer for ITS and CTX-M cluster 1 genes	AAGTGGTATCACGCCATCACCCGAAGATG	none		Modified from: Xu et al., 2018; MetaWater, 2016
CTXMC1`F	CTX-M cluster 1 genes	GCGTGATACCACTTCACCTC	none	260	Xu et al., 2018
CTXMC1`R	CTX-M cluster 1 genes	TGAAGTAAGTGACCAGAATCAGC	none		Modified from: Xu et al., 2018
NH_2-ITS`F	ITS region	CAATTTTCGTGTCCCCTTCGTC	5'-NH_2-C12	400	Modified from: Khan et al., 2007
DET`R-BIO	CTX-M cluster 1 genes	GTGACCAGAATCAGCGGCGCACGATC	5'-Biotin		This work
phoE`F	phoE region	GGTCTGGTGGATGGCCTGGATCTGACCCTGCA	none	119	Modified from: Shannon et al., 2007
phoE`R-CTXMC1`F	Bridge primer for phoE and CTX-M cluster 1 genes	TGAAGTGGTATCACGCAGCTTAACGAGGTGCC	none		This work, Xu et al., 2018

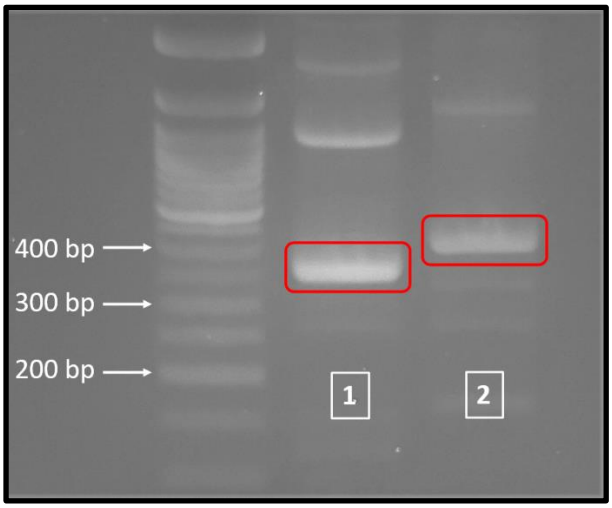

Figure 18: Agarose gel image of fusion products formed by homogeneous RPA during the primer testing process. The *K. pneumoniae* phoE-CTXM-55 fusion product of 363 base pairs is shown in lane 1, red box. The *E. coli* ITS-CTX-M-1 fusion product of 422 base pairs is shown in lane 2, red box. The picture was taken with a smartphone camera while the DNA in the gel was visualized on a blue light table. The bands marked by red boxes were cut out from the gel and the containing DNA was cleaned up and sent for sequencing.[20]

A

```
1 CAATTTTCGT GTCCCCTTCG TCTAGGGGCC CAGGACACCG CCCTTTCACG GCGGTAACAG
2 CAATTTTCGN GTCCCCTTCG TCTAGNGGCC CAGGACACCG CCCTTTCACG GCGGTAACAG

1 GGGTTCGAAT CCCCTAGGGG ACGCCACTTG CTGGTTTGTG AGTGAAAGTC ACCTGCCTTA
2 GGGTTCGAAT CCCCTAGGGG ACGCCACTTG CTGGTTTGTG AGTGAAAGTC ACCTGCCTTA

1 ATATCTCAAA ACTCATCTTC GGGTGATGGC GTGATACCAC TTCACCTCGG GCAATGGCGC
2 ATATCTCAAA ACTCATCTTC GGGTGATGGC GTGATACCAC TTCACCTCGG GCAATGGCGC

1 AAACTCTGCG GAATCTGACG CTGGGTAAAG CATTGGGCGA CAGCCAACGG GCGCAGCTGG
2 AAACTCTGCG GAATCTGACG CTGGGTAAAG CATTGGGCGA CAGCCAACGG GCGCAGCTGG

1 TGACATGGAT GAAAGGCAAT ACCACCGGTG CAGCGAGCAT TCAGGCTGGA CTGCCTGCTT
2 TGACATGGAT GAAAGGCAAT ACCACCGGTG CAGCGAGCAT TCAGGCTGGA CTGCCTGCTT

1 CCTGGGTTGT GGGGGATAAA ACCGGCAGCG GTGGCTATGG CACCACCAAC GATATCGCGG
2 CCTGGGTTGT GGGGGATAAA ACCGGCAGCG GTGGCTATGG CACCACCAAC GATATCGCGG

1 TGATCTGGCC AAAAGATCGT GCGCCGCTGA TTCTGGTCAC TTACTTCA
2 TGATCTGGCC AAAAGATCGT GCGCCGCTGA TTCTGGTCAC TTACTTCA
```

B

```
1 CTTCGGTCTG GTGGATGGCC TGGATCTGAC CCTGCAGTAC CAGGGTAAAA ACGAAGGCCG
2 ----GGTCTG GTGGATGGCC TGGATCTGAC CCTGCAGTAC CAGGGTAAAA ACGAAGGCCG

1 TGAAGCGAAG AAACAGAACG GCGACGGCGT CGGCACCTCG TTAAGCTGCG TGATACCACT
2 TGAAGCGAAG AAACAGAACG GCGACGGCGT CGGCACCTCG TTAAGCTGCG TGATACCACT

1 TCACCTCGGG CAATGGCGCA AACTCTGCGT AATCTGACGC TGGGTAAAGC ATTGGGCGAC
2 TCACCTCGGG CAATGGCGCA AACTCTGCGG AATCTGACGC TGGGTAAAGC ATTGGGCGAC

1 AGCCAACGGG CGCAGCTGGT GACATGGATG AAAGGCAATA CCACCGGTGC AGCGAGCATT
2 AGCCAACGGG CGCAGCTGGT GACATGGATG AAAGGCAATA CCACCGGTGC AGCGAGCATT

1 CAGGCTGGAC TGCCTGCTTC CTGGGTTGTG GGGGATAAAA CCGGCAGCGG TGGCTATGGC
2 CAGGCTGGAC TGCCTGCTTC CTGGGTTGTG GGGGATAAAA CCGGCAGCGG TGGCTATGGC

1 ACCACCAACG ATATCGCGGT GATCTGGCCA AAAGATCGTG CGCCGCTGAT TCTGGTCACT
2 ACCACCAACG ATATCGCGGT GATCTGGCCA AAAGATCGTG CGCCGCTGAT TCTGGTCACT

1 TACTTCACC
2 TACTTCA--
```

Figure 19: Sequencing results of the *E. coli* and *K. pneumoniae* fusion RPA amplicons aligned with *in silico* designed fusion products. The *E. coli* **A** fusion amplicon band was cleaned up from the agarose gel shown in Figure 18 and was sequenced by Sanger sequencing. Sequencing was performed using the primers ITS'F and CTXMC1'R. The resulting forward and reverse sequencing data was combined (2) and aligned to an *in silico* designed fusion product sequence (1). The DNA of the *K. pneumoniae* fusion product **B** was cleaned up from the agarose gel shown in Figure 18 sequenced by Sanger sequencing as well. Here, sequencing was performed using the primers phoE`F and CTXMC1'R. The resulting forward and reverse sequencing data was combined (2) and aligned to an *in silico* designed fusion product sequence (1). Red color represents gaps or mismatches. The alignments and the *in silico* designs of the fusion products were done with CLC Genomics Workbench 20.0.3 by QIAGEN .[20]

4.1.3. Heterogeneous fusion product formation

As described in Figure 17, after homogeneous fusion product formation, the detection step was aimed to be done by haRPA. Therefore, a primer system for the detection step needed to be developed. When using haRPA, primers can work quite differently than in homogeneous RPA. For immobilization on the surface, the forward primer, namely ITS'F or phoE'F were chosen. Different detection primers targeting the CTX-M part of the amplicon were tested and the DET'R primer shown in Table 5 was used. Unfortunately, when trying to detect both the *K. pneumoniae* and *E. coli* fusion products at the same time, it was noticed that DET'R shows interaction with phoE'F. As there was no time to develop a new phoE'F primer, it was decided to continue with the assay for *E. coli* as a proof-of-principle. Further optimization of this assay showed that the optimal NH_2-ITS`F primer, DET`R primer and CTXMC1`R primer concentrations were 75 µM, 5 µM and 0.1 µM, respectively. Details about this can be found in the Master's Thesis of Philipp Streich which is part of this work.[200]

When looking at the entire colony-fusion-haRPA workflow (Figure 16), it resulted in an assay time of under 90 minutes. The colony lysis amounts to 15 minutes, the single-gene amplification, the fusion product amplification and the haRPA take 20 minutes each and the detection step additional 10 minutes. It is worth noting that, as the chip has two flow cells, two samples can be handled at the same time.

4.1.4. Specificity testing of fusion haRPA

As this method was aimed to be used for surface water samples, the specificity of the developed primer system needed to be confirmed. Therefore, other species which can potentially contain CTX-M genes of the cluster 1 were analyzed with the colony-fusion-haRPA workflow. Therefore, *E. coli* colonies, carrying CTX-M-1/3/15 genes, *K. pneumoniae* colonies carrying CTX-M-15/55 genes, and *E. cloacae* colonies carrying CTX-M-15 genes were analyzed as all these genes belong to cluster 1. For comparison, *E. coli* colonies carrying CTX-M-2/9/14/27 genes which belong to other clusters of CTX-M genes were analyzed as well. For all following figures involving the haRPA detection, colonies of CTX-M-15 carrying *E. coli* were analyzed with each chip batch. As these colonies consistently gave the highest signal, their mean value was set as 100% signal for the respective chip batch. The results of the specificity analysis can be seen in Figure 20.

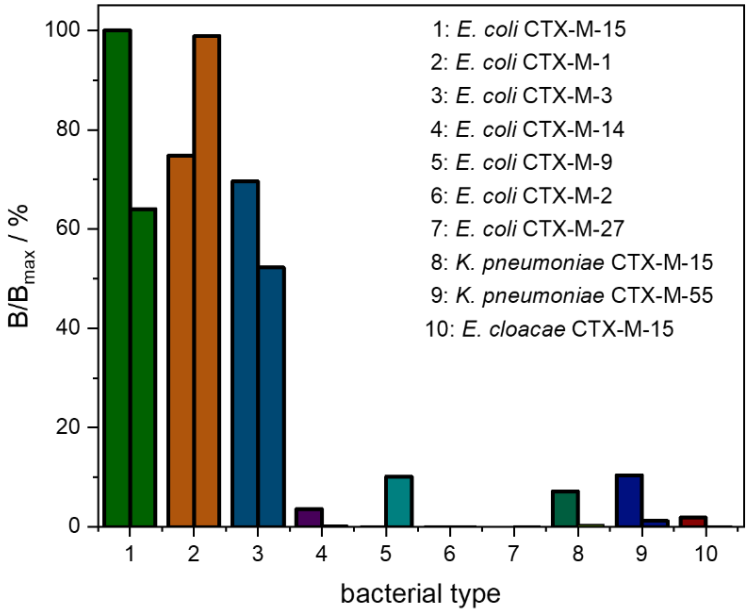

Figure 20: Specificity of the developed fusion haRPA primer system. Signal intensities are shown in relation (%) to the maximum value (B_{max}), determined by an *E. coli* colony carrying a CTX-M-15 gene (bar 1.1). Each bar belonging to one bacterial type represents one colony. Two colonies per sample type (1−10) were analyzed. The signal intensities shown are the mean values of four spots in one row on the microarray chip.[20]

The signal intensities for cluster 1 gene carriers were 42−99% higher compared to those of non-*E. coli* and non-cluster 1 carriers. This indeed demonstrates that the developed colony-fusion-haRPA primer system is specific for *E. coli* carrying CTX-M genes of the cluster 1. As the aspect of specificity is especially crucial when working with environmental samples, a more extensive study covering more genes and more species is needed in the future.

4.1.5. Cutoff determination using colony-fusion haRPA

In order to be able to discriminate between positive samples (*E coli* CTX-M cluster 1) and negative samples (non-*E. coli* CTX-M cluster 1 or *E. coli* non-CTX-M cluster 1) a signal range in which this could be determined was required. For this purpose, a cutoff determination experiment was performed. In order to be as realistic as possible, environmental sampling was mimicked. All available bacterial types belonging to a "negative" group were mixed and cultivated creating a "negative" sample plate. These were *E. coli* carrying CTX-M-2/9/14/27 genes, *K. pneumoniae* carrying CTX-M-15/55 genes, and *E. cloacae* carrying CTX-M-15 genes. The same was done with all available bacterial types classifying as "positive" to create a "positive" sample plate. These were *E. coli* carrying CTX-M-1/3/15 genes. For cutoff determination, 20 "negative" and 24 "positive" colonies were analyzed with the colony-fusion-haRPA workflow. As can be seen in Figure 24, "negative" sample colonies resulted in signals of 2-11% whereas "positive" sample colonies produced signals in the range of 23-108%. Interestingly, no false-negative or false-positive incidences were observed. This made the calculation of the cutoff value according to standard methods (using selectivity, specificity and the confidence interval) impossible.[201–203] It was therefore defined as the mean value of the "negative" samples, plus three times standard deviation. This is a method which is often used in these cases.[204,205] The cutoff was thereby placed at 17% of the maximum signal determined by the mean value of three *E. coli* colonies carrying CTX-M-15 genes. This dataset must be seen as a training dataset, a more extensive study with a broader variety of bacterial types and a higher sample number is needed to narrow down the cutoff value in the future.

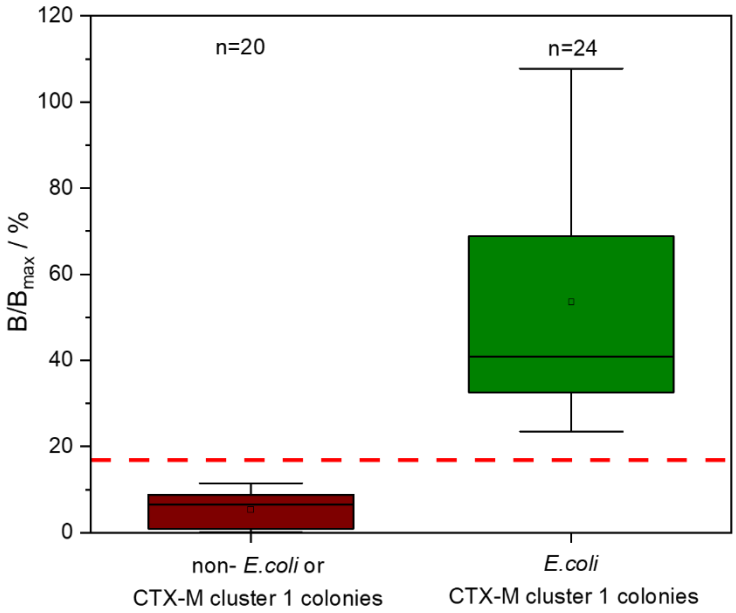

Figure 21: Cutoff value determination for the colony-fusion-haRPA workflow. Signals are presented in percentage of the maximum value (B_{max}), defined by the mean signal of three *E. coli* colonies carrying a CTX-M-15 gene. Non-*E. coli* CTX-M cluster 1 colonies (left) are constituted by a mixture of colonies of *E. coli* carrying CTX-M-2/9/14/27 genes, *K. pneumoniae* carrying CTX-M-15/55 genes, and *E. cloacae* carrying CTX-M-15 genes. *E. coli* CTX-M cluster 1 colonies (right) are constituted by a mixture of colonies of *E. coli* carrying CTX-M-1/3/15 genes. The red line at 17% marks the cutoff value for positive samples. n is the number of colonies measured. The boxes display 25−75% of values. The squares inside the boxes indicate the mean and the lines the median values. The whisker-ends correspond to the highest or lowest values of the sample groups.[20]

4.1.6. Analysis of river water samples

The method which is mostly used for analysis of environmental water samples is cultivation.[206–208] This is also the main reason why the method presented here was developed to start from bacterial colonies, so that it could be compatible with currently used strategies. It was therefore crucial to test whether the colony-fusion-haRPA workflow is applicable for environmental samples. For this purpose, water from the river Lech in Augsburg was collected just downstream of the outlet of a wastewater treatment plant. The samples were then cultivated on plates containing cefotaxime for 16 hours. In order to be able to screen a large number of colonies, colony-PCR was used. 150 colonies were screened with PCR primers

specific for the CTX-M cluster 1[137] and for the *E. coli* specific ITS region (Table 6).[197,198] The screening was done by visualizing amplicons on agarose gels. Of these colonies, only two showed amplicons for both genes. These two colonies and four random negative colonies were regrown and the colony-PCR was repeated. The gel image of this experiment can be seen in Figure 22. The bands of the positive colonies were cut from the gel, the DNA was cleaned up and sent for sequencing. As can be seen in Figure 23, the sequencing results show that indeed the colonies belonged to the species *E. coli* and both contained a CTX-M-15 gene. Once this was confirmed, colony-fusion-haRPA was performed on the two positive and four random negative colonies to have a comparison. As can be seen in Figure 24 the signal of the two positive colonies is above the cutoff of 17% with 36% and 52%, respectively. The four negative colonies all gave signals well below the cutoff line with 3.8%, 1.0%, 0.8% and 0.1%, respectively. As the results of the colony-PCR could be reproduced with the fusion haRPA workflow, this indicates a good applicability of the system for environmental samples. In the future a more extensive study with higher sample numbers will have to be performed.

Table 6.: Primers used for colony-PCR[20]

Detection of:	Amplification of:	Primer sequence (5'-3')	Amplicon length /bp	Source
E.coli	Conserved ITS genomic region	F: CAATTTTCGTGTCCCCTTCG	148	Khan et al., 2007
		R: CATCACCCGAAGATGAGTTTT		MetaWater, 2016
CTX-M cluster 1 genes	Conserved CTX-M cluster 1 genomic region	F: GCGTGATACCACTTCACCTC	260	Modified from Xu et al., 2018
		R: TGAAGTAAGTGACCAGAATCAGC		

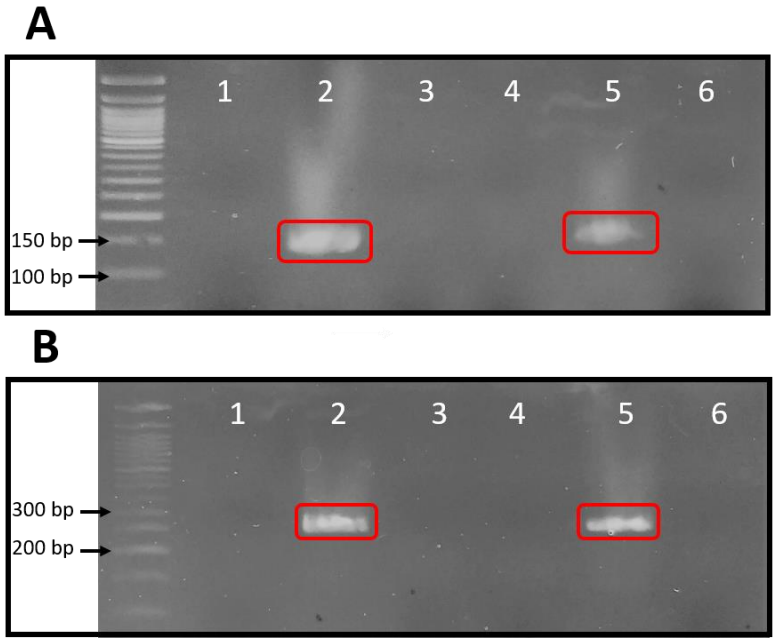

Figure 22: Agarose gel images of the analysis of the colony-PCR reactions done for the screening of the environmental samples. Colony-PCR was performed for screening of 150 environmental colonies with primers targeting the ITS region **A** and the conserved CTX-M cluster 1 region **B** (Primers are depicted in Table 6). Of the 150 screened colonies only two resulted positive for both genes. These two and four random negative colonies were regrown and the colony-PCR was repeated. The results are depicted in this agarose gel images. The six lanes in the gels represent these six environmental colonies. Positive samples (lane 3 and 5) display a band of 148 base pairs corresponding to the ITS gene region in **A** and of 260 base pairs corresponding to the CTX-M cluster 1 conserved region in **B**. For negative samples no amplicons were generated at these sizes. The bands in the red boxes were cut out of the gels and the containing DNA was cleaned up and sent for sequencing. Sequencing data is shown in Figure 23.[20]

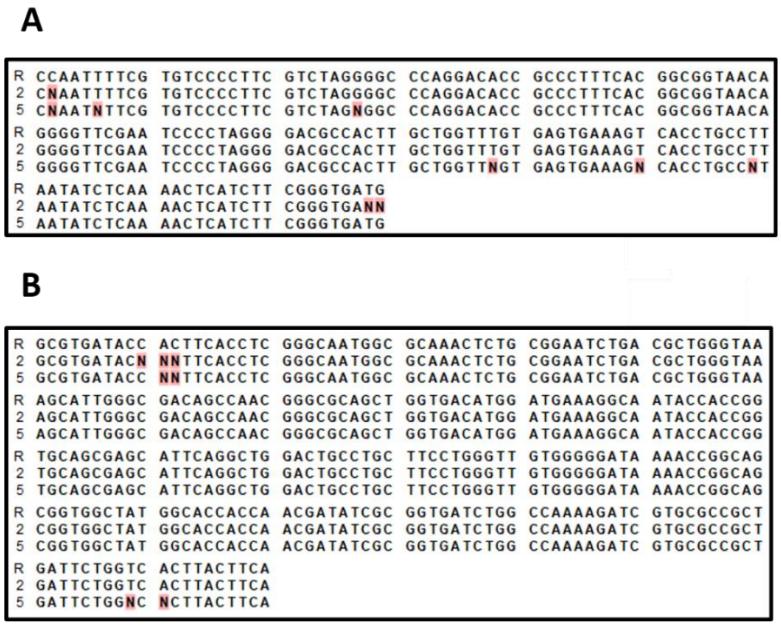

Figure 23: Sequencing results from the colony-PCR reactions of the two positive environmental colonies aligned with their ITS and CTX-M-15 template sequences. The bands visible in lanes 2 and 5 of Figure 22 were cut out of the gel, the containing DNA was cleaned up and sent for Senger sequencing. The alignment of the sequencing results of the ITS gene of sample 2 (2) and sample 5 (5) to the reference ITS sequence (R) is visible in **A**. **B** shows the alignment of the sequencing results of the CTX-M-15 gene of sample 2 (2) and sample 5 (5) to the reference CTX-M-15 sequence (R). Sequencing was performed with the same primers as the colony-PCR. The resulting forward and reverse sequences were combined and aligned to the reference sequences. Red color represents gaps or mismatches. The alignments were performed with the CLC Genomics Workbench 20.0.3 by QIAGEN.[20]

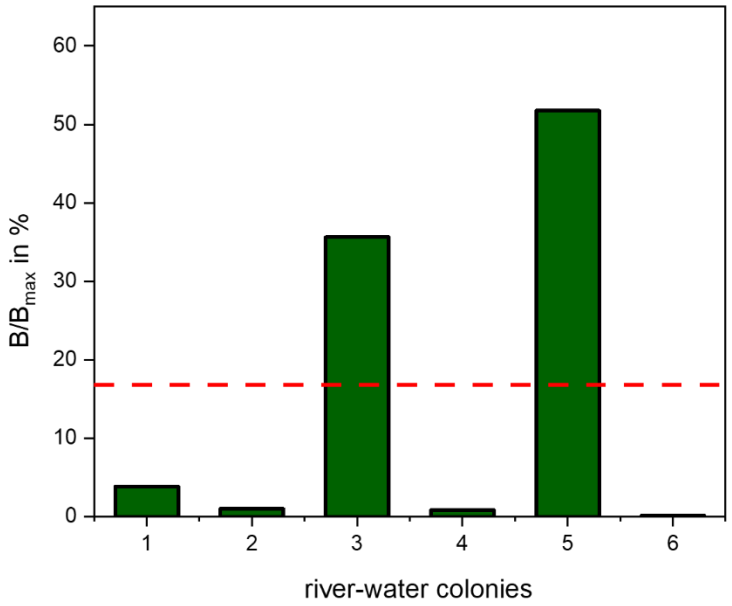

Figure 24: Analysis of a river water sample with the fusion-haRPA workflow. Signals are depicted in percentage of the maximum value (B_{max}), defined by the mean signal given by three *E. coli* colonies carrying a CTX-M-15 gene. Numbers 1-6 correspond to colonies picked from an environmental river-water sample plate and measured by fusion-haRPA. The red line indicates the 17 % threshold value above which samples were considered positive. The signals depicted are the mean values of four spots on the microarray chip.[20]

5. Development of an immobilization strategy for diclofenac on polycarbonate surfaces for a chip-based, regenerable, indirect competitive immunoassay

5.1.1. Aim of this project

During the Master Thesis of Andreas Auernhammer, which was part of this work, an immobilization strategy for diclofenac on glass surfaces was developed based on chip chemistry previously used at the institute.[179] The long-term aim of this project was the establishment of an assay comparable to the one published by Kloth et al.[48] for a number of different classes of chemicals instead of just antibiotics. The immobilization of diclofenac was achieved by using EDC/S-NHS mediated cross linking of the carboxyl group of diclofenac to the amino group of the activated glass surface.[179] The MRL for diclofenac in milk is 100 ng/L. This assay only reached an LoD of 264 ng/L with an IC_{50} of 1 µg/L in milk and an LoD of 66 ng/L with an IC_{50} of 450 ng/L in water. Interestingly, ELISAs with the same antibody yield an LoD and IC_{50} of 7.8 and 44 ng/L, respectively.[58] During the Master's thesis, different approaches such as a variation in spotting concentrations of diclofenac, incubation times and flow rates, were tried to improve the assay but none of them succeeded.[209] This is why, a different approach was tested. Combining the advantages of plastic chips with the advantages of a regenerable assay, would drastically improve the method. Polycarbonate surfaces are more cost-effective, easier, and faster to produce while also providing a more environmentally friendly alternative to the solvent-intensive activation of glass chip surfaces. At the same time, regenerablity means one chip can be used for multiple measurements which is optimal for fast and automated monitoring. Because of this, the transfer of the assay onto polycarbonate surfaces was attempted. Whether or not polycarbonate surfaces can be used for regenerable assay formats had never been tested before so in this chapter the right immobilization strategy had to be identified. Firstly, coating conditions for coating with unmodified Jeffamine® needed to be found. On top of that, spotting buffer compositions were aimed to

be examined together with the amount of immobilized diclofenac. In the end, the system needed to be calibrated to investigate if the new assay yielded a lower LoD.

5.1.2. Testing of different Jeffamine® concentrations for coating and different diclofenac concentrations for spotting of polycarbonate chips

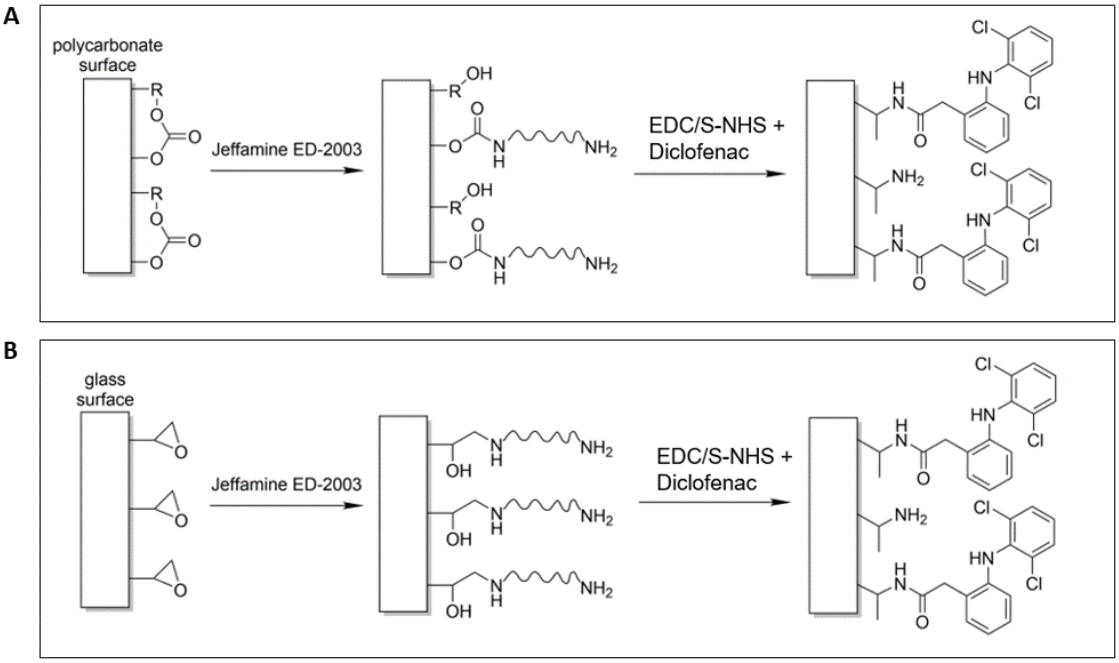

Figure 25: Comparison of the surface functionalizations for immobilization of diclofenac on polycarbonate (A) and glass surfaces (B) with Jeffamine®.

In previous research, only succinylated Jeffamine® had been used to coat polycarbonate surfaces.[27,59] For the purpose of this project, unmodified Jeffamine® carrying an amino group at each end of the molecule was needed in order to crosslink the carboxyl group of diclofenac to the surface. The difference in chip chemistries can be seen in Figure 25. For glass, Jeffamine® is added onto the hydrophobic epoxy surface and the amino groups of Jeffamine® react with the epoxy groups, creating exposed amino groups.[179] For polycarbonate surfaces,

Jeffamine® is directly added and the reaction takes place via an attack of the primary amine on the carbonyl C of polycarbonate. This as well, creates a surface with exposed amino groups. As in previous research, polycarbonate chips were only coated with succinylated Jeffamine® by screen printing,[27,59] these experiments were based on this experience as well as on information provided by Julia Neumair, who also tested coating with unmodified Jeffamine® for other purposes. Bemetz et. al [59] developed an efficient coating method by screen printing a sheet of polycarbonate chips with succinylated Jeffamine® and then incubating the sheet at 100 °C for 2 hours. This is why, this method was used for coating in this work as well. The conditions which were tested can be seen in Figure 26, namely incubation of Jeffamine® on the chips after coating for either 2 hours or overnight at temperatures of 70 °C and 100 °C each. The used diclofenac concentrations for spotting ranged from 1.5 to 5 mg/ml. For testing of the system, blank measurements in milk were performed, revealing the maximum signal intensity of each condition. This is important as the blank signal intensity gives information about how much analyte has bound to the surface. The more analyte on the surface, the higher the signal. High signal coming from a high density of analyte on the surface often correlates with a higher sensitivity as well. One chip per condition was measured for five times. The first two measurements were discarded, as stable signal is only achieved from the third measurement on. The standard deviations result from these three measurements which also represent the regenerability of the chip surface. As can be seen in Figure 26 the maximum signal intensities varied a lot among these conditions. The highest intensity with 14,900 was achieved with 2 hours incubation at 100 °C (Figure 26, A), followed by overnight incubation at 70 °C with a maximum signal of 12,800 (Figure 26, D). Both these conditions have in common that the highest signal was achieved by immobilization of 5 mg/ml diclofenac, meaning the surface was not yet saturated. The other two conditions resulted in rather low signals of 8,000 with 4 mg/ml immobilized diclofenac when incubated for 2 hours at 70 °C (Figure 26, C) and 2,500 with 5 mg/ml immobilized diclofenac for overnight incubation at 100 °C (Figure 26, B). These results indicate that similar amounts of analyte were bound to the surface when using 2 hours incubation at 100 °C and overnight incubation at 70 °C. Not only the signal intensity is important, but also the homogeneity and

transparency of the surface. Pictures of the surfaces can be seen in Figure 27. Chips incubated at 100 °C were a lot opaquer than those incubated at 70 °C. Also, the surface of the latter was very inhomogeneous. Incubation for 2 hours at 100 °C resulted in the seemingly thickest layer of Jeffamine®. Chips incubated at 70 °C were more transparent and homogeneous. When incubated at 70 °C overnight the surfaces seemed almost transparent. Due to the combination between a high signal and a very transparent and homogeneous surface, the condition of incubation at 70 °C overnight was chosen for further use.

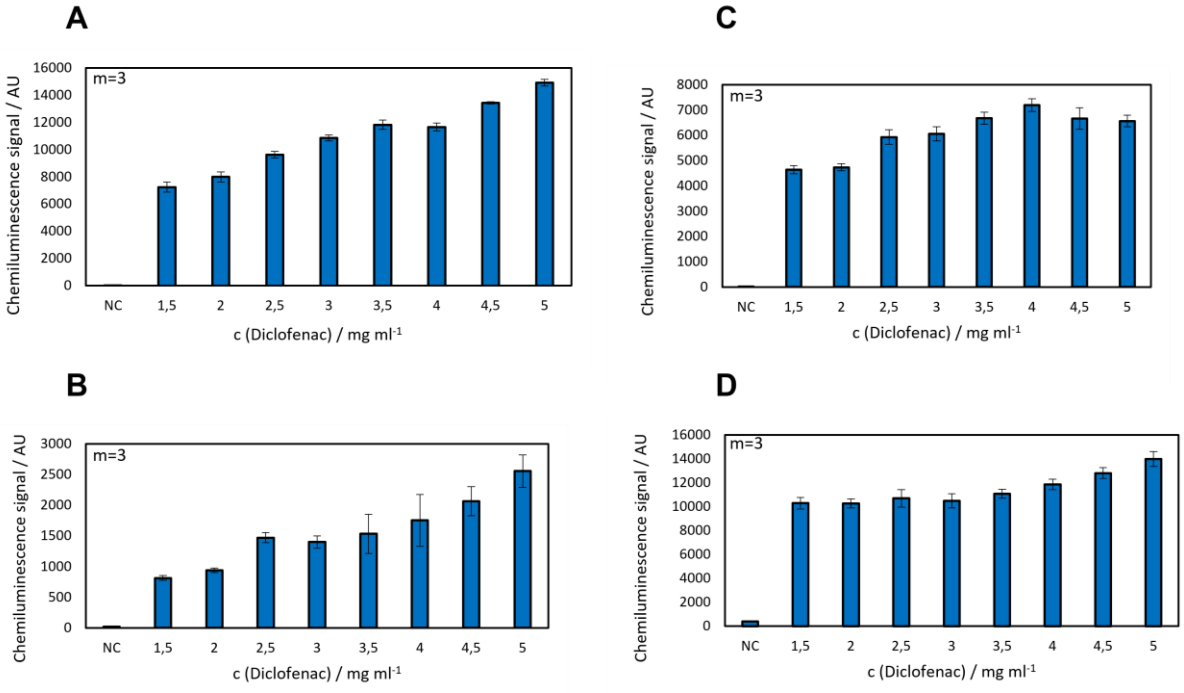

Figure 26: Bar plots showing the signal intensities of polycarbonate chips coated with Jeffamine® at different conditions and spotted with different concentrations of diclofenac. On the upper left **A** the chips were incubated for 2 hours at 100 °C after Jeffamine® coating. On the lower left **B** they were incubated overnight at 100 °C. On the upper right **C** and lower right **D**, chips were incubated for 2 h at 70 °C and overnight at 70 °C, respectively. The concentrations of diclofenac in the spotting buffer used for spotting of the chips are depicted on the X axes. The signal intensities are depicted as chemiluminescence signals in AU. Every bar represents three consecutive measurements on the same chip including standard deviations.

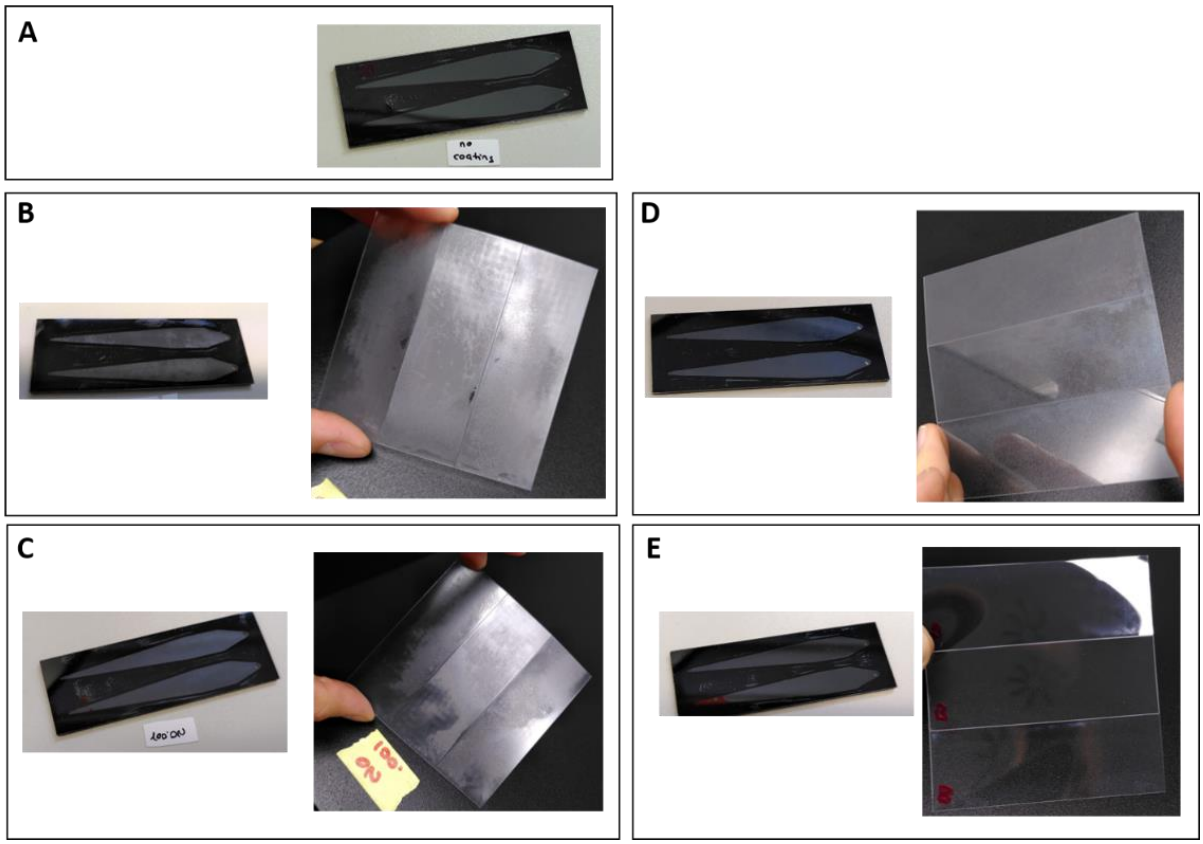

Figure 27: Images of assembled and non-assembled polycarbonate chips after coating with Jeffamine® under different conditions. Pictures were taken of a non-coated chip **A**, coated chips which were incubated for 2 hours at 100 °C **B** and overnight at 100 °C **C** as well as for 2 hours at 70 °C **D** and overnight at 70 °C **E**.

5.1.3. Testing of different spotting buffer compositions

For testing the optimal coating conditions, the spotting buffer composition which had been optimized for glass surfaces[209] was used. As it was not clear whether this was also the optimal composition for polycarbonate surfaces, different concentrations of crosslinking agents were tested. A high excess in crosslinking reagents to the analyte can improve immobilization efficiency. Therefore, different higher concentrations of EDC and S-NHS were added to the spotting buffer. Figure 28 shows the results which were obtained from spotting with 2 times (**A**), 5 times (**B**) and 10 times (**C**) the amount of which was originally used. This time, the amount of diclofenac in the spotting buffer ranged from 5 to 30 mg/ml as previous

experiments showed the surface was not yet saturated. The concentration point of 5 mg/ml shows that doubling the amount of crosslinking reagents to 8 mg/ml EDC and S-NHS each resulted in a lower signal. In this case it dropped from 14,000 (Figure 28, D) to 7,600 (Figure 28, A).

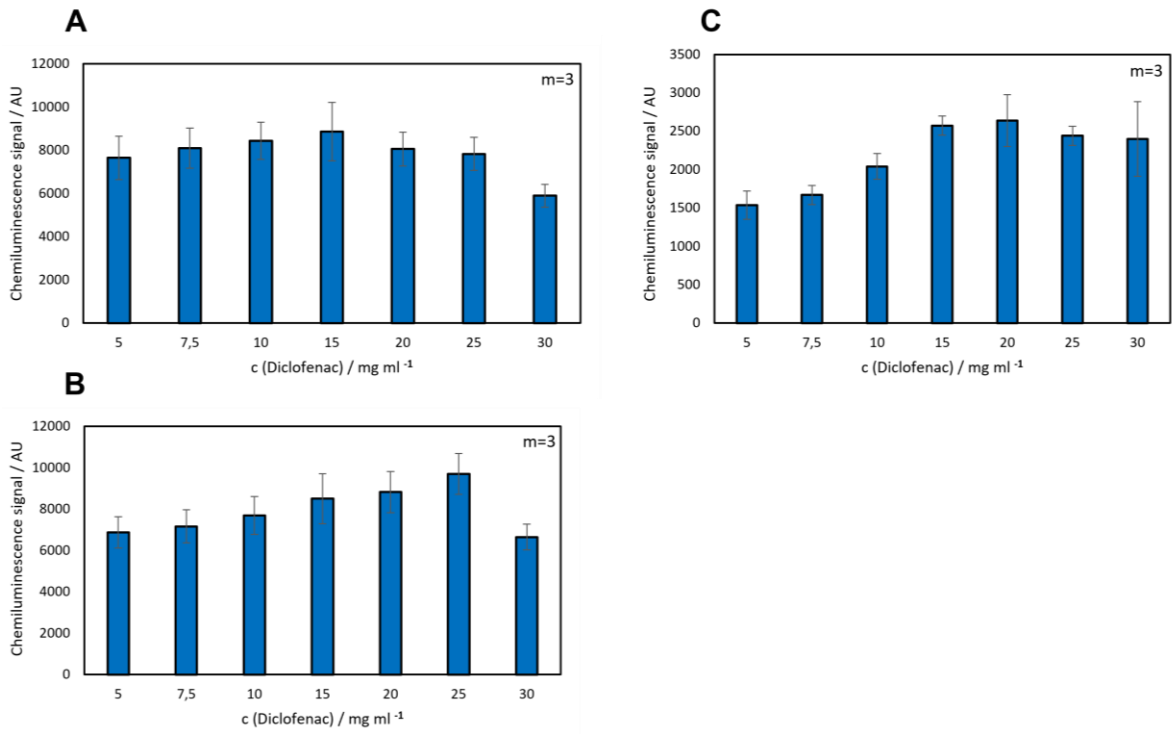

Figure 28: Bar plots showing the signal intensities of polycarbonate chips spotted with different spotting buffer compositions containing different concentrations of crosslinking reagents and diclofenac. On the upper left **A** the spotting buffer contained 8 mg/ml EDC and S-NHS respectively. On the lower left **B** it contained 20 mg/ml EDC and S-NHS respectively while on the upper right **C** it contained 40 mg/ml EDC and S-NHS respectively. All chips were incubated with Jeffamine® overnight at 70 °C. The concentrations depicted on the x-axes are the concentrations of diclofenac in the spotting buffer. The signal intensities are depicted as chemiluminescence signals in AU. Every bar represents three consecutive measurements on the same chip including standard deviations.

Looking at Figure 28, A the highest signal results from 15 mg/ml diclofenac in the spotting buffer with a signal of 8,900 (Figure 28, A). When using 5 times the amount of crosslinking reagents, the signal at 5 mg/ml diclofenac in the spotting buffer decreases to 6,800, with the highest signal being 9,700 at 25 mg/ml diclofenac in the spotting buffer (Figure 28, B). An increase to a 10-fold quantity of crosslinking reagents to a concentration of 40 mg/ml each then resulted in a drastic drop of signal to 1,500 for 5 mg/ml diclofenac in the spotting buffer

and a maximum signal of 2,600 with 20 mg/ml diclofenac in the spotting buffer (Figure 28, C). These results indicate that the previously used spotting buffer composition was better for the used system than a high excess of crosslinking reagent to the analyte. Interestingly, when looking at the concentration of diclofenac in the spotting buffer, optimal concentrations range between 15 to 25 mg/ml (Figure 28). This is why these concentrations were also used again in the next optimization step.

5.1.4. Testing of a quick washing procedure

After the spotting process, the spots on the chip surfaces were very well visible by eye. From their appearance, crystals seemed to have formed on the surface. In the measurement program of the MCR 3, the first step is the rinsing of the flow cell. Nevertheless, a quick washing step after spotting was tested. The chip wafer was dipped in ddH_20 under moderate shaking for 20 seconds. Surprisingly, as can be seen in Figure 29 this resulted in a drastic increase of signal intensity. When measuring the chips without washing (Figure 29, A), a concentration of 5 mg/ml of diclofenac in the spotting buffer resulted in the highest signal intensity with 17,800. When the chips were washed before the measurements (Figure 29, B), 10 mg/ml diclofenac in the spotting buffer yielded the highest intensity with 22,100. This is an increase of signal intensity of 20%. In each measurement, antibody bound to loose analyte must have been washed away, therefore rendering the signal smaller than it could have been. By previously washing away any loose analyte, this artefact could be avoided. Another notable fact is the reduction of the standard deviation if the chips were washed (Figure 29, B). Likely, the standard deviation without washing mainly results from washing away of the analyte during the measurements. By adding the washing procedure, this step was already done before measurements took place, therefore allowing a more stable signal for multiple measurements. In this experiment, the primary antibody concentration was increased from 1:1,500 to 1:100 as well, explaining the overall increase of maximum signal intensity in comparison to previous experiments.

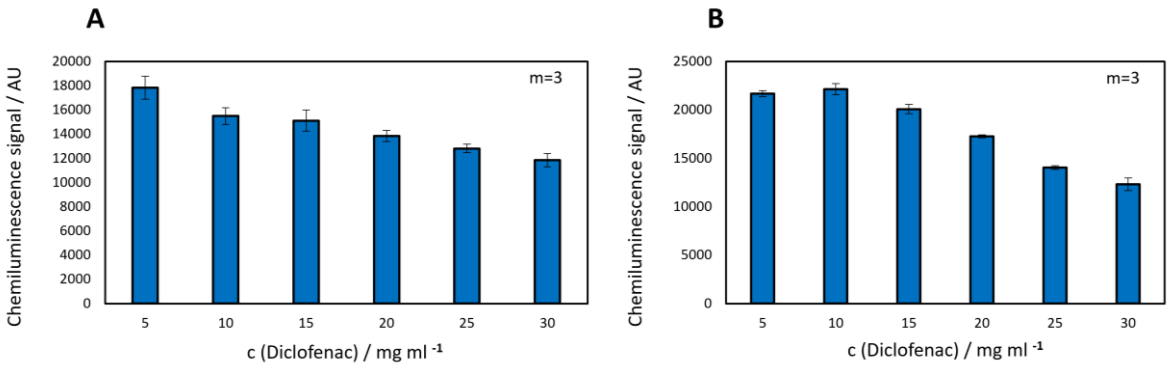

Figure 29: Bar plots showing the signal intensities of polycarbonate chips with and without a washing procedure before measuring. Chips were either measured according to the standard protocol **A** or washed in water for 20 seconds beforehand **B**. The concentrations depicted on the x-axes are the concentrations of diclofenac in the spotting buffer. The signal intensities are depicted as chemiluminescence signals in AU. Every bar represents three consecutive measurements on the same chip including standard deviations.

5.1.5. Regenerability analysis with optimized conditions

The sensitivity performance of such assays strongly depends on the regenerability of the surface. As in the previous experiments the signals were obtained from one chip which was measured three times. It was known that the surface was in principle regenerable. In a next step, the recovery of the signal after 12 regeneration cycles was investigated with the optimized assay conditions. 12 regenerations represent the cycle number needed for a full calibration. Figure 30 shows that the blank signals before and after 12 regeneration cycles, differ by 26%. This means that only 74% of the initial signal can be recovered after 12 surface regeneration cycles which indicates that the regeneration conditions used here were not ideal for polycarbonate surfaces. The same assay on glass surfaces showed a signal loss of only 21% after 35 cycles of regeneration.[209] Possibly the conditions are too harsh and thereby remove too much of the immobilized analyte and decreasing the sensitivity over time. In future work, other regeneration buffer compositions may be tested.

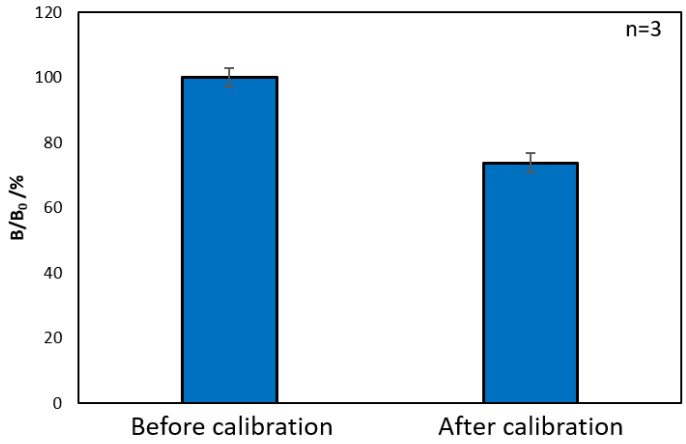

Figure 30.: Recovery of the signal on polycarbonate chips after 12 cycles of regeneration. Blank signals before and after calibration measurements are depicted. Maximum signal intensity before the calibration was set as B_0. Chemiluminescence signal intensities are depicted as B/B_0. Bars are mean values of three chips (n=3) including standard deviations.

5.1.6. Calibration with optimized conditions

Knowing which of the tested conditions yielded the highest signal, a calibration experiment was performed in order to assess the sensitivity of the system. For a 10-point calibration, at least 13 measurements per chip are needed. In this experiment, 3 chips were measured for 15 times each. The first two measurements were blank and were discarded. The last three measurements were blank again, of which the first two were discarded due to residual analyte in the system. This last blank measurement was compared to the first one in order to assess the signal recovery shown in Figure 30. In between these blank measurements, the calibration samples were measured. The concentrations of diclofenac in the samples ranged from 0.001 to 1,000 µg/L. The resulting calibration curve is depicted in Figure 31. The LoD of this assay lies at 0.174 µg/L with a working range from 0.300 – 1.850 µg/L and an IC_{50} at 0.745 µg/L. This shows that, unfortunately, in comparison to glass chips, the LoD and the IC_{50} did not improve much. Table 7 shows the direct comparison of the values. In conclusion, this means that an increase of analyte concentration on the surface does not directly result in a higher sensitivity but nevertheless a regenerable assay was successfully implemented on polycarbonate chips for the first time.

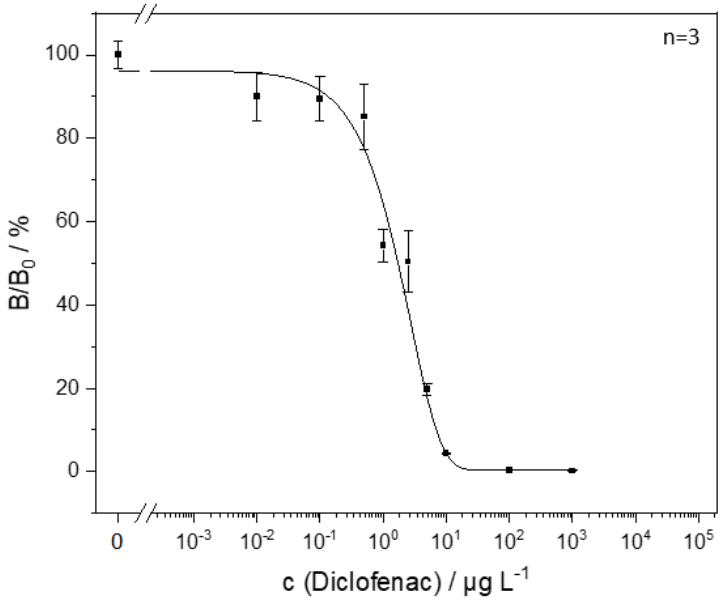

Figure 31: Calibration curve with optimized conditions for polycarbonate chips. Blank signal was set as B_0. Chemiluminescence signal intensities are depicted as B/B_0. Dots are mean values of three chips (n=3) including standard deviations.

Table 7.: Comparison of limits of detection and IC_{50} values of indirect competitive immunoassays performed by ELISA or on glass or polycarbonate chips on the MCR 3. The same primary antibody was used in all assays.[58,209]

	LoD (µg/L)	IC50 (µg/L)
ELISA (waste water)	0.08	0.04
Glass chips (milk)	0.26	1.0
Polycabonate chips (milk)	0.17	0.75

When it comes to the lower sensitivity, previous experiments with this assay on glass surfaces showed that analyte-antibody interaction times could be excluded as reasons as well as secondary antibody quantitiy.[209] As already mentioned in the theoretical background section,

the reaction mechanism of an ELISA is quite different to the flow-based assay format performed on the chip surfaces. There are several possible reasons why the antibody could perform better in ELISA assays. As the interaction time and surface is a lot smaller in the chip-based assay, no equilibrium can be formed between the primary antibody and the analyte. Even when increasing the interaction time, as was done for glass chips[209], an equilibrium cannot be achieved simply by the nature of a microfluidic system. With these systems, interaction is only possible when antibody and analyte get into close proximity which is achieved by pumping the liquid over the surface, while in ELISA, diffusion is another route. It is possible that due to this, the antibody cannot perform equally well. The precise binding pocket of this antibody is unknown, so all assumptions are of speculative nature. However, another reason could be steric hindrance, as diclofenac in ELISA is immobilized as a BSA-conjugate. Therefore, it is attached to a large protein, creating distance to the surface of the well. This could result in a better accessibility by the antibody than when diclofenac is immobilized on the chips. By adding an additional spacer molecule to diclofenac for immobilization, this hypothesis could be tested in the future.

6. Conclusion and outlook

6.1. Summary and outlooks on the research topics of this work

Modern human life leaves imprints on our surroundings everywhere. The air we breathe, the water we drink and the food we consume is often contaminated with residuals from daily industrialized life. This thesis looked at three areas where human health is affected by contaminants of different kinds. And even though the topics, mycotoxin producers in air, antibiotic resistant bacteria in water and pharmaceuticals in food are very different, they all represent areas where monitoring and surveillance are important. With the development of three chemiluminescence bioassays to detect the latter this work contributed to the pressing need of fast, automated, on site, easy to use methods for environmental surveillance.

6.1.1. Summary and outlook on the haRPA-based detection method for mycotoxin producers

Monitoring tools which deliver reliable, quantitative results are needed for modern mold analytics. This work introduced a culture-independent molecular biological technique for this purpose. By using a flow-based chemiluminescence haRPA assay for the detection of zearalenone producers, a method which can produce quantitative results was developed. A primer set targeting a conserved zearalenone biosynthesis gene was confirmed to be specific using *F. culmorum* as model zearalenone producer. After this, the assay was transferred from glass to polycarbonate surfaces which are faster, cheaper and easier to produce. In order to be as realistic as possible for calibration, a workflow was established. Pure spore suspensions of *F. culmorum* were generated in order to mimic bioaerosol samples. Instead of kit-based DNA extraction which is often more cost and time intensive, the spore suspensions were mechanically and enzymatically lysed. The lysis supernatants were used as templates for haRPA reactions. By generation of a dose-response curve, a sigmoidal correlation between chemiluminescence signal and the log of the spore concentration was shown. The LoD of the assay was determined to be 2.7×10^5 spores/ml. This result shows that the method is usable for risk assessment in medium to highly contaminated environments. In the future, the primer set will have to be tested on more zearalenone producers and bioaerosol samples of indoor air. A second zearalenone producer, namely *F. oxysporum*, which is often present in indoor air, was tested with the primer set and showed positive results as well. However, signal intensities were very different for this species. This points at a common problem regarding the simultaneous detection of different mold species. The lysis efficiencies of spores of different species can vary a lot as well as the quantity of DNA they contain. As there are too many potential indoor mold species to cover all of them, a powerful analytical tool might need to be calibrated with all relevant species. Additionally, preliminary experiments, testing a trichothecene producer-specific primer set showed promising results in prospect of a multiplex mycotoxin producer chip. In the future, a number of different primer sets could be immobilized on the chip surface, creating a mycotoxin producer chip which, enables the

simultaneous detection of various organism types. If a mycotoxin producer would be identified, other methods could be used to assess the presence of mycotoxins. This assay might be a powerful tool in combination with bioaerosol collection, especially with impingement and impaction methods. Once microorganisms are captured in a liquid or in a gel-like substance, the lysis protocol of this method is the ideal follow-up. Testing this theory would be the next step in development of its applicability for environmental surveillance. To be applicable on-site, it would be very useful to miniaturize the device and automate the whole method. The here presented assay has great potential for reliable on-site risk assessment of mold contamination.

6.1.2. Summary and outlook on the colony-fusion-haRPA workflow for the detection of ARGs and their hosts

By development of the colony-fusion-haRPA method, a monitoring technique for resistance genes and their carrying species was created. The major novel aspects of this method are the start from colonies instead of DNA extracts and the fusion product formation, both using RPA. The use of colony RPA makes this method especially easy-to-use in combination with standard environmental sampling techniques. Fusion product formation enabled the simultaneous detection of both the resistance gene and the carrying species which is difficult with standard molecular biological methods. In this proof-of-principle study, *E. coli* and *K. pneumoniae* carrying CTX-M genes of the cluster 1 were chosen as targets. During the development of the primer system for the colony-fusion-haRPA workflow it became clear that the *K. pneumoniae* primer set would need further improvement. Therefore, the assay development was continued using only *E. coli*. The final workflow was confirmed to be specific for *E. coli* carrying CTX-M cluster 1 resistance genes. A cutoff value of 17% above which samples could be classified as CTX-M cluster 1 containing *E. coli* could be set without compromise of false-negative or false-positive samples. When environmental samples were analyzed with the colony-fusion-haRPA method, they were classified correctly indicating the applicability of the

method for environmental monitoring. One of the main advantages of the chip system used in this study is their multiplex-ability. In the future, a chip as exemplary shown in Figure 32 which can determine multiple CTX-M cluster 1 carriers, is meant to be developed.

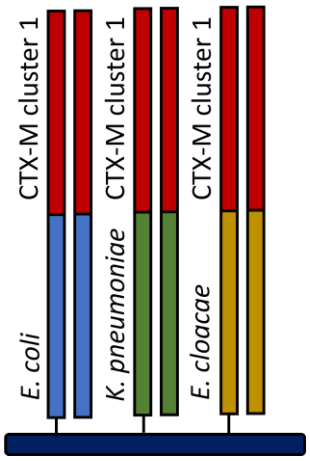

Figure 32.: Exemplary scheme of a multiplex chip to detect CTX.M cluster 1 resistance genes in multiple species

For this purpose, the primer set which was successfully tested for fusion product formation with homogeneous RPA for *K. pneumoniae* can be optimized. Another interesting species would be *E. cloacae*. The more species are included, the more challenging the development of the primer system becomes but also the more useful it will be for monitoring purposes. The surveillance of gene transfer events in particular water settings would be a powerful use for this method. By monitoring how genes distribute one might even be able to prevent or to react to clinical outbreaks. A miniaturization of the MCR 3 would further increase the in-field applicability of the system. A fully portable device would be particularly useful for a method such as this. An automated colony-fusion-haRPA workflow on a miniaturized MCR 3 would be a good basis for further development of new assays and applications for this method. Not only environmental monitoring but also food safety and diagnostics could be good candidate fields for the colony-fusion-haRPA.

6.1.3. Summary and outlook on the development of a chip-based, regenerable immunoassay on polycarbonate surfaces for diclofenac

The aim of this project was the transfer of a regenerable immunoassay for the detection of diclofenac from glass to polycarbonate surfaces and to investigate its behavior and properties. Firstly, different coating conditions of polycarbonate chips with Jeffamine® were tested for their highest maximum signal, transparency and homogeneity. Here, an incubation of chips with 90% Jeffamine® overnight at 70 °C was chosen. Next, different spotting buffer compositions were tested but remained unchanged as the original one performed best. Also, a washing step was introduced after spotting which resulted in an increase of the maximum signal of 20%. During these experiments, different concentrations of diclofenac in the spotting buffer were tested, too. The best composition, yielding the highest maximum signal resulted to contain 5 mg/ml diclofenac. With these optimized conditions, a calibration experiment was performed. The sensitivity of the system with 0.174 µg/L as LoD and 0.745 µg/L as IC_{50} did only yield a small improvement to the previous assay on glass. Reasons for this can be numerous. The assay principle is different to ELISA and so is the antibody performance and the analyte immobilization. Missing equilibrium formation and steric hindrances are possible reasons. On top of this, the calibration experiment also showed that after 14 cycles of surface regeneration, only 74% of the initial maximum signal could be recovered. Improving regenerability could also increase the sensitivity. In the future, placing a spacer molecule between diclofenac and the surface as well as changing the regeneration buffer composition may be tested.

6.2. Outlook on the MCR 3 as platform for molecular biological- and immunoassays for environmental monitoring

The MCR 3 has had its breakthrough in analytics in 2009, when an assay for the simultaneous detection of 13 different antibiotics in bovine milk was developed.[48] This assay and the MCR 3 have then been used by the Bavarian Association for raw milk testing (Milchprüfring Bayern e.V.) to monitor antibiotics in raw milk. Since then, the look and setup of the MCR 3 for immunoassays has much improved, as the Legiotyper (MCR-R) has been developed by GWK Präzisionstechnik.[210] For this system, an assay for the rapid detection of *Legionella* has been successfully developed (unpublished) and a Covid-19 antibody test is on its way. DNA-based haRPA assays have only ever been performed on the original MCR 3[20,21,23,27,28] but in the future this will be changed. This work showed how valuable haRPA can be for environmental monitoring purposes. Successful monitoring includes an easy-to use and portable device. Unlike immunoassays, haRPA measurements do not require a complex microfluidic system, as the amplification reaction itself is static. If reproducible enough, an injection of the sample into the chip by hand could be considered for this purpose as well. Although, automatic sample preparation would be more interesting for potential users. Including the lysis step in the device would enable the assay to be fully independent from laboratory equipment. In the case of spore lysis, this could pose a problem, as spores need to be lysed mechanically which could be tested to be exchanged by cycles of boiling and freezing. In the case of colony-lysis this is easier as only enzymes need to be added or a single boiling step performed. The separation of the cell debris from the supernatant poses another challenge. An alternative to centrifugation could be achieved by pressure-based pumping of the lysis extract through a filter, allowing only the DNA containing supernatant to pass.[211] A miniaturized MCR 3 would therefore need to be able to heat and cool samples, to add reagents to them and to separate supernatants from cell debris. If the sample sizes would be miniaturized this could be achieved by using lab-on-a-chip type systems where reagents are stored in small cavities in chips and are then mixed together by microfluidics. Thermal reactions can be achieved by using heating wires and solutions can be mixed together by pumping and use of vents and

valves.[212] By decreasing the reaction volume, also the sample amount decreases, so sensitivity would have to be investigated in detail. The detection of the chemiluminescence could be achieved by a miniature CCD camera[211,213] which could be attached to a smartphone or tablet for evaluation. An exemplary potential microchip is shown in Figure 33. A new haRPA-MCR system designed like this would be a valuable tool for environmental analytics as well as for diagnostics.

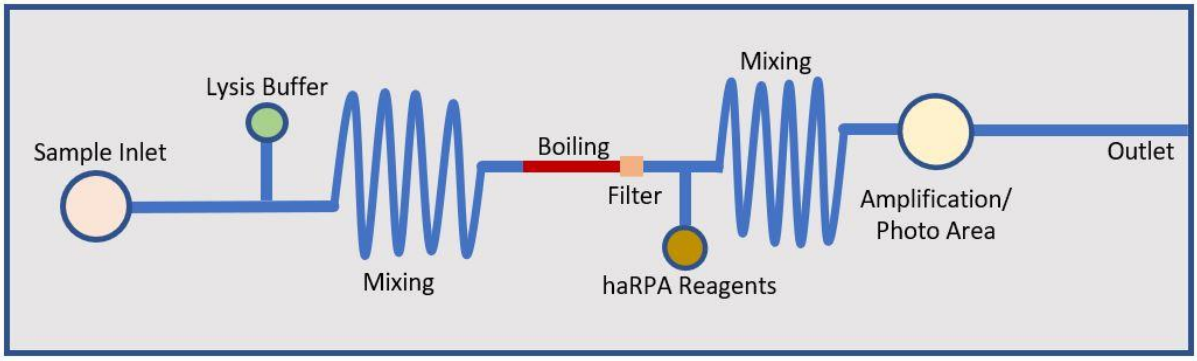

Figure 33: Scheme of an exemplary microchip for haRPA applications. The untreated sample could be injected into the inlet. Thereafter it is mixed with the lysis buffer in a mixing loop. After that, boiling would occur in a channel lined with a heatable wire. The cell debris would be separated from the supernatant by a filter. After that, the supernatant would be combined with the haRPA reagents in another mixing loop. The amplification reaction would occur in a slightly bigger space which could or could not have clusters of different immobilized primers for multiplexing. The micro-CCD camera would be placed directly above in order to record the amplification real time by taking pictures every few seconds.

7. Materials and instrumentation

7.1. Devices

Device	Manufacturer
Autoclave (Laboklav SHP)	Satuelle, Germany
Beakers	Schott (Mainz, Germany)
Bench-top centrifuge	Carl Roth (Karlsruhe, Germany)
BioOdyssey™ Calligrapher™ Miniarrayer	Bio-Rad (Eschwege, Germany)
Blue Light Table	SERVA electrophoresis GmbH (Heidelberg, Germany)
Bottles	Schott (Mainz, Germany)
Centrifuge 5804 R	Eppendorf (Hamburg, Germany)
Cutting Plotter CE6000-40	Graphtec (Yokohama, Japan)
DNA/RNA UV-Box	SIA biosan (Riga, Latvia)
Drying cabinet	Memmert (Schwabach, Germany)
Electrophoresis system	Bio-Rad (Feldkirchen, Germany)
Gel electrophoresis unit	Bio-Rad Laboratories (Munich, Germany)
Glass slide holder for staining trough	Kartell Labware (Noviglio, Italy)
Hemocytometer	Carl Roth (Karlsruhe, Germany)
Ice machine	Wessamat (Kaiserslautern, Germany)
Incubator	Heraeus (Hanau, Germany)
Incubator	Brunswick scientific (Nürtingen, Germany)
Incubator	Memmert (Büchenbach, Germany)
LightCycler 480	Roche Diagnostics GmbH (Mannheim, Germany)
Magnetic stirrer	Heidolph (Schwabach, Germany)
Magnetic stirrer	IKA Labortechnik (Staufen im Breisgau, Germany)
MCR 3	GWK Präzisionstechnik (Munich, Germany)
Microchip assembly equipment	Institute of Hydrochemistry (Munich, Germany)
Microscope	Leica (Wetzlar, Deutschland)
Microwave	Lidl (Neckarsulm, Deutschland)
Milli-Q plus 185	Millipore (Bedford, MA, USA)
Nano-Photometer	IMPLEN (München, Germany)
pH-Meter	Mettler-Toledo (Columbus, USA)
Pipettes	Eppendorf (Hamburg, Germany)
Precision balance	Mettler (Columbus, OH, USA)
Rotary evaporator	Büchi (Flawil, Schweiz)
Scale	Kern (Balingen, Germany)
sciFLEXARRAYER S1	Scienion AG (Berlin, Germany)
Signograph	Proxxon (Föhren, Deutschland)
Staining trough	Kartell Labware (Noviglio, Italy)
Sterile bench	BCK Luft- & Reinraumtechnik GmbH (Sonnenbühl-Genkingen, Germany)

Sterile bench	Kendro Laboratory Products GmbH (Langenselbold, Germany)
ThermoMixer C	Eppendorf (Hamburg, Germany)
Ultrasonic bath Sonorex RK510S	Bandelin (Berlin, Germany)
Vortexer	Fisher Scientific (Pittsburgh, PA, USA)

7.2. Consumables

Consumable	Catalog number	Manufacturer
Autoclave bags SEKUROKA®	Carl Roth: E706.1	Carl Roth (Karlsruhe, Germany)
Balloons ROTILABO®	Carl Roth: 0933.1	Carl Roth (Karlsruhe, Germany)
Boxes for glass slides ROTILABO®	Carl Roth: T208.1	Carl Roth (Karlsruhe, Germany)
Canula: size 1, G 20 × 1 ½" / ø 0,90 × 40 mm, size 2, G 21 × 1 ½" / ø 0,80 × 40 mm, Sterican®	Carl Roth: X134.1, C721.1	B. Braun (Melsungen, Germany)
Centrifuge tubes PP, 15 ml, 50 ml	Carl Roth: AN77.1, AN79.1	Kartell Labware (Noviglio, Italy)
Double-sided adhesive tape ARcare, Acryl-Hybrid	90106	Adhesive Research Ireland (Limerick, Ireland)
Foldable canister ROTILABO® 10 L	Carl Roth: N369.1	Carl Roth (Karlsruhe, Germany)
Glass slides, soda lime glass, 26 × 76 × 1 mm, ± 0.1 mm	Carl Roth: 0656.1	Marienfeld Laboratory Glassware (Lauda-Königshofen, Germany)
LightCycler 480 Multiwell plate 96		Roche Diagnostics GmbH (Mannheim, Germany)
Lysing Matrix E, 2 ml	MP: 116914050-CF	MP Biomedicals (Eschenwege, Deutschland)
Parafilm®	Merck: P6543	Sigma-Aldrich (Taufkirchen, Germany)
Petri dishes glass	Carl Roth: 0690.1	Carl Roth (Karlsruhe, Germany)
Petri dishes PS	Carl Roth: N221.2	Carl Roth (Karlsruhe, Germany)
PCR-tubes Mμlti®, 200 µl, 500µl	Carl Roth: H560.1, A774.1	Sorenson BioScience (Salt Lake City, Utah, USA)
PCR-tubes ROTILABO®	Carl Roth: CEL6.1	Carl Roth (Karlsruhe, Germany)
Pipet tips 0.1-10 µl, 10-100 µl, 100-1000 µl, **1-5 ml**	Carl Roth: K138.1, 2395.2, 2679.1, 5846.1	Carl Roth (Karlsruhe, Germany)
PMMA carriers with inlets and outlets for flow cells		Institute of Hydrochemistry (Munich, Germany)

Polycarbonate sheets 1 mm Makrolon®		Covestro AG (Leverkusen, Germany)
Sample beakers with screw closure	Carl Roth: PT10.1	Boettger (Bodenmais, Germany)
sciSOURCEPLATE-384-PP		Scienion AG (Berlin, Germany)
Sealing-films ROTILABO®	Carl Roth: EN82.1	Carl Roth (Karlsruhe, Germany)
Single use syringes, BD Plastipak™ Luer-Lock, PP, 50 mL	300865	Becton Dickinson (Franklin Lakes, NJ, USA)
Single use syringes Inkjet® PP/PS, 1 mL, 5 mL and 25 mL	Carl Roth: 0056.1, 0057.1, 0058.1, 0059.1	B. Braun (Melsungen, Germany)
Single use pasteur pipettes 5 ml	Carl Roth: EA61.1	
Snap cap vials 5 mL, 10 mL, 25 mL	Carl Roth: CLA8.1, CLA3.1, CLC1.1	Hecht Glaswarenfabrik (Sondheim vor der Rhön, Germany)
Syringe filters 0,22 µM ROTILABO®	Carl Roth: P668.1	Carl Roth (Karlsruhe, Germany)

7.3. Chemicals

Chemical	Catalog number	Manufacturer
(3-Glycidyloxypropyl)-trimethoxysilane (GOTPS)	440167	Sigma-Aldrich (Taufkirchen, Germany)
1,1'-Carbonyldiimidazole	6992	Carl Roth (Karlsruhe, Germany)
1,4-Dioxane	1601521	Sigma-Aldrich (Taufkirchen, Germany)
4-(2-hydroxyethyl)-1-piperazineethane-sulfonic acid	ENAH93E75468	Sigma-Aldrich (Taufkirchen, Germany)
Acetonitrile	1012699	Sigma-Aldrich (Taufkirchen, Germany)
Agar Agar	2266	Carl Roth (Karlsruhe, Germany)
Agarose	2267	Carl Roth (Karlsruhe, Germany)
Bovine Serum Albumine	A7030	Sigma-Aldrich (Taufkirchen, Germany)
Casein (from milk)	C3400	Sigma-Aldrich (Taufkirchen, Germany)
Cefotaxime	C0685000	Sigma-Aldrich (Taufkirchen, Germany)
Chloramphenicol	3886	Carl Roth (Karlsruhe, Germany)
Diclofenac sodium salt	D6899	Sigma-Aldrich (Taufkirchen, Germany)

Diethylamine	KK00	Carl Roth (Karlsruhe, Germany)
Dimethylaminopyridine (DMAP)	107700	Sigma-Aldrich (Taufkirchen, Germany)
Dimethylformamide (DMF)	227056	Sigma-Aldrich (Taufkirchen, Germany)
Dipotassium hydrogen phosphate	9683	Carl Roth (Karlsruhe, Germany)
Disuccinimidyl-carbonate (DSC)	43720	Sigma-Aldrich (Taufkirchen, Germany)
DNA ladder, 50 bp	B7025	New England Biolabs (Ipswich, USA)
DNA Stain Clear G	39804	Serva Electrophoresis GmbH (Heidelberg, Germany)
EDTA	8043	Carl Roth (Karlsruhe, Germany)
Ethanol, ≧ 99.8%	493511	Sigma-Aldrich (Taufkirchen, Germany)
EZ-Link™ amine-PEG_2-biotin	21346	Thermofisher Scientific (Waltham, MA, USA)
Glacial acetic acid	6755	Carl Roth (Karlsruhe, Germany)
Glucose	HN06	Carl Roth (Karlsruhe, Germany)
Glycerin	3783	Carl Roth (Karlsruhe, Germany)
Glycine	3783	Sigma-Aldrich (Taufkirchen, Germany)
Hellmanex III	9-307-011-4-507	Hellma GmbH (Mühlheim, Germany)
Hydrochloric acid, 37%	258148	Sigma-Aldrich (Taufkirchen, Germany)
Hydrogen peroxide, Westar Supernova	XLS3	Cyanagen (Bologna, Italy)
Jeffamine ED-2003	14529	Sigma-Aldrich (Taufkirchen, Germany)
LB Media	6669	Carl Roth (Karlsruhe, Germany)
Luminol, Westar Supernova	XLS3	Cyanagen (Bologna, Italy)
Magnesium chloride	M8266	Sigma-Aldrich (Taufkirchen, Germany)
Malt Extract	X976	Carl Roth (Karlsruhe, Germany)
Methanol	34860	Sigma-Aldrich (Taufkirchen, Germany)

Methyl tertiary butyl ether (MTBE), 99.8%	306975	Sigma-Aldrich (Taufkirchen, Germany)
Nuclease-free water	AM9932	Invitrogen AG (Carlsbad, USA)
Peptone	2832	Carl Roth (Karlsruhe, Germany)
Pluronic F 68	24040032	Thermofisher Scientific (Waltham, MA, USA)
Polyglycerol-3-glycidyl-ether (CL9)	CL 9	Ipox chemicals (Laupheim, Germany)
Potassium dihydrogen phosphate	P0662	Sigma-Aldrich (Taufkirchen, Germany)
Potassium sulfate	X889	Carl Roth (Karlsruhe, Germany)
Proteinase K	7528	Carl Roth (Karlsruhe, Germany)
RNAse A	7156	Carl Roth (Karlsruhe, Germany)
sciClean 8	C-5283	Scienion AG (Berlin, Germany)
Sodium azide	S2002	Sigma-Aldrich (Taufkirchen, Germany)
Sodium carbonate	S7795	Sigma-Aldrich (Taufkirchen, Germany)
Sodium chloride	3957	Carl Roth (Karlsruhe, Germany)
Sodium dodecyl sulfate	L3771	Sigma-Aldrich (Taufkirchen, Germany)
Sodium hydrogen carbonate	S5761	Sigma-Aldrich (Taufkirchen, Germany)
Sodium hypochlorite,	6846	Carl Roth (Karlsruhe, Germany)
Sodium thiosulfate	72049	Sigma-Aldrich (Taufkirchen, Germany)
Streptavidin horseradish peroxide	VEC-SA-5004	Biozol (Eching, Germany)
Sulfuric acid, 97%	07208-M	Sigma-Aldrich (Taufkirchen, Germany)
TE-buffer	12090015	Thermofisher Scientific (Waltham, MA, USA)
Toluene, 99.8%	244511	Sigma-Aldrich (Taufkirchen, Germany)
Trehalose	8897	Carl Roth (Karlsruhe, Germany)
Triethylamine	T0886	Sigma-Aldrich (Taufkirchen, Germany)

Tris(hydroxymethyl)-aminomethane	252859	Sigma-Aldrich (Taufkirchen, Germany)
Triton X-100	X100	Sigma-Aldrich (Taufkirchen, Germany)
Tween®-20	9127	Carl Roth (Karlsruhe, Germany)
Yeast Extract	2904	Carl Roth (Karlsruhe, Germany)

7.4. Reaction Kits

Reaction Kit	Manufacturer
InnuSPEED Bacteria/FUNGI DNA Kit	Analytik Jena AG (Jena, Deutschland)
Monarch® PCR & DNA Cleanup Kit	New England Biolabs (Ipswich, USA)
Monarch® DNA Gel Extraction Kit	New England Biolabs (Ipswich, USA)
Phusion® High-Fidelity PCR Kit	New England Biolabs (Ipswich, USA)
QIAamp DNA Mini Kit	QIAGEN (Hilden, Germany)
Taq PCR Kit	New England Biolabs (Ipswich, USA)
TwistDx RPA Basic Kit	TwistDx™ Limited (Cambridge, UK)

7.5. Software

Software	Developer
ApE	M. Wayne Davis
Avis FITS Viewer	MSB di F. Cavicchio (Ravenna, Italy)
BioOdyssey Calligrapher 2.0	Bio-Rad Laboratories (München, Germany)
BLAST®, blastn suite	National Center for Biotechnology Information (Rockville Pike, USA)
ChemDraw Professional 19	PerkinElmer (Waltham, MA, USA)
CLC Genomics Workbench 12	Quiagen (Hilden, Germany)
GIMP	Spencer Kimball, P. Mattis
Image J 1.49	Rasband (NIH, Bethesda, USA)
MCRImageAnalyzer	GWK Präzisionstechnik (Munich, Germany)
MCR_Spot_Reader	Stefan Weißenberger in collaboration with the institute of Hydrochemistry (Munich, Germany)
Microsoft Excel 2016	Microsoft (Redmond, WA, USA)
Microsoft Power Point 2016	Microsoft (Redmond, WA, USA)
Microsoft Word 2016	Microsoft (Redmond, WA, USA)
Multiple Primer Analyzer	ThermoFisher Scientific
Oligo Calc	University of Pittsburgh, School of Medicine
Origin 2017 – 2020	OriginLab (Northampton, MA, USA)

8. Abbreviations

ARG	Antibiotic resistance gene
CCD	Charge coupled device
CFU	Colony forming units
DNA	Deoxyribonucleic acid
dsDNA	Double stranded DNA
DSC	N,N-dissucinimidylcarbonate
ELISA	Enzyme-linked immunosorbent assay
EU	European Union
ESBL	Extended spectrum β-lactamase
FAO	Food and Agriculture Organization
haRPA	Heterogeneous asymmetric recombinase polymerase amplification
HPLC	High performance liquid chromatography
HRP	Horseradish peroxidase
IC_{50}	Half maximal inhibitory concentration
ITS	Internal transcribed spacer
LAMP	Loop-mediated isothermal amplification
LoD	Limit of detection
LB	Lysogeny broth
MCR 3	Microarray chip reader, third generation
MEA	Malt extract agar
MIA	Microarray immunoassay
MS	Mass spectrometry
NAMA	Nucleic acid amplification and microarray analysis
NAT	Nucleic acid amplification test
NCBI	National Center of Biotechnology Information
PBS	Phosphate buffered saline

PCR	Polymerase chain reaction
PEG	Polyethylene glycol
PKS4	Polyketide synthase 4
PMMA	Polymethylacrylate
qPCR	Quantitative PCR
RPA	Recombinase Polymerase Amplification
Strep	Streptavidin
TE	Tris EDTA
TTC	Threshold of toxicological concern
WHO	World Health Organisation

7 Literature

(1) Power, A. L.; Tennant, R. K.; Jones, R. T.; Tang, Y.; Du, J.; Worsley, A. T.; Love, J. Monitoring Impacts of Urbanisation and Industrialisation on Air Quality in the Anthropocene Using Urban Pond Sediments. *Front. Earth Sci.* **2018**, *6*, 131. https://doi.org/10.3389/feart.2018.00131.

(2) Waters, C. N.; Zalasiewicz, J.; Summerhayes, C.; Barnosky, A. D.; Poirier, C.; Ga uszka, A.; Cearreta, A.; Edgeworth, M.; Ellis, E. C.; Ellis, M.; Jeandel, C.; Leinfelder, R.; McNeill, J. R.; Richter, D. d.; Steffen, W.; Syvitski, J.; Vidas, D.; Wagreich, M.; Williams, M.; Zhisheng, A.; Grinevald, J.; Odada, E.; Oreskes, N.; Wolfe, A. P. The Anthropocene Is Functionally and Stratigraphically Distinct from the Holocene. *Science* **2016**, *351* (6269), aad2622–aad2622. https://doi.org/10.1126/science.aad2622.

(3) Kampa, M.; Castanas, E. Human Health Effects of Air Pollution. *Environ. Pollut.* **2008**, *151* (2), 362–367. https://doi.org/10.1016/j.envpol.2007.06.012.

(4) Schwarzenbach, R. P.; Egli, T.; Hofstetter, T. B.; von Gunten, U.; Wehrli, B. Global Water Pollution and Human Health. *Annu. Rev. Environ. Resour.* **2010**, *35* (1), 109–136. https://doi.org/10.1146/annurev-environ-100809-125342.

(5) Gwynne, M. D. The Global Environment Monitoring System (GEMS): Some Recent Developments. *Environ. Monit. Assess.* **1988**, *11* (3), 219–223. https://doi.org/10.1007/BF00394671.

(6) *Environmental Monitoring and Characterization*; Artiola, J. F., Pepper, I. L., Brusseau, M. L., Eds.; Elsevier Academic Press: Amsterdam ; Boston, 2004.

(7) UN Environment Programme-Water.

(8) UN Environment Programme-Air.

(9) Schweizer, C.; Edwards, R. D.; Bayer-Oglesby, L.; Gauderman, W. J.; Ilacqua, V.; Juhani Jantunen, M.; Lai, H. K.; Nieuwenhuijsen, M.; Künzli, N. Indoor Time–Microenvironment–Activity Patterns in Seven Regions of Europe. *J. Expo. Sci. Environ. Epidemiol.* **2007**, *17* (2), 170–181. https://doi.org/10.1038/sj.jes.7500490.

(10) Haleem Khan, A. A.; Mohan Karuppayil, S. Fungal Pollution of Indoor Environments and Its Management. *Saudi J. Biol. Sci.* **2012**, *19* (4), 405–426. https://doi.org/10.1016/j.sjbs.2012.06.002.

(11) World Health Organization. WHO publishes list of bacteria for which new antibiotics are urgently needed https://www.who.int/en/news-room/detail/27-02-2017-who-publishes-list-of-bacteria-for-which-new-antibiotics-are-urgently-needed.

(12) Dasenaki, M. E.; Thomaidis, N. S. Multi-Residue Determination of 115 Veterinary Drugs and Pharmaceutical Residues in Milk Powder, Butter, Fish Tissue and Eggs Using Liquid Chromatography–Tandem Mass Spectrometry. *Anal. Chim. Acta* **2015**, *880*, 103–121. https://doi.org/10.1016/j.aca.2015.04.013.

(13) Lenoir, T.; Giannella, E. The Emergence and Diffusion of DNA Microarray Technology. *J. Biomed. Discov. Collab.* **2006**, *1* (1), 11. https://doi.org/10.1186/1747-5333-1-11.

(14) Affymetric-Corporate History.

(15) Ekins, R.; Chu, F. Multianalyte Microspot Immunoassay. The Microanalytical “compact Disk” of the Future. *Ann. Biol. Clin. (Paris)* **1992**, *50* (5), 337–353.

(16) Schena, M.; Shalon, D.; Davis, R. W.; Brown, P. O. Quantitative Monitoring of Gene Expression Patterns with a Complementary DNA Microarray. *Science* **1995**, *270* (5235), 467–470. https://doi.org/10.1126/science.270.5235.467.

(17) Niemitz, E. The Microarray Revolution: Microarray Technology. *Nat. Rev. Genet.* **2007**, *8* (S1), S15–S15. https://doi.org/10.1038/nrg2259.

(18) Leimanis, S.; Hernández, M.; Fernández, S.; Boyer, F.; Burns, M.; Bruderer, S.; Glouden, T.; Harris, N.; Kaeppeli, O.; Philipp, P.; Pla, M.; Puigdomènech, P.; Vaitilingom, M.; Bertheau, Y.; Remacle, J. A Microarray-Based Detection System for Genetically Modified (GM) Food Ingredients. *Plant Mol. Biol.* **2006**, *61* (1–2), 123–139. https://doi.org/10.1007/s11103-005-6173-4.

(19) Koyuncu, S.; Andersson, G.; Vos, P.; Häggblom, P. DNA Microarray for Tracing Salmonella in the Feed Chain. *Int. J. Food Microbiol.* **2011**, *145*, S18–S22. https://doi.org/10.1016/j.ijfoodmicro.2010.07.012.

(20) Sollweck, K.; Streich, P.; Elsner, M.; Seidel, M. A Chip-Based Colony Fusion Recombinase Polymerase Amplification Assay for Monitoring of Antimicrobial Resistance Genes and Their Carrying Species in Surface Water. *ACS EST Water* **2021**, acsestwater.0c00110. https://doi.org/10.1021/acsestwater.0c00110.

(21) Kober, C.; Niessner, R.; Seidel, M. Quantification of Viable and Non-Viable Legionella Spp. by Heterogeneous Asymmetric Recombinase Polymerase Amplification (HaRPA) on a Flow-Based Chemiluminescence Microarray. *Biosens. Bioelectron.* **2018**, *100*, 49–55. https://doi.org/10.1016/j.bios.2017.08.053.

(22) Taranova, N. A.; Byzova, N. A.; Zaiko, V. V.; Starovoitova, T. A.; Vengerov, Y. Yu.; Zherdev, A. V.; Dzantiev, B. B. Integration of Lateral Flow and Microarray Technologies for Multiplex Immunoassay: Application to the Determination of Drugs of Abuse. *Microchim. Acta* **2013**, *180* (11–12), 1165–1172. https://doi.org/10.1007/s00604-013-1043-2.

(23) Kunze, A.; Dilcher, M.; Abd El Wahed, A.; Hufert, F.; Niessner, R.; Seidel, M. On-Chip Isothermal Nucleic Acid Amplification on Flow-Based Chemiluminescence Microarray Analysis Platform for the Detection of Viruses and Bacteria. *Anal. Chem.* **2016**, *88* (1), 898–905. https://doi.org/10.1021/acs.analchem.5b03540.

(24) Szkola, A.; Linares, E. M.; Worbs, S.; Dorner, B. G.; Dietrich, R.; Märtlbauer, E.; Niessner, R.; Seidel, M. Rapid and Simultaneous Detection of Ricin, Staphylococcal Enterotoxin B and Saxitoxin by Chemiluminescence-Based Microarray Immunoassay. *The Analyst* **2014**, *139* (22), 5885–5892. https://doi.org/10.1039/C4AN00345D.

(25) Wutz, K.; Meyer, V. K.; Wacheck, S.; Krol, P.; Gareis, M.; Nölting, C.; Struck, F.; Soutschek, E.; Böcher, O.; Niessner, R.; Seidel, M. New Route for Fast Detection of Antibodies against Zoonotic Pathogens in Sera of Slaughtered Pigs by Means of Flow-through Chemiluminescence Immunochips. *Anal. Chem.* **2013**, *85* (10), 5279–5285. https://doi.org/10.1021/ac400781t.

(26) Kohler, C.; Dunachie, S. J.; Müller, E.; Kohler, A.; Jenjaroen, K.; Teparrukkul, P.; Baier, V.; Ehricht, R.; Steinmetz, I. Rapid and Sensitive Multiplex Detection of Burkholderia Pseudomallei-Specific Antibodies in Melioidosis Patients Based on a Protein Microarray Approach. *PLoS Negl. Trop. Dis.* **2016**, *10* (7), e0004847. https://doi.org/10.1371/journal.pntd.0004847.

(27) Sollweck, K.; Schwaiger, G.; Seidel, M. A Chemiluminescence-Based Heterogeneous Asymmetric Recombinase Polymerase Amplification Assay for the Molecular Detection of Mycotoxin Producers. *The Analyst* **2021**, 10.1039.D0AN02000A. https://doi.org/10.1039/D0AN02000A.

(28) Göpfert, L.; Elsner, M.; Seidel, M. Isothermal HaRPA Detection of BlaCTX-M in Bacterial Isolates from Water Samples and Comparison with QPCR. *Anal. Methods Adv. Methods Appl.* **2021**, *13* (4), 552–557. https://doi.org/10.1039/d0ay02000a.

(29) Belleville, E.; Dufva, M.; Aamand, J.; Bruun, L.; Clausen, L.; Christensen, C. B. V. Quantitative Microarray Pesticide Analysis. *J. Immunol. Methods* **2004**, *286* (1–2), 219–229. https://doi.org/10.1016/j.jim.2004.01.004.

(30) Shreffler, W. G.; Beyer, K.; Chu, T.-H. T.; Burks, A. W.; Sampson, H. A. Microarray Immunoassay: Association of Clinical History, in Vitro IgE Function, and Heterogeneity of Allergenic Peanut Epitopes. *J. Allergy Clin. Immunol.* **2004**, *113* (4), 776–782. https://doi.org/10.1016/j.jaci.2003.12.588.
(31) Seidel, M.; Niessner, R. Chemiluminescence Microarrays in Analytical Chemistry: A Critical Review. *Anal. Bioanal. Chem.* **2014**, *406* (23), 5589–5612. https://doi.org/10.1007/s00216-014-7968-4.
(32) Carvalho, B. High Resolution Microarray Comparative Genomic Hybridisation Analysis Using Spotted Oligonucleotides. *J. Clin. Pathol.* **2004**, *57* (6), 644–646. https://doi.org/10.1136/jcp.2003.013029.
(33) Ling, D. I.; Flores, L. L.; Riley, L. W.; Pai, M. Commercial Nucleic-Acid Amplification Tests for Diagnosis of Pulmonary Tuberculosis in Respiratory Specimens: Meta-Analysis and Meta-Regression. *PLoS ONE* **2008**, *3* (2), e1536. https://doi.org/10.1371/journal.pone.0001536.
(34) Seidel, M.; Niessner, R. Automated Analytical Microarrays: A Critical Review. *Anal. Bioanal. Chem.* **2008**, *391* (5), 1521–1544. https://doi.org/10.1007/s00216-008-2039-3.
(35) Tiede, C.; Bedford, R.; Heseltine, S. J.; Smith, G.; Wijetunga, I.; Ross, R.; AlQallaf, D.; Roberts, A. P.; Balls, A.; Curd, A.; Hughes, R. E.; Martin, H.; Needham, S. R.; Zanetti-Domingues, L. C.; Sadigh, Y.; Peacock, T. P.; Tang, A. A.; Gibson, N.; Kyle, H.; Platt, G. W.; Ingram, N.; Taylor, T.; Coletta, L. P.; Manfield, I.; Knowles, M.; Bell, S.; Esteves, F.; Maqbool, A.; Prasad, R. K.; Drinkhill, M.; Bon, R. S.; Patel, V.; Goodchild, S. A.; Martin-Fernandez, M.; Owens, R. J.; Nettleship, J. E.; Webb, M. E.; Harrison, M.; Lippiat, J. D.; Ponnambalam, S.; Peckham, M.; Smith, A.; Ferrigno, P. K.; Johnson, M.; McPherson, M. J.; Tomlinson, D. C. Affimer Proteins Are Versatile and Renewable Affinity Reagents. *eLife* **2017**, *6*. https://doi.org/10.7554/eLife.24903.
(36) Moran, G. Comparative Genomics Using Candida Albicans DNA Microarrays Reveals Absence and Divergence of Virulence-Associated Genes in Candida Dubliniensis. *Microbiology* **2004**, *150* (10), 3363–3382. https://doi.org/10.1099/mic.0.27221-0.
(37) Vora, G. J.; Meador, C. E.; Stenger, D. A.; Andreadis, J. D. Nucleic Acid Amplification Strategies for DNA Microarray-Based Pathogen Detection. *Appl. Environ. Microbiol.* **2004**, *70* (5), 3047–3054. https://doi.org/10.1128/AEM.70.5.3047-3054.2004.
(38) Nagl, S.; Schaeferling, M.; Wolfbeis, O. S. Fluorescence Analysis in Microarray Technology. *Microchim. Acta* **2005**, *151* (1–2), 1–21. https://doi.org/10.1007/s00604-005-0393-9.
(39) Cooper, M.; Ebner, A.; Briggs, M.; Burrows, M.; Gardner, N.; Richardson, R.; West, R. Cy3B™: Improving the Performance of Cyanine Dyes. *J. Fluoresc.* **2004**, *14* (2), 145–150. https://doi.org/10.1023/B:JOFL.0000016286.62641.59.
(40) Panchuk-Voloshina, N.; Haugland, R. P.; Bishop-Stewart, J.; Bhalgat, M. K.; Millard, P. J.; Mao, F.; Leung, W.-Y.; Haugland, R. P. Alexa Dyes, a Series of New Fluorescent Dyes That Yield Exceptionally Bright, Photostable Conjugates. *J. Histochem. Cytochem.* **1999**, *47* (9), 1179–1188. https://doi.org/10.1177/002215549904700910.
(41) Worsfold, P. J.; Townshend, A.; Poole, C. F. *Encyclopedia of Analytical Science*; Elsevier: S.l., 2010.
(42) Yu, X.; Xu, D.; Cheng, Q. Label-Free Detection Methods for Protein Microarrays. *PROTEOMICS* **2006**, *6* (20), 5493–5503. https://doi.org/10.1002/pmic.200600216.
(43) Cesewski, E.; Johnson, B. N. Electrochemical Biosensors for Pathogen Detection. *Biosens. Bioelectron.* **2020**, *159*, 112214. https://doi.org/10.1016/j.bios.2020.112214.
(44) Liu, M.; Lin, Z.; Lin, J.-M. A Review on Applications of Chemiluminescence Detection in Food Analysis. *Anal. Chim. Acta* **2010**, *670* (1–2), 1–10. https://doi.org/10.1016/j.aca.2010.04.039.

(45) Fortunato, A. DSC: History, Instruments and Devices. In *Drug-Biomembrane Interaction Studies*; Elsevier, 2013; pp 169–212. https://doi.org/10.1533/9781908818348.169.
(46) Roda, A.; Guardigli, M.; Pasini, P.; Mirasoli, M.; Michelini, E.; Musiani, M. Bio- and Chemiluminescence Imaging in Analytical Chemistry. *Anal. Chim. Acta* **2005**, *541* (1–2), 25–35. https://doi.org/10.1016/j.aca.2004.11.083.
(47) Kricka, L. J.; Park, J. Y. Assay Principles in Clinical Pathology. In *Pathobiology of Human Disease*; Elsevier, 2014; pp 3207–3221. https://doi.org/10.1016/B978-0-12-386456-7.06302-4.
(48) Kloth, K.; Rye-Johnsen, M.; Didier, A.; Dietrich, R.; Märtlbauer, E.; Niessner, R.; Seidel, M. A Regenerable Immunochip for the Rapid Determination of 13 Different Antibiotics in Raw Milk. *The Analyst* **2009**, *134* (7), 1433–1439. https://doi.org/10.1039/b817836d.
(49) Weißenberger, S. MCR_Spot_Reader Software, 2019. https://github.com/swbg/MCR-Spot-Reader
(50) Weller, M. G.; Schuetz, A. J.; Winklmair, M.; Niessner, R. Highly Parallel Affinity Sensor for the Detection of Environmental Contaminants in Water1Parts of This Work Were Presented at the Fifth World Congress on Biosensors, Berlin, Germany, 1998.1. *Anal. Chim. Acta* **1999**, *393* (1–3), 29–41. https://doi.org/10.1016/S0003-2670(98)00855-1.
(51) Knecht, B. G.; Strasser, A.; Dietrich, R.; Märtlbauer, E.; Niessner, R.; Weller, M. G. Automated Microarray System for the Simultaneous Detection of Antibiotics in Milk. *Anal. Chem.* **2004**, *76* (3), 646–654. https://doi.org/10.1021/ac035028i.
(52) Donhauser, S. C.; Niessner, R.; Seidel, M. Quantification of E. Coli DNA on a Flow-through Chemiluminescence Microarray Readout System after PCR Amplification. *Anal. Sci.* **2009**, *25* (5), 669–674. https://doi.org/10.2116/analsci.25.669.
(53) Meyer, V. K.; Meloni, D.; Olivo, F.; Märtlbauer, E.; Dietrich, R.; Niessner, R.; Seidel, M. Validation Procedure for Multiplex Antibiotic Immunoassays Using Flow-Based Chemiluminescence Microarrays. *Methods Mol. Biol. Clifton NJ* **2017**, *1518*, 195–212. https://doi.org/10.1007/978-1-4939-6584-7_13.
(54) Wutz, K.; Niessner, R.; Seidel, M. Simultaneous Determination of Four Different Antibiotic Residues in Honey by Chemiluminescence Multianalyte Chip Immunoassays. *Microchim. Acta* **2011**, *173* (1–2), 1–9. https://doi.org/10.1007/s00604-011-0548-9.
(55) Sauceda-Friebe, J. C.; Karsunke, X. Y. Z.; Vazac, S.; Biselli, S.; Niessner, R.; Knopp, D. Regenerable Immuno-Biochip for Screening Ochratoxin A in Green Coffee Extract Using an Automated Microarray Chip Reader with Chemiluminescence Detection. *Anal. Chim. Acta* **2011**, *689* (2), 234–242. https://doi.org/10.1016/j.aca.2011.01.030.
(56) Oswald, S.; Karsunke, X. Y. Z.; Dietrich, R.; Märtlbauer, E.; Niessner, R.; Knopp, D. Automated Regenerable Microarray-Based Immunoassay for Rapid Parallel Quantification of Mycotoxins in Cereals. *Anal. Bioanal. Chem.* **2013**, *405* (20), 6405–6415. https://doi.org/10.1007/s00216-013-6920-3.
(57) Szkola, A.; Campbell, K.; Elliott, C. T.; Niessner, R.; Seidel, M. Automated, High Performance, Flow-through Chemiluminescence Microarray for the Multiplexed Detection of Phycotoxins. *Anal. Chim. Acta* **2013**, *787*, 211–218. https://doi.org/10.1016/j.aca.2013.05.028.
(58) Huebner, M.; Weber, E.; Niessner, R.; Boujday, S.; Knopp, D. Rapid Analysis of Diclofenac in Freshwater and Wastewater by a Monoclonal Antibody-Based Highly Sensitive ELISA. *Anal. Bioanal. Chem.* **2015**, *407* (29), 8873–8882. https://doi.org/10.1007/s00216-015-9048-9.
(59) Bemetz, J.; Kober, C.; Meyer, V. K.; Niessner, R.; Seidel, M. Succinylated Jeffamine ED-2003 Coated Polycarbonate Chips for Low-Cost Analytical Microarrays. *Anal. Bioanal. Chem.* **2019**, *411* (10), 1943–1955. https://doi.org/10.1007/s00216-019-01594-8.

(60) Daher, R. K.; Stewart, G.; Boissinot, M.; Bergeron, M. G. Recombinase Polymerase Amplification for Diagnostic Applications. 12.
(61) Li, J.; Macdonald, J.; von Stetten, F. Review: A Comprehensive Summary of a Decade Development of the Recombinase Polymerase Amplification. *The Analyst* **2019**, *144* (1), 31–67. https://doi.org/10.1039/C8AN01621F.
(62) Lobato, I. M.; O'Sullivan, C. K. Recombinase Polymerase Amplification: Basics, Applications and Recent Advances. *TrAC Trends Anal. Chem.* **2018**, *98*, 19–35. https://doi.org/10.1016/j.trac.2017.10.015.
(63) Hardin, B. D.; Kelman, B. J.; Saxon, A. Adverse Human Health Effects Associated with Molds in the Indoor Environment. *J. Occup. Environ. Med.* **2003**, *45* (5), 470–478. https://doi.org/10.1097/00043764-200305000-00006.
(64) *WHO Guidelines for Indoor Air Quality: Dampness and Mould*; Heseltine, E., Rosen, J., World Health Organization, Eds.; WHO: Copenhagen, 2009.
(65) Brasche, S.; Bischof, W. Daily Time Spent Indoors in German Homes – Baseline Data for the Assessment of Indoor Exposure of German Occupants. *Int. J. Hyg. Environ. Health* **2005**, *208* (4), 247–253. https://doi.org/10.1016/j.ijheh.2005.03.003.
(66) Ammann, H. M. Inhalation Exposure and Toxic Effects of Mycotoxins. In *Biology of Microfungi*; Li, D.-W., Ed.; Fungal Biology; Springer International Publishing: Cham, 2016; pp 495–523. https://doi.org/10.1007/978-3-319-29137-6_20.
(67) Ammann, H. M. Is Indoor Mold Contamination a Threat to Health? Part Two. *J. Environ. Health* **2003**, *66* (2), 47–49.
(68) Fisk, W. J.; Lei-Gomez, Q.; Mendell, M. J. Meta-Analyses of the Associations of Respiratory Health Effects with Dampness and Mold in Homes. *Indoor Air* **2007**, *17* (4), 284–296. https://doi.org/10.1111/j.1600-0668.2007.00475.x.
(69) Vennewald, I.; Wollina, U. Cutaneous Infections Due to Opportunistic Molds: Uncommon Presentations. *Clin. Dermatol.* **2005**, *23* (6), 565–571. https://doi.org/10.1016/j.clindermatol.2005.01.003.
(70) Li, D.-W.; Johanning, E.; Yang, C. S. Airborne Fungi and Mycotoxins. In *Manual of Environmental Microbiology*; Yates, M. V., Nakatsu, C. H., Miller, R. V., Pillai, S. D., Eds.; ASM Press: Washington, DC, USA, 2015; p 3.2.5-1-3.2.5-21. https://doi.org/10.1128/9781555818821.ch3.2.5.
(71) Schimmelpilzbelastung in Innenräumen – Befunderhebung, gesundheitliche Bewertung und Maßnahmen: Mitteilung der Kommission „Methoden und Qualitätssicherung in der Umweltmedizin". *Bundesgesundheitsblatt - Gesundheitsforschung - Gesundheitsschutz* **2007**, *50* (10), 1308–1323. https://doi.org/10.1007/s00103-007-0339-y.
(72) *Report No. 12: Biological Particles in Indoor Environments*; Commission of the European Communities: Luxenburg, 1994.
(73) Eduarda, W.; Heederik, D. Methods for Quantitative Assessment of Airborne Levels of Noninfectious Microorganisms in Highly Contaminated Work Environments. *Am. Ind. Hyg. Assoc. J.* **1998**, *59* (2), 113–127. https://doi.org/10.1080/15428119891010370.
(74) Klug, K.; Weidner, U.; Linsel, G.; Hebisch, R.; Martin, E.; Otto, C.; Jäckel, U. *Gefahrstoffe - Reinhaltung Der Luft*; Institut für Arbeisschutz der DGUV und VDI, 2011.
(75) Moriske, H. J.; Szewzyk, R.; Tappler, P.; Valtanen, K. *Leitfaden Zur Vorbeugung, Erfassung Und Sanierung von Schimmelbefall in Gebäuden*; Umweltbundesamt Innenraumlufthygiene-Kommission des Umweltbundesamtes, 2017.
(76) Jarvis, B. B.; Miller, J. D. Mycotoxins as Harmful Indoor Air Contaminants. *Appl. Microbiol. Biotechnol.* **2005**, *66* (4), 367–372. https://doi.org/10.1007/s00253-004-1753-9.

(77) Hussein, H. Toxicity, Metabolism, and Impact of Mycotoxins on Humans and Animals. *Toxicology* **2001**, *167* (2), 101–134. https://doi.org/10.1016/S0300-483X(01)00471-1.
(78) Kelman, B. J.; Robbins, C. A.; Swenson, L. J.; Hardin, B. D. Risk from Inhaled Mycotoxins in Indoor Office and Residential Environments. *Int. J. Toxicol.* **2004**, *23* (1), 3–10. https://doi.org/10.1080/10915810490265423.
(79) Straus, D. C. Molds, Mycotoxins, and Sick Building Syndrome. *Toxicol. Ind. Health* **2009**, *25* (9–10), 617–635. https://doi.org/10.1177/0748233709348287.
(80) Hardin, B. D.; Robbins, C. A.; Fallah, P.; Kelman, B. J. The Concentration of No Toxicologic Concern (CoNTC) and Airborne Mycotoxins. *J. Toxicol. Environ. Health A* **2009**, *72* (9), 585–598. https://doi.org/10.1080/15287390802706389.
(81) Mendell, M. J.; Mirer, A. G.; Cheung, K.; Tong, M.; Douwes, J. Respiratory and Allergic Health Effects of Dampness, Mold, and Dampness-Related Agents: A Review of the Epidemiologic Evidence. *Environ. Health Perspect.* **2011**, *119* (6), 748–756. https://doi.org/10.1289/ehp.1002410.
(82) Bennett, J. W.; Klich, M. Mycotoxins. *Clin. Microbiol. Rev.* **2003**, *16* (3), 497–516. https://doi.org/10.1128/cmr.16.3.497-516.2003.
(83) Croft, W. A.; Jarvis, B. B.; Yatawara, C. S. Airborne Outbreak of Trichothecene Toxicosis. *Atmospheric Environ. 1967* **1986**, *20* (3), 549–552. https://doi.org/10.1016/0004-6981(86)90096-X.
(84) Hintikka, E.-L.; Nikulin, M. Airborne Mycotoxins in Agricultural and Indoor Environments. *Indoor Air* **1998**, *8* (S4), 66–70. https://doi.org/10.1111/j.1600-0668.1998.tb00011.x.
(85) Wang, Y.; Chai, T.; Lu, G.; Quan, C.; Duan, H.; Yao, M.; Zucker, B.-A.; Schlenker, G. Simultaneous Detection of Airborne Aflatoxin, Ochratoxin and Zearalenone in a Poultry House by Immunoaffinity Clean-up and High-Performance Liquid Chromatography. *Environ. Res.* **2008**, *107* (2), 139–144. https://doi.org/10.1016/j.envres.2008.01.008.
(86) Smoragiewicz, W.; Cossette, B.; Boutard, A.; Krzystyniak, K. Trichothecene Mycotoxins in the Dust of Ventilation Systems in Office Buildings. *Int. Arch. Occup. Environ. Health* **1993**, *65* (2), 113–117. https://doi.org/10.1007/BF00405729.
(87) Verdier, T.; Coutand, M.; Bertron, A.; Roques, C. A Review of Indoor Microbial Growth across Building Materials and Sampling and Analysis Methods. *Build. Environ.* **2014**, *80*, 136–149. https://doi.org/10.1016/j.buildenv.2014.05.030.
(88) Karlsson, K.; Malmberg, P. Characterization of Exposure to Molds and Actinomycetes in Agricultural Dusts by Scanning Electron Microscopy, Fluorescence Microscopy and the Culture Method. *Scand. J. Work. Environ. Health* **1989**, *15* (5), 353–359. https://doi.org/10.5271/sjweh.1847.
(89) Heldal, K.; Asbjørn, S.; Wijnand, E. IMPROVEMENTS IN THE QUANTIFICATION OF AIRBORNE MICRO-ORGANISMS IN THE FARM ENVIRONMENT BY EPIFLUORESCENCE MICROSCOPY. *Ann. Occup. Hyg.* **1996**. https://doi.org/10.1093/annhyg/40.4.437.
(90) Bloom, E.; Nyman, E.; Must, A.; Pehrson, C.; Larsson, L. Molds and Mycotoxins in Indoor Environments — A Survey in Water-Damaged Buildings. *J. Occup. Environ. Hyg.* **2009**, *6* (11), 671–678. https://doi.org/10.1080/15459620903252053.
(91) Meklin, T.; Reponen, T.; McKinstry, C.; Cho, S.-H.; Grinshpun, S. A.; Nevalainen, A.; Vepsäläinen, A.; Haugland, R. A.; LeMasters, G.; Vesper, S. J. Comparison of Mold Concentrations Quantified by MSQPCR in Indoor and Outdoor Air Sampled Simultaneously. *Sci. Total Environ.* **2007**, *382* (1), 130–134. https://doi.org/10.1016/j.scitotenv.2007.03.031.
(92) Meklin, T.; Haugland, R. A.; Reponen, T.; Varma, M.; Lummus, Z.; Bernstein, D.; Wymer, L. J.; Vesper, S. J. Quantitative PCR Analysis of House Dust Can Reveal Abnormal Mold Conditions. *J. Environ. Monit.* **2004**, *6* (7), 615. https://doi.org/10.1039/b400250d.

(93) Rodríguez, A.; Isabel Luque, M.; Andrade, M. J.; Rodríguez, M.; Asensio, M. A.; Córdoba, J. J. Development of Real-Time PCR Methods to Quantify Patulin-Producing Molds in Food Products. *Food Microbiol.* **2011**, *28* (6), 1190–1199. https://doi.org/10.1016/j.fm.2011.04.004.
(94) Lignell, U.; Meklin, T.; Rintala, H.; Hyvärinen, A.; Vepsäläinen, A.; Pekkanen, J.; Nevalainen, A. Evaluation of Quantitative PCR and Culture Methods for Detection of House Dust Fungi and Streptomycetes in Relation to Moisture Damage of the House. *Lett. Appl. Microbiol.* **2008**, *47* (4), 303–308. https://doi.org/10.1111/j.1472-765X.2008.02431.x.
(95) Rodríguez, A.; Rodríguez, M.; Luque, M. I.; Justesen, A. F.; Córdoba, J. J. Quantification of Ochratoxin A-Producing Molds in Food Products by SYBR Green and TaqMan Real-Time PCR Methods. *Int. J. Food Microbiol.* **2011**, *149* (3), 226–235. https://doi.org/10.1016/j.ijfoodmicro.2011.06.019.
(96) Rodríguez, A.; Rodríguez, M.; Andrade, M. J.; Córdoba, J. J. Development of a Multiplex Real-Time PCR to Quantify Aflatoxin, Ochratoxin A and Patulin Producing Molds in Foods. *Int. J. Food Microbiol.* **2012**, *155* (1–2), 10–18. https://doi.org/10.1016/j.ijfoodmicro.2012.01.007.
(97) Suanthie, Y.; Cousin, M. A.; Woloshuk, C. P. Multiplex Real-Time PCR for Detection and Quantification of Mycotoxigenic Aspergillus, Penicillium and Fusarium. *J. Stored Prod. Res.* **2009**, *45* (2), 139–145. https://doi.org/10.1016/j.jspr.2008.12.001.
(98) Fredlund, E.; Gidlund, A.; Olsen, M.; Börjesson, T.; Spliid, N. H. H.; Simonsson, M. Method Evaluation of Fusarium DNA Extraction from Mycelia and Wheat for Down-Stream Real-Time PCR Quantification and Correlation to Mycotoxin Levels. *J. Microbiol. Methods* **2008**, *73* (1), 33–40. https://doi.org/10.1016/j.mimet.2008.01.007.
(99) Nakayama, T.; Yamazaki, T.; Yo, A.; Tone, K.; Mahdi Alshahni, M.; Fujisaki, R.; Makimura, K. Detection of Fungi from an Indoor Environment Using Loop-Mediated Isothermal Amplification (LAMP) Method. *Biocontrol Sci.* **2017**, *22* (2), 97–104. https://doi.org/10.4265/bio.22.97.
(100) Niessen, L. Current State and Future Perspectives of Loop-Mediated Isothermal Amplification (LAMP)-Based Diagnosis of Filamentous Fungi and Yeasts. *Appl. Microbiol. Biotechnol.* **2015**, *99* (2), 553–574. https://doi.org/10.1007/s00253-014-6196-3.
(101) Niessen, L. The Application of Loop-Mediated Isothermal Amplification (LAMP) Assays for the Rapid Diagnosis of Food-Borne Mycotoxigenic Fungi. *Curr. Opin. Food Sci.* **2018**, *23*, 11–22. https://doi.org/10.1016/j.cofs.2018.02.007.
(102) Lee, P. L. M. DNA Amplification in the Field: Move over PCR, Here Comes LAMP. *Mol. Ecol. Resour.* **2017**, *17* (2), 138–141. https://doi.org/10.1111/1755-0998.12548.
(103) Notomi, T.; Mori, Y.; Tomita, N.; Kanda, H. Loop-Mediated Isothermal Amplification (LAMP): Principle, Features, and Future Prospects. *J. Microbiol.* **2015**, *53* (1), 1–5. https://doi.org/10.1007/s12275-015-4656-9.
(104) TwistDx. TwistAmp® DNA Amplification Kits - Assay Design Manual https://www.twistdx.co.uk/docs/default-source/RPA-assay-design/twistamp-assay-design-manual-v2-5.pdf?sfvrsn=29.
(105) Yu, J.; Shen, D.; Dai, T.; Lu, X.; Xu, H.; Dou, D. Rapid and Equipment-free Detection of *Phytophthora Capsici* Using Lateral Flow Strip-based Recombinase Polymerase Amplification Assay. *Lett. Appl. Microbiol.* **2019**, lam.13166. https://doi.org/10.1111/lam.13166.
(106) Lei, R.; Kong, J.; Qiu, Y.; Chen, N.; Zhu, S.; Wang, X.; Wu, P. Rapid Detection of the Pathogenic Fungi Causing Blackleg of Brassica Napus Using a Portable Real-Time Fluorescence Detector. *Food Chem.* **2019**, *288*, 57–67. https://doi.org/10.1016/j.foodchem.2019.02.089.
(107) Karakkat, B. B.; Hockemeyer, K.; Franchett, M.; Olson, M.; Mullenberg, C.; Koch, P. L. Detection of Root-Infecting Fungi on Cool-Season Turfgrasses Using Loop-Mediated

Isothermal Amplification and Recombinase Polymerase Amplification. *J. Microbiol. Methods* **2018**, *151*, 90–98. https://doi.org/10.1016/j.mimet.2018.06.011.

(108) Brasel, T. L.; Martin, J. M.; Carriker, C. G.; Wilson, S. C.; Straus, D. C. Detection of Airborne Stachybotrys Chartarum Macrocyclic Trichothecene Mycotoxins in the Indoor Environment. *Appl. Environ. Microbiol.* **2005**, *71* (11), 7376–7388. https://doi.org/10.1128/AEM.71.11.7376-7388.2005.

(109) Bloom, E.; Bal, K.; Nyman, E.; Must, A.; Larsson, L. Mass Spectrometry-Based Strategy for Direct Detection and Quantification of Some Mycotoxins Produced by Stachybotrys and Aspergillus Spp. in Indoor Environments. *Appl. Environ. Microbiol.* **2007**, *73* (13), 4211–4217. https://doi.org/10.1128/AEM.00343-07.

(110) Polizzi, V.; Adams, A.; De Saeger, S.; Van Peteghem, C.; Moretti, A.; De Kimpe, N. Influence of Various Growth Parameters on Fungal Growth and Volatile Metabolite Production by Indoor Molds. *Sci. Total Environ.* **2012**, *414*, 277–286. https://doi.org/10.1016/j.scitotenv.2011.10.035.

(111) Hendry, K. M.; Cole, E. C. A Review of Mycotoxins in Indoor Air. *J. Toxicol. Environ. Health* **1993**, *38* (2), 183–198. https://doi.org/10.1080/15287399309531711.

(112) *Antimicrobial Resistance: Global Report on Surveillance*; World Health Organization, Ed.; World Health Organization: Geneva, Switzerland, 2014.

(113) Wennergren, G.; Lagercrantz, H. "One Sometimes Finds What One Is Not Looking for" (Sir Alexander Fleming): The Most Important Medical Discovery of the 20th Century. *Acta Paediatr.* **2007**, *96* (1), 141–144. https://doi.org/10.1111/j.1651-2227.2007.00098.x.

(114) Pärnänen, K. M. M.; Narciso-da-Rocha, C.; Kneis, D.; Berendonk, T. U.; Cacace, D.; Do, T. T.; Elpers, C.; Fatta-Kassinos, D.; Henriques, I.; Jaeger, T.; Karkman, A.; Martinez, J. L.; Michael, S. G.; Michael-Kordatou, I.; O'Sullivan, K.; Rodriguez-Mozaz, S.; Schwartz, T.; Sheng, H.; Sørum, H.; Stedtfeld, R. D.; Tiedje, J. M.; Giustina, S. V. D.; Walsh, F.; Vaz-Moreira, I.; Virta, M.; Manaia, C. M. Antibiotic Resistance in European Wastewater Treatment Plants Mirrors the Pattern of Clinical Antibiotic Resistance Prevalence. *Sci. Adv.* **2019**, *5* (3), eaau9124.

(115) Cassini, A.; Högberg, L. D.; Plachouras, D.; Quattrocchi, A.; Hoxha, A.; Simonsen, G. S.; Colomb-Cotinat, M.; Kretzschmar, M. E.; Devleesschauwer, B.; Cecchini, M.; Ouakrim, D. A.; Oliveira, T. C.; Struelens, M. J.; Suetens, C.; Monnet, D. L.; Strauss, R.; Mertens, K.; Struyf, T.; Catry, B.; Latour, K.; Ivanov, I. N.; Dobreva, E. G.; Tambic Andraševic, A.; Soprek, S.; Budimir, A.; Paphitou, N.; Žemlicková, H.; Schytte Olsen, S.; Wolff Sönksen, U.; Märtin, P.; Ivanova, M.; Lyytikäinen, O.; Jalava, J.; Coignard, B.; Eckmanns, T.; Abu Sin, M.; Haller, S.; Daikos, G. L.; Gikas, A.; Tsiodras, S.; Kontopidou, F.; Tóth, Á.; Hajdu, Á.; Guólaugsson, Ó.; Kristinsson, K. G.; Murchan, S.; Burns, K.; Pezzotti, P.; Gagliotti, C.; Dumpis, U.; Liuimiene, A.; Perrin, M.; Borg, M. A.; de Greeff, S. C.; Monen, J. C.; Koek, M. B.; Elstrøm, P.; Zabicka, D.; Deptula, A.; Hryniewicz, W.; Caniça, M.; Nogueira, P. J.; Fernandes, P. A.; Manageiro, V.; Popescu, G. A.; Serban, R. I.; Schréterová, E.; Litvová, S.; Štefkovicová, M.; Kolman, J.; Klavs, I.; Korošec, A.; Aracil, B.; Asensio, A.; Pérez-Vázquez, M.; Billström, H.; Larsson, S.; Reilly, J. S.; Johnson, A.; Hopkins, S. Attributable Deaths and Disability-Adjusted Life-Years Caused by Infections with Antibiotic-Resistant Bacteria in the EU and the European Economic Area in 2015: A Population-Level Modelling Analysis. *Lancet Infect. Dis.* **2019**, *19* (1), 56–66.

(116) European Commission. The New EU ONE HEALTH Action Plan against Antimicrobial Resistance-Summary of the Action Plan. official website of the European Union: https://ec.europa.eu/health/amr/ 2017.

(117) Thorpe, K. E.; Joski, P.; Johnston, K. J. Antibiotic-Resistant Infection Treatment Costs Have Doubled Since 2002, Now Exceeding $2 Billion Annually. *Health Aff. (Millwood)* **2018**, *37* (4), 662–669. https://doi.org/10.1377/hlthaff.2017.1153.

(118) Paulson, J. R.; Mahmoud, I. Y.; Al-Musharafi, S. K.; Al-Bahry, S. N. Antibiotic Resistant Bacteria in the Environment as Bio-Indicators of Pollution. *Open Biotechnol. J.* **2016**, *10* (1), 342–351.
(119) Heuer, H.; Schmitt, H.; Smalla, K. Antibiotic Resistance Gene Spread Due to Manure Application on Agricultural Fields. *Curr. Opin. Microbiol.* **2011**, *14* (3), 236–243.
(120) Pruden, A.; Larsson, D. G. J.; Amézquita, A.; Collignon, P.; Brandt, K. K.; Graham, D. W.; Lazorchak, J. M.; Suzuki, S.; Silley, P.; Snape, J. R.; Topp, E.; Zhang, T.; Zhu, Y.-G. Management Options for Reducing the Release of Antibiotics and Antibiotic Resistance Genes to the Environment. *Environ. Health Perspect.* **2013**, *121* (8), 878–885.
(121) Manaia, C. M.; Rocha, J.; Scaccia, N.; Marano, R.; Radu, E.; Biancullo, F.; Cerqueira, F.; Fortunato, G.; Iakovides, I. C.; Zammit, I.; Kampouris, I.; Vaz-Moreira, I.; Nunes, O. C. Antibiotic Resistance in Wastewater Treatment Plants: Tackling the Black Box. *Environ. Int.* **2018**, *115*, 312–324.
(122) Birošová, L.; Mackuľak, T.; Bodík, I.; Ryba, J.; Škubák, J.; Grabic, R. Pilot Study of Seasonal Occurrence and Distribution of Antibiotics and Drug Resistant Bacteria in Wastewater Treatment Plants in Slovakia. *Sci. Total Environ.* **2014**, *490*, 440–444.
(123) Karkman, A.; Do, T. T.; Walsh, F.; Virta, M. P. J. Antibiotic-Resistance Genes in Waste Water. *Trends Microbiol.* **2018**, *26* (3), 220–228. https://doi.org/10.1016/j.tim.2017.09.005.
(124) von Wintersdorff, C. J. H.; Penders, J.; van Niekerk, J. M.; Mills, N. D.; Majumder, S.; van Alphen, L. B.; Savelkoul, P. H. M.; Wolffs, P. F. G. Dissemination of Antimicrobial Resistance in Microbial Ecosystems through Horizontal Gene Transfer. *Front. Microbiol.* **2016**, *7*.
(125) Nordmann, P.; Dortet, L.; Poirel, L. Carbapenem Resistance in Enterobacteriaceae: Here Is the Storm! *Trends Mol. Med.* **2012**, *18* (5), 263–272. https://doi.org/10.1016/j.molmed.2012.03.003.
(126) Cantón, R.; Coque, T. M. The CTX-M β-Lactamase Pandemic. *Curr. Opin. Microbiol.* **2006**, *9* (5), 466–475.
(127) Cantón, R.; González-Alba, J. M.; Galán, J. C. CTX-M Enzymes: Origin and Diffusion. *Front. Microbiol.* **2012**, *3*.
(128) Davies, J.; Davies, D. Origins and Evolution of Antibiotic Resistance. *Microbiol. Mol. Biol. Rev.* **2010**, *74* (3), 417–433. https://doi.org/10.1128/MMBR.00016-10.
(129) Bevan, E. R.; Jones, A. M.; Hawkey, P. M. Global Epidemiology of CTX-M β-Lactamases: Temporal and Geographical Shifts in Genotype. *J. Antimicrob. Chemother.* **2017**, *72* (8), 2145–2155.
(130) Zhao, W.-H.; Hu, Z.-Q. Epidemiology and Genetics of CTX-M Extended-Spectrum β-Lactamases in Gram-Negative Bacteria. *Crit. Rev. Microbiol.* **2013**, *39* (1), 79–101.
(131) Bauernfeind, A.; Schweighart, S.; Grimm, H. A New Plasmidic Cefotaximase in a Clinical Isolate of Escherichia Coli. *Infection* **1990**, *18* (5), 294–298. https://doi.org/10.1007/BF01647010.
(132) Aali, R.; Nikaeen, M.; Khanahmad, H.; Hassanzadeh, A. Monitoring and Comparison of Antibiotic Resistant Bacteria and Their Resistance Genes in Municipal and Hospital Wastewaters. *Int. J. Prev. Med.* **2014**, *5* (7), 887–894.
(133) McLain, J. E.; Cytryn, E.; Durso, L. M.; Young, S. Culture-Based Methods for Detection of Antibiotic Resistance in Agroecosystems: Advantages, Challenges, and Gaps in Knowledge. *J. Environ. Qual.* **2016**, *45* (2), 432–440.
(134) Exner, M.; Schwartz, T. RiSKWa-Statuspapier Bewertungskonzepte Der Mikrobiologie Mit Den Schwerpunkten Neue Krankheitserreger Und Antibiotikaresistenzen Ergebnisse Des Querschnittsthemas „Bewertungskonzepte Der Mikrobiologie“. BMBF-Fördermaßnahme 2015.

(135) Watkinson, A. J.; Micalizzi, G. R.; Bates, J. R.; Costanzo, S. D. Novel Method for Rapid Assessment of Antibiotic Resistance in Escherichia Coli Isolates from Environmental Waters by Use of a Modified Chromogenic Agar. *Appl. Environ. Microbiol.* **2007**, *73* (7), 2224–2229.
(136) Wada, M.; Lkhagvadorj, E.; Bian, L.; Wang, C.; Chiba, Y.; Nagata, S.; Shimizu, T.; Yamashiro, Y.; Asahara, T.; Nomoto, K. Quantitative Reverse Transcription-PCR Assay for the Rapid Detection of Methicillin-Resistant Staphylococcus Aureus. *J. Appl. Microbiol.* **2010**, *108* (3), 779–788.
(137) Xu, L. Rapid and Simple Detection of BlaCTX-M Genes by Multiplex PCR Assay. *J. Med. Microbiol.* **2005**, *54* (12), 1183–1187. https://doi.org/10.1099/jmm.0.46160-0.
(138) Zhang, G.-L.; Feng, Y.-L.; Song, J.-L.; Zhou, X.-S. Zearalenone: A Mycotoxin With Different Toxic Effect in Domestic and Laboratory Animals' Granulosa Cells. *Front. Genet.* **2018**, *9*, 667. https://doi.org/10.3389/fgene.2018.00667.
(139) Spencer, S. J.; Tamminen, M. V.; Preheim, S. P.; Guo, M. T.; Briggs, A. W.; Brito, I. L.; A Weitz, D.; Pitkänen, L. K.; Vigneault, F.; Virta, M. Pj.; Alm, E. J. Massively Parallel Sequencing of Single Cells by EpicPCR Links Functional Genes with Phylogenetic Markers. *ISME J.* **2016**, *10* (2), 427–436.
(140) Hultman, J.; Tamminen, M.; Pärnänen, K.; Cairns, J.; Karkman, A.; Virta, M. Host Range of Antibiotic Resistance Genes in Wastewater Treatment Plant Influent and Effluent. *FEMS Microbiol. Ecol.* **2018**, *94* (4).
(141) Rice, E. W.; Wang, P.; Smith, A. L.; Stadler, L. B. Determining Hosts of Antibiotic Resistance Genes: A Review of Methodological Advances. *Environ. Sci. Technol. Lett.* **2020**, *7* (5), 282–291.
(142) Hu, C.; Kalsi, S.; Zeimpekis, I.; Sun, K.; Ashburn, P.; Turner, C.; Sutton, J. M.; Morgan, H. Ultra-Fast Electronic Detection of Antimicrobial Resistance Genes Using Isothermal Amplification and Thin Film Transistor Sensors. *Biosens. Bioelectron.* **2017**, *96*, 281–287.
(143) Ota, Y.; Furuhashi, K.; Nanba, T.; Yamanaka, K.; Ishikawa, J.; Nagura, O.; Hamada, E.; Maekawa, M. A Rapid and Simple Detection Method for Phenotypic Antimicrobial Resistance in Escherichia Coli by Loop-Mediated Isothermal Amplification. *J. Med. Microbiol.* **2019**, *68* (2), 169–177.
(144) Zhong, L.-L.; Zhou, Q.; Tan, C.; Roberts, A. P.; El-Sayed Ahmed, M. A. E.-G.; Chen, G.; Dai, M.; Yang, F.; Xia, Y.; Liao, K.; Liang, Y.; Yang, Y.; Feng, S.; Zheng, X.; Tian, G.-B. Multiplex Loop-Mediated Isothermal Amplification (Multi-LAMP) Assay for Rapid Detection of Mcr-1 to Mcr-5 in Colistin-Resistant Bacteria. *Infect. Drug Resist.* **2019**, *Volume 12*, 1877–1887.
(145) Bergkessel, M.; Guthrie, C. Colony PCR. In *Methods in Enzymology*; Elsevier, 2013; Vol. 529, pp 299–309.
(146) Kong, P.; Richardson, P. A.; Hong, C. Direct Colony PCR-SSCP for Detection of Multiple Pythiaceous Oomycetes in Environmental Samples. *J. Microbiol. Methods* **2005**, *61* (1), 25–32. https://doi.org/10.1016/j.mimet.2004.10.019.
(147) Bottoni, P.; Caroli, S. Presence of Residues and Metabolites of Pharmaceuticals in Environmental Compartments, Food Commodities and Workplaces: A Review Spanning the Three-Year Period 2014–2016. *Microchem. J.* **2018**, *136*, 2–24. https://doi.org/10.1016/j.microc.2017.06.016.
(148) Rana, M. S.; Lee, S. Y.; Kang, H. J.; Hur, S. J. Reducing Veterinary Drug Residues in Animal Products: A Review. *Food Sci. Anim. Resour.* **2019**, *39* (5), 687–703. https://doi.org/10.5851/kosfa.2019.e65.
(149) Beyene, T. Veterinary Drug Residues in Food-Animal Products: Its Risk Factors and Potential Effects on Public Health. *J. Vet. Sci. Technol.* **2015**, *07* (01). https://doi.org/10.4172/2157-7579.1000285.

(150) Van Hecken, A.; Schwartz, J. I.; Depré, M.; De Lepeleire, I.; Dallob, A.; Tanaka, W.; Wynants, K.; Buntinx, A.; Arnout, J.; Wong, P. H.; Ebel, D. L.; Gertz, B. J.; De Schepper, P. J. Comparative Inhibitory Activity of Rofecoxib, Meloxicam, Diclofenac, Ibuprofen, and Naproxen on COX-2 versus COX-1 in Healthy Volunteers. *J. Clin. Pharmacol.* **2000**, *40* (10), 1109–1120.
(151) Blobaum, A. L.; Marnett, L. J. Structural and Functional Basis of Cyclooxygenase Inhibition. *J. Med. Chem.* **2007**, *50* (7), 1425–1441. https://doi.org/10.1021/jm0613166.
(152) Lonappan, L.; Brar, S. K.; Das, R. K.; Verma, M.; Surampalli, R. Y. Diclofenac and Its Transformation Products: Environmental Occurrence and Toxicity - A Review. *Environ. Int.* **2016**, *96*, 127–138. https://doi.org/10.1016/j.envint.2016.09.014.
(153) Gallo, P.; Fabbrocino, S.; Dowling, G.; Salini, M.; Fiori, M.; Perretta, G.; Serpe, L. Confirmatory Analysis of Non-Steroidal Anti-Inflammatory Drugs in Bovine Milk by High-Performance Liquid Chromatography with Fluorescence Detection. *J. Chromatogr. A* **2010**, *1217* (17), 2832–2839. https://doi.org/10.1016/j.chroma.2010.02.047.
(154) Jedziniak, P.; Szprengier-Juszkiewicz, T.; Pietruk, K.; Śledzińska, E.; Żmudzki, J. Determination of Non-Steroidal Anti-Inflammatory Drugs and Their Metabolites in Milk by Liquid Chromatography–Tandem Mass Spectrometry. *Anal. Bioanal. Chem.* **2012**, *403* (10), 2955–2963. https://doi.org/10.1007/s00216-012-5860-7.
(155) Mainero Rocca, L.; Gentili, A.; Pérez-Fernández, V.; Tomai, P. Veterinary Drugs Residues: A Review of the Latest Analytical Research on Sample Preparation and LC-MS Based Methods. *Food Addit. Contam. Part A* **2017**, 1–19. https://doi.org/10.1080/19440049.2017.1298846.
(156) Swan, G. E.; Cuthbert, R.; Quevedo, M.; Green, R. E.; Pain, D. J.; Bartels, P.; Cunningham, A. A.; Duncan, N.; Meharg, A. A.; Lindsay Oaks, J.; Parry-Jones, J.; Shultz, S.; Taggart, M. A.; Verdoorn, G.; Wolter, K. Toxicity of Diclofenac to *Gyps* Vultures. *Biol. Lett.* **2006**, *2* (2), 279–282. https://doi.org/10.1098/rsbl.2005.0425.
(157) Naidoo, V.; Wolter, K.; Cuthbert, R.; Duncan, N. Veterinary Diclofenac Threatens Africa's Endangered Vulture Species. *Regul. Toxicol. Pharmacol.* **2009**, *53* (3), 205–208. https://doi.org/10.1016/j.yrtph.2009.01.010.
(158) Prakash, V.; Bishwakarma, M. C.; Chaudhary, A.; Cuthbert, R.; Dave, R.; Kulkarni, M.; Kumar, S.; Paudel, K.; Ranade, S.; Shringarpure, R.; Green, R. E. The Population Decline of Gyps Vultures in India and Nepal Has Slowed since Veterinary Use of Diclofenac Was Banned. *PLoS ONE* **2012**, *7* (11), e49118. https://doi.org/10.1371/journal.pone.0049118.
(159) Paudel, K.; Amano, T.; Acharya, R.; Chaudhary, A.; Baral, H. S.; Bhusal, K. P.; Chaudhary, I. P.; Green, R. E.; Cuthbert, R. J.; Galligan, T. H. Population Trends in Himalayan Griffon in Upper Mustang, Nepal, before and after the Ban on Diclofenac. *Bird Conserv. Int.* **2016**, *26* (3), 286–292. https://doi.org/10.1017/S0959270915000192.
(160) European Commission. Commission Regulation (EU) No 37/2010 of 22 December 2009 on Pharmacologically Active Substances and Their Classification Regarding Maximum Residue Limits in Foodstuffs of Animal Origin. EUR-Lex 2009.
(161) Margalida, A.; Oliva-Vidal, P. The Shadow of Diclofenac Hangs over European Vultures. *Nat. Ecol. Evol.* **2017**, *1* (8), 1050–1050. https://doi.org/10.1038/s41559-017-0255-y.
(162) Alvine Coralie Mehinto. Impacts of the Human Pharmaceutical Diclofenac in the Aquatic Environment. October 2009.
(163) Fent, K.; Weston, A.; Caminada, D. Ecotoxicology of Human Pharmaceuticals. *Aquat. Toxicol.* **2006**, *76* (2), 122–159. https://doi.org/10.1016/j.aquatox.2005.09.009.
(164) Acuña, V.; Ginebreda, A.; Mor, J. R.; Petrovic, M.; Sabater, S.; Sumpter, J.; Barceló, D. Balancing the Health Benefits and Environmental Risks of Pharmaceuticals: Diclofenac as an Example. *Environ. Int.* **2015**, *85*, 327–333. https://doi.org/10.1016/j.envint.2015.09.023.

(165) Davanzo, R.; Bua, J.; Paloni, G.; Facchina, G. Breastfeeding and Migraine Drugs. *Eur. J. Clin. Pharmacol.* **2014**, *70* (11), 1313–1324. https://doi.org/10.1007/s00228-014-1748-0.
(166) Amundsen, S.; Nordeng, H.; Nezvalová-Henriksen, K.; Stovner, L. J.; Spigset, O. Pharmacological Treatment of Migraine during Pregnancy and Breastfeeding. *Nat. Rev. Neurol.* **2015**, *11* (4), 209–219. https://doi.org/10.1038/nrneurol.2015.29.
(167) Bewertungsbericht Zu Den Ergebnissen Des Nationalen Rückstandskontrollplans Und Des Einfuhrüberwachungsplans 2016. Bundesinstitut für Risikobewertung April 2019.
(168) Rückstandskontrollprogramm 2017 Für Milch, Eier Und Honig. Bundesministerium für Arbeit, Soziales, Gesundheit und Konsumentenschutz (BMASGK) Österreichische Agentur für Gesundheit und Ernährungssicherheit GmbH (AGES) May 2018.
(169) Dowling, G.; Gallo, P.; Fabbrocino, S.; Serpe, L.; Regan, L. Determination of Ibuprofen, Ketoprofen, Diclofenac and Phenylbutazone in Bovine Milk by Gas Chromatography-Tandem Mass Spectrometry. *Food Addit. Contam. Part A* **2008**, *25* (12), 1497–1508. https://doi.org/10.1080/02652030802383160.
(170) *Analysis of Antibiotic/Drug Residues in Food Products of Animal Origin*; 1992.
(171) Reig, M.; Toldrá, F. Patents for ELISA Tests to Detect Antibiotic Residues in Foods of Animal Origin. *Recent Pat. Food Nutr. Agric.* **2011**, *3* (2), 110–114.
(172) Ahmed, S.; Ning, J.; Peng, D.; Chen, T.; Ahmad, I.; Ali, A.; Lei, Z.; Abu bakr Shabbir, M.; Cheng, G.; Yuan, Z. Current Advances in Immunoassays for the Detection of Antibiotics Residues: A Review. *Food Agric. Immunol.* **2020**, *31* (1), 268–290. https://doi.org/10.1080/09540105.2019.1707171.
(173) Aydin, S. A Short History, Principles, and Types of ELISA, and Our Laboratory Experience with Peptide/Protein Analyses Using ELISA. *Peptides* **2015**, *72*, 4–15. https://doi.org/10.1016/j.peptides.2015.04.012.
(174) Fadlalla, M. H.; Ling, S.; Wang, R.; Li, X.; Yuan, J.; Xiao, S.; Wang, K.; Tang, S.; Elsir, H.; Wang, S. Development of ELISA and Lateral Flow Immunoassays for Ochratoxins (OTA and OTB) Detection Based on Monoclonal Antibody. *Front. Cell. Infect. Microbiol.* **2020**, *10*, 80. https://doi.org/10.3389/fcimb.2020.00080.
(175) Abate, M. F.; Ahmed, M. G.; Li, X.; Yang, C.; Zhu, Z. Distance-Based Paper/PMMA Integrated ELISA-Chip for Quantitative Detection of Immunoglobulin G. *Lab. Chip* **2020**, *20* (19), 3625–3632. https://doi.org/10.1039/D0LC00505C.
(176) Han, K. N.; Li, C. A.; Seong, G. H. Microfluidic Chips for Immunoassays. *Annu. Rev. Anal. Chem.* **2013**, *6* (1), 119–141. https://doi.org/10.1146/annurev-anchem-062012-092616.
(177) Rasooly, A.; Bruck, H. A.; Kostov, Y. An ELISA Lab-on-a-Chip (ELISA-LOC). *Methods Mol. Biol. Clifton NJ* **2013**, *949*, 451–471. https://doi.org/10.1007/978-1-62703-134-9_29.
(178) Singh, B.; Flampouri, E.; Dempsey, E. Electrochemical Enzyme-Linked Immunosorbent Assay (e-ELISA) for Parasitic Nematode *Ostertagia Ostertagi* (Brown Stomach Worm) Infections in Dairy Cattle. *The Analyst* **2019**, *144* (19), 5748–5754. https://doi.org/10.1039/C9AN00982E.
(179) Hübner, M. Development of Immunological Methods for the Detection of Micropollutants in Fresh Water Samples. Dissertation 2015.
(180) Meyer, V. K.; Kober, C.; Niessner, R.; Seidel, M. Regeneration of Recombinant Antigen Microarrays for the Automated Monitoring of Antibodies against Zoonotic Pathogens in Swine Sera. *Sensors* **2015**, *15* (2), 2614–2628. https://doi.org/10.3390/s150202614.
(181) Atoui, A.; El Khoury, A.; Kallassy, M.; Lebrihi, A. Quantification of Fusarium Graminearum and Fusarium Culmorum by Real-Time PCR System and Zearalenone Assessment in Maize. *Int. J. Food Microbiol.* **2012**, *154* (1–2), 59–65. https://doi.org/10.1016/j.ijfoodmicro.2011.12.022.

(182) Rodríguez, A.; Rodríguez, M.; Luque, M. I.; Martín, A.; Córdoba, J. J. Real-Time PCR Assays for Detection and Quantification of Aflatoxin-Producing Molds in Foods. *Food Microbiol.* **2012**, *31* (1), 89–99. https://doi.org/10.1016/j.fm.2012.02.009.
(183) Niessen, L. PCR-Based Diagnosis and Quantification of Mycotoxin Producing Fungi. *Int. J. Food Microbiol.* **2007**, *119* (1–2), 38–46. https://doi.org/10.1016/j.ijfoodmicro.2007.07.023.
(184) Meng, K.; Wang, Y.; Yang, P.; Luo, H.; Bai, Y.; Shi, P.; Yuan, T.; Ma, R.; Yao, B. Rapid Detection and Quantification of Zearalenone-Producing Fusarium Species by Targeting the Zearalenone Synthase Gene PKS4. *Food Control* **2010**, *21* (2), 207–211. https://doi.org/10.1016/j.foodcont.2009.05.014.
(185) Fung, F.; Clark, R. F. Health Effects of Mycotoxins: A Toxicological Overview. *J. Toxicol. Clin. Toxicol.* **2004**, *42* (2), 217–234. https://doi.org/10.1081/CLT-120030947.
(186) Schwaiger, G. Detection of Mycotoxin Producers via Microarray-Assisted Amplification. Master Thesis 2019.
(187) Solomon, G. M.; Hjelmroos-Koski, M.; Rotkin-Ellman, M.; Hammond, S. K. Airborne Mold and Endotoxin Concentrations in New Orleans, Louisiana, after Flooding, October through November 2005. *Environ. Health Perspect.* **2006**, *114* (9), 1381–1386. https://doi.org/10.1289/ehp.9198.
(188) Inal, A.; Karakoc, G. B.; Altintas, D. U.; Guvenmez, H. K.; Aka, Y.; Gelisken, R.; Yilmaz, M.; Kendirli, S. G. Effect of Indoor Mold Concentrations on Daily Symptom Severity of Children with Asthma and/or Rhinitis Monosensitized to Molds. *J. Asthma* **2007**, *44* (7), 543–546. https://doi.org/10.1080/02770900701496130.
(189) Reboux, G.; Bellanger, A. P.; Roussel, S.; Grenouillet, F.; Sornin, S.; Piarroux, R.; Dalphin, J. C.; Millon, L. Indoor Mold Concentration in Eastern France: Indoor Mold in France. *Indoor Air* **2009**, *19* (6), 446–453. https://doi.org/10.1111/j.1600-0668.2009.00598.x.
(190) Ergänzung zum Standard der baubiologischen Messtechnik SBM-2015, Baubiologische Richtwerte für Schlafbereiceh https://www.gesundes-haus.ch/files/content/materialempfehlungen/SBM%20Standard%20baubiologische%20Messtechnik%202008/richtwerte-schlafbereiche-15.pdf.
(191) Viegas, C. *Exposure to Microbiological Agents in Indoor and Occupational Environments*, 1st edition.; Springer Berlin Heidelberg: New York, NY, 2017.
(192) Khan, A. A. H.; Karuppayil, S. M.; Manoharachary, C.; Kunwar, I. K.; Waghray, S. Isolation, Identification and Testing for Allergenicity of Fungi from Air-Conditioned Indoor Environments. *Aerobiologia* **2009**, *25* (2), 119–123. https://doi.org/10.1007/s10453-009-9114-x.
(193) Niessen, M. L.; Vogel, R. F. Group Specific PCR-Detection of Potential Trichothecene-Producing Fusarium-Species in Pure Cultures and Cereal Samples. *Syst. Appl. Microbiol.* **1998**, *21* (4), 618–631. https://doi.org/10.1016/S0723-2020(98)80075-1.
(194) Quarta, A.; Mita, G.; Haidukowski, M.; Santino, A.; Mulè, G.; Visconti, A. Assessment of Trichothecene Chemotypes of *Fusarium Culmorum* Occurring in Europe. *Food Addit. Contam.* **2005**, *22* (4), 309–315. https://doi.org/10.1080/02652030500058361.
(195) Szewczyk, E.; Nayak, T.; Oakley, C. E.; Edgerton, H.; Xiong, Y.; Taheri-Talesh, N.; Osmani, S. A.; Oakley, B. R. Fusion PCR and Gene Targeting in Aspergillus Nidulans. *Nat. Protoc.* **2006**, *1* (6), 3111–3120.
(196) Liu, Y.; Chen, J.; Thygesen, A. Efficient One-Step Fusion PCR Based on Dual-Asymmetric Primers and Two-Step Annealing. *Mol. Biotechnol.* **2018**, *60* (2), 92–99. https://doi.org/10.1007/s12033-017-0050-7.
(197) Khan, I. U. H.; Gannon, V.; Kent, R.; Koning, W.; Lapen, D. R.; Miller, J.; Neumann, N.; Phillips, R.; Robertson, W.; Topp, E.; van Bochove, E.; Edge, T. A. Development of a Rapid Quantitative

PCR Assay for Direct Detection and Quantification of Culturable and Non-Culturable Escherichia Coli from Agriculture Watersheds. *J. Microbiol. Methods* **2007**, *69* (3), 480–488.
(198) MetaWater- MetaGenomics of Water.
(199) Shannon, K. E.; Lee, D.-Y.; Trevors, J. T.; Beaudette, L. A. Application of Real-Time Quantitative PCR for the Detection of Selected Bacterial Pathogens during Municipal Wastewater Treatment. *Sci. Total Environ.* **2007**, *382* (1), 121–129.
(200) Streich, P. Development of a Chip-Based Detection System for Rapid Identification of Antibiotic Resistance Genes in Klebsiella Pneumoniae and Escherichia Coli via Molecular Fusion. Masters Thesis 2020.
(201) Lattanzio, V. M. T.; von Holst, C.; Visconti, A. Experimental Design for In-House Validation of a Screening Immunoassay Kit. The Case of a Multiplex Dipstick for Fusarium Mycotoxins in Cereals. *Anal. Bioanal. Chem.* **2013**, *405* (24), 7773–7782.
(202) The European Commission. COMMISSION REGULATION (EU) No 519/2014 of 16 May 2014 Amending Regulation (EC) No 401/2006 as Regards Methods of Sampling of Large Lots, Spices and Food Supplements, Performance Criteria for T-2, HT-2 Toxin and Citrinin and Screening Methods of Analysis. Official Journal of the European Union.
(203) Bewick, V.; Cheek, L.; Ball, J. Statistics Review 13: Receiver Operating Characteristic Curves. *Crit. Care* **2004**, *8* (6), 508.
(204) Banerjee, G. Comparative Study of Biofilm Formation in Pseudomonas Aeruginosa Isolates from Patients of Lower Respiratory Tract Infection. *J. Clin. Diagn. Res.* **2014**.
(205) Lardeux, F.; Torrico, G.; Aliaga, C. Calculation of the ELISA's Cut-off Based on the Change-Point Analysis Method for Detection of Trypanosoma Cruzi Infection in Bolivian Dogs in the Absence of Controls. *Mem. Inst. Oswaldo Cruz* **2016**, *111* (8), 501–504.
(206) Fernando, D. M.; Tun, H. M.; Poole, J.; Patidar, R.; Li, R.; Mi, R.; Amarawansha, G. E. A.; Fernando, W. G. D.; Khafipour, E.; Farenhorst, A.; Kumar, A. Detection of Antibiotic Resistance Genes in Source and Drinking Water Samples from a First Nations Community in Canada. *Appl. Environ. Microbiol.* **2016**, *82* (15), 4767–4775.
(207) Schwartz, T.; Kohnen, W.; Jansen, B.; Obst, U. Detection of Antibiotic-Resistant Bacteria and Their Resistance Genes in Wastewater, Surface Water, and Drinking Water Biofilms. *FEMS Microbiol. Ecol.* **2003**, *43* (3), 325–335.
(208) Xi, C.; Zhang, Y.; Marrs, C. F.; Ye, W.; Simon, C.; Foxman, B.; Nriagu, J. Prevalence of Antibiotic Resistance in Drinking Water Treatment and Distribution Systems. *Appl. Environ. Microbiol.* **2009**, *75* (17), 5714–5718.
(209) Auernhammer, A. Development of a Residue Analysis Microarray Chip for Milk. Masters Thesis April 14, 2020.
(210) Detektionssystem Zur Schnellen Risikobewertung von Legionellenexpositionen (LegioTyper).
(211) Mauk, M. G.; Liu, C.; Song, J.; Bau, H. H. Integrated Microfluidic Nucleic Acid Isolation, Isothermal Amplification, and Amplicon Quantification. *Microarrays Basel Switz.* **2015**, *4* (4), 474–489. https://doi.org/10.3390/microarrays4040474.
(212) Burns, M. A.; Johnson, B. N.; Brahmasandra, S. N.; Handique, K.; Webster, J. R.; Krishnan, M.; Sammarco, T. S.; Man, P. M.; Jones, D.; Heldsinger, D.; Mastrangelo, C. H.; Burke, D. T. An Integrated Nanoliter DNA Analysis Device. *Science* **1998**, *282* (5388), 484–487. https://doi.org/10.1126/science.282.5388.484.
(213) Rector, D. M.; Poe, G. R.; Redgrave, P.; Harper, R. M. A Miniature CCD Video Camera for High-Sensitivity Light Measurements in Freely Behaving Animals. *J. Neurosci. Methods* **1997**, *78* (1–2), 85–91. https://doi.org/10.1016/s0165-0270(97)00137-4.